

CUTTING STRATEGIES FOR FORGING DIE  
MANUFACTURING ON CNC MILLING MACHINES

A THESIS SUBMITTED TO  
THE GRADUATE SCHOOL OF NATURAL AND APPLIED SCIENCES  
OF  
MIDDLE EAST TECHNICAL UNIVERSITY

BY

ARDA ÖZGEN

IN PARTIAL FULFILLMENT OF THE REQUIREMENTS  
FOR  
THE DEGREE OF MASTER OF SCIENCE  
IN  
MECHANICAL ENGINEERING

MARCH 2008

Approval of the thesis:

**CUTTING STRATEGIES FOR FORGING DIE  
MANUFACTURING ON CNC MILLING MACHINES**

submitted by **ARDA ÖZGEN** in partial fulfillment of the requirements for the degree of **Master of Science in Mechanical Engineering, Middle East Technical University** by,

Prof. Dr. Canan Özgen  
Dean, Graduate School of **Natural and Applied Sciences** \_\_\_\_\_

Prof. Dr. Kemal İDER  
Head of the Department, **Mechanical Engineering** \_\_\_\_\_

Prof. Dr. Mustafa İlhan GÖKLER  
Supervisor, **Mechanical Engineering Dept., METU** \_\_\_\_\_

**Examining Committee Members:**

Prof. Dr. A. Demir Bayka  
Mechanical Engineering Dept., METU \_\_\_\_\_

Prof. Dr. Mustafa İlhan GÖKLER  
Mechanical Engineering Dept., METU \_\_\_\_\_

Prof. Dr. S. Engin KILIÇ  
Mechanical Engineering Dept., METU \_\_\_\_\_

Prof. Dr. R. Orhan YILDIRIM  
Mechanical Engineering Dept., METU \_\_\_\_\_

Prof. Dr. Can ÇOĞUN  
Mechanical Engineering Dept., Gazi University \_\_\_\_\_

**Date:** March 27<sup>th</sup>, 2008

**I hereby declare that all information in this document has been obtained and presented in accordance with academic rules and ethical conduct. I also declare that, as required by these rules and conduct, I have fully cited and referenced all material and results that are not original to this work.**

Name, Last name: Arda Özgen

Signature:

## **ABSTRACT**

### **CUTTING STRATEGIES FOR FORGING DIE MANUFACTURING ON CNC MILLING MACHINES**

Özgen, Arda

M.Sc., Department of Mechanical Engineering

Supervisor: Prof. Dr. Mustafa İlhan Gökler

March 2008, 110 pages

Manufacturing of dies has been presenting greater requirements of geometrical accuracy, dimensional precision and surface quality as well as decrease in costs and manufacturing times. Although proper cutting parameter values are utilized to obtain high geometrical accuracy and surface quality, there may exist geometrical discrepancy between the designed and the manufactured surface profile of the die cavities. In milling process; cutting speed, step over and feed are the main cutting parameters and these parameters affect geometrical accuracy and surface quality of the forging die cavities.

In this study, effects of the cutting parameters on geometrical error have been examined on a representative die cavity profile. To remove undesired volume in the die cavities, available cutting strategies are investigated. Feed rate optimization is performed to maintain the constant metal removal rate along the trajectory of the milling cutter during rough cutting process.

In the finish cutting process of the die cavities, Design of Experiment Method has been employed to find out the effects of the cutting parameters on the geometrical accuracy of the manufactured cavity profile. Prediction formula is derived to estimate the geometrical error value in terms of the values of the cutting parameters.

Validity of the prediction formula has been tested by conducting verification experiments for the representative die geometry and die cavity geometry of a forging part used in industry. Good agreement between the predicted error values and the measured error values has been observed.

**Keywords:** Forging Dies, Milling Process, Geometrical Error, Design of Experiment.

## ÖZ

### DÖVME KALIPLARININ CNC FREZE TEZGAHLARINDA ÜRETİMİ İÇİN KESİM YÖNTEMLERİ

Özgen, Arda

Yüksek Lisans, Makina Mühendisliği Bölümü  
Tez Yöneticisi: Prof. Dr. Mustafa İlhan Gökler

Mart 2008, 110 sayfa

Kalıp üretiminde geometrik doğruluk, ölçüsel netlik ve yüzey kalitesi bakımından daha fazla gereksinimlerin yanında, maliyetlerde ve üretim zamanlarında azalma talep edilmektedir. Yüksek geometrik doğruluğu ve yüzey kalitesini elde etmek için uygun kesim parametre değerleri uygulansa bile, tasarlanan ve imal edilen kalıp boşluğunun yüzey profili arasında geometrik farklılıklar bulunabilir. Frezeleme işleminde; kesim hızı, yanal adım ve takım ilerlemesi esas kesim parametreleri olup, dövme kalıplarının geometrik doğruluğunu ve yüzey kalitesini bu parametreler etkiler.

Bu çalışmada, kesim parametrelerinin geometrik hata üzerine etkileri temsili bir kalıp boşluğu profili üzerinde incelenmiştir. Kalıp boşluklarındaki istenmeyen hacmi boşaltmak için mevcut kesim stratejileri araştırılmıştır. Kaba kesim işlemi sırasında, kesici takımın yolu boyunca sabit talaş kaldırma hızını sağlamak için takım ilerleme optimizasyonu yapılmıştır.

Kalıp boşluklarının nihai kesim işleminde; kesim parametrelerinin imal edilen boşluk profilinin geometrik doğruluğu üzerine etkilerinin bulunması amacıyla, deneysel tasarım metodu kullanılmıştır. Geometrik hatanın kesim parametrelerinin değerleri cinsinden hesaplanabilmesi için tahmin formülü çıkarılmıştır. Tahmin formülünün

geçerliliđi, temsili kalıp geometrisi ve endüstride kullanılan bir dövme parçasının kalıp boşluğu geometrisi için doğrulama deneyleri yapılarak test edilmiştir. Tahmin edilen hata değerleri ile ölçülen hata değerleri arasında iyi uyum gözlemlenmiştir.

**Anahtar Kelimeler:** Dövme Kalıpları, Frezeleme İşlemi, Geometrik Hata, Deney Tasarımı.

*To whom, they make this study  
possible with their contributions*

## ACKNOWLEDGEMENTS

I would like to express my deepest gratitude to my supervisor Prof. Dr. Mustafa İlhan Gökler for his guidance, advice, criticism, encouragement and insight throughout the study.

The author was supported by The Scientific and Technological Research Council of Turkey (TÜBİTAK) with National Scholarship Program for MSc Students (Program no: 2210).

I express sincere appreciation to Mechanical Engineering Department of METU for the facilities conducted in the study.

I wish to thank to METU-BİLTİR Research and Application Center, AKSAN Steel Forging Company for the research applications performed during the experimental study.

I also would like to thank to my senior colleagues Kazım Arda Çelik, Mehmet Maşat, Sevgi Saraç, İlker Durukan for their valuable support and assistance.

Special thanks go to my colleagues, Hüseyin Öztürk, Cihat Özcan, Özgür Cavbozar, Ulaş Göçmen, Ali Murat Kayıran, Halit Şahin, Ali Demir and Hüseyin Ali Atmaca for their endless efforts and aids.

I am deeply indebt to my parents, Ayfer and Turgut Özgen for their encouragement and faith in me.

## TABLE OF CONTENTS

ABSTRACT.....	iv
ÖZ .....	vi
ACKNOWLEDGEMENTS .....	ix
TABLE OF CONTENTS.....	x
LIST OF TABLES .....	xiii
LIST OF FIGURES .....	xv
LIST OF SYMBOLS .....	xviii
CHAPTER	
1. INTRODUCTION.....	1
1.1 Forging Process.....	1
1.2 Precision Forging .....	2
1.3 Forging Die Manufacturing .....	5
1.4 CNC Milling vs. EDM Process in Die Manufacturing .....	8
1.5 Importance of Geometric Accuracy and Manufacturing Time in Forging Die Manufacturing .....	9
1.6 Some Previous Studies.....	11
1.7 Scope of the Thesis .....	12
2. GEOMETRIC DIMENSIONING AND TOLERANCING IN FORGING DIES.	14
2.1 Definition of Geometric Dimensioning and Tolerancing .....	14
2.2 Feature Control Frame in GD&T.....	16

2.3	Advantages of GD&T over Coordinate Dimensioning and Tolerancing....	17
2.4	Profile Tolerancing .....	19
2.5	Dimensional Tolerances of Dies .....	23
2.6	Design Considerations of Forging Dies .....	25
2.6.1	Fillet and Corner Radii.....	26
2.6.2	Draft Angle .....	27
2.7	Determination of the Experimental Geometry for the Study .....	28
3.	ROUGH CUT MILLING OF EXPERIMENTAL DIE CAVITIES .....	34
3.1	Importance of Rough Cutting Operations in Forging Die Manufacturing..	34
3.2	Cutting Parameters for Rough Machining .....	35
3.3	Constant Metal Removal Rate in Rough Cut.....	38
3.4	Tool Path Generation for Rough Machining.....	39
3.5	Deficiencies of Spiral Tool Path .....	43
3.6	Rough Cutting Parameters for the Selected Geometry .....	45
3.7	Rough Cut Optimization .....	47
4.	FINISH CUT MILLING OF EXPERIMENTAL DIE CAVITIES .....	52
4.1	Three Level Factorial Design.....	52
4.2	Finish Cut Experiments and Experimental Details .....	53
4.3	Geometrical Measurement .....	60
4.3.1	Measurement Setup.....	60
4.3.2	Scanning Technique on CMM .....	61
4.3.3	Geometrical Error Analysis.....	63
5.	ANALYSIS OF THE EXPERIMENTS AND DERIVATION	
	OF GEOMETRICAL ERROR PREDICTION FORMULA .....	67
5.1	Geometrical Error Analysis of the First Set of Experiments .....	67

5.2	Geometrical Error Analysis of the Second Set of Experiments .....	73
5.3	Geometrical Error Prediction Formula.....	79
5.4	Verification Analysis for the Finish Cut Experiments .....	80
5.5	Case Study.....	82
6.	CONCLUSION .....	86
6.1	Conclusions .....	86
6.2	Recommendations for Future Work.....	89
	REFERENCES.....	90
	APPENDICES	
A.	MAZAK VARIAXIS 630-5X CNC MILLING CENTER .....	94
B.	DIEVAR PREMIUM HOT WORK TOOL STEEL .....	96
B.1	General .....	96
B.2	Hot Work Applications .....	97
B.3	Properties .....	97
C.	PROPERTIES OF THE CUTTING TOOLS .....	99
	USED IN ROUGH AND FINISH CUT MILLING .....	99
C.1	General .....	99
C.2	Cutting Data Recommendations of Dievar Tool Steel for Carbide Tools.....	100
D.	ORIGINAL TOOL PATH VS. OPTIMIZED TOOL PATH.....	101
E.	REGRESSION ANALYSIS OF THE FINISH CUT EXPERIMENTS .....	109

## LIST OF TABLES

### TABLES

Table 1.1 Comparison of EDM process with CNC milling application .....	9
Table 2.1 Tolerance symbols with their descriptions.....	15
Table 2.2 Forging tolerances for length, width, and height .....	25
Table 2.3 Recommendations for minimum fillet and corner radii.....	27
Table 2.4 List of the parts forged by 1000 ton press at Aksan Steel Forging Company .....	29
Table 3.1 Cutting strategies vs. cycle time .....	43
Table 3.2 Rough cutting parameters .....	46
Table 3.3 Cutting coordinates of die cavities wrt reference coordinate.....	51
Table 4.1 Cutting data recommendations for end milling.....	54
Table 4.2 Selected factors and levels for the first set of finish cut experiments.....	58
Table 4.3 Selected factors and levels for the second set of finish cut experiments ...	58
Table 4.4 Design matrix for the experiments.....	59
Table 5.1 Results of the first set of experiments.....	69
Table 5.2 Comparison of geometrical error values with production time values .....	73
Table 5.3 Results of the second set of experiments .....	75
Table 5.4 Comparison of geometrical error values with production time values .....	79
Table 5.5 Results of the verification experiments.....	80
Table 5.6 Comparison of predicted error values with measured error values .....	82

Table 5.7 Cutting strategies vs. cycle time .....	83
Table 5.8 Results of the case study .....	84
Table 5.9 Comparison of predicted error values with measured error values .....	85
Table B.1 General characteristics of Dievar .....	96
Table B.2 Physical properties of Dievar .....	97
Table B.3 Mechanical properties of Dievar .....	98
Table C.1 Cutting data recommendations for end milling.....	100

## LIST OF FIGURES

### FIGURES

Figure 1.1 Precisely forged parts .....	3
Figure 1.2 Precision and conventionally forged components .....	4
Figure 1.3 Flow diagram of the die manufacturing processes of Aksan Steel Forging Company .....	6
Figure 1.4 Lead times in manufacturing of dies .....	7
Figure 2.1 Feature control frame.....	17
Figure 2.2 Traditional plus or minus tolerancing system.....	18
Figure 2.3 Bilateral tolerance on a profile .....	20
Figure 2.4 Unilateral tolerance outside on a profile.....	20
Figure 2.5 Unilateral tolerance inside on a profile.....	21
Figure 2.6 Unequally distributed bilateral tolerance on a profile .....	21
Figure 2.7 All around tolerance symbol.....	22
Figure 2.8 Between tolerance symbol.....	22
Figure 2.9 All over tolerance symbol.....	23
Figure 2.10 Corner radii and fillet radii in forging dies.....	26
Figure 2.11 Types of draft angles in forging dies .....	28
Figure 2.12 Entities of the designed profile .....	30
Figure 2.13 Profile used in the experiments .....	31
Figure 2.14 Experimental die cavity geometry .....	32

Figure 2.15 Profile tolerance of the experimental cavity.....	33
Figure 3.1 Up and down milling .....	37
Figure 3.2 Parameters of metal removal rate .....	39
Figure 3.3 NC programming [10] .....	40
Figure 3.4 Pro/Engineer Wildfire 3 cutting strategy library .....	41
Figure 3.5 Type spiral tool path.....	42
Figure 3.6 First deficiency of spiral tool path.....	44
Figure 3.7 Second deficiency of spiral tool path.....	45
Figure 3.8 Sample of optimized code .....	48
Figure 3.9 Geometrical distribution of the die cavities with experiment numbers....	50
Figure 3.10 Datum surfaces for reference coordinate.....	50
Figure 4.1 Treatment combinations in 3 <sup>2</sup> design .....	52
Figure 4.2 Scallop formations during ball nose finishing .....	55
Figure 4.3 Tool path with 0.10 mm step over.....	56
Figure 4.4 Tool path with 0.20 mm step over.....	56
Figure 4.5 Tool path with 0.30 mm step over.....	57
Figure 4.6 CMM used in the study .....	60
Figure 4.7 Scanning technique on CMM .....	62
Figure 4.8 Scanning directions.....	63
Figure 4.9 Geometrical error analysis process.....	64
Figure 4.10 Geometrical error measurement .....	65
Figure 5.1 Design matrix for the first set of experiments .....	67
Figure 5.2 Photograph of the first set of experiments.....	68
Figure 5.3 Main effect plot of the first input parameter.....	70
Figure 5.4 Main effect plot of the second input parameter .....	70

Figure 5.5 Interaction effect plot of the input parameters.....	71
Figure 5.6 Surface plot of the response variable geometrical error .....	72
Figure 5.7 Design matrix for the second set of experiments .....	73
Figure 5.8 Photograph of the second set of experiments .....	74
Figure 5.9 Main effect plot of the first input parameter.....	76
Figure 5.10 Main effect plot of the second input parameter .....	76
Figure 5.11 Interaction effect plot of the input parameters.....	77
Figure 5.12 Surface plot of the response variable geometrical error .....	78
Figure 5.13 Photograph of the verification experiments.....	81
Figure 5.14 Die and forging part geometries for the case study .....	83
Figure 5.15 Photograph of the case study .....	84
Figure A.1 Mazak Variaxis 630-5x milling center .....	94
Figure C.1 Dimensional properties of the rough cutter.....	99
Figure C.2 Dimensional properties of the finish cutter.....	100

## LIST OF SYMBOLS

### SYMBOLS

$a_p$	: Axial depth of cut
$a_e$	: Radial depth of cut (i.e. Step over)
$V_f$	: Feed rate
$V_f'$	: Optimized feed rate
$V_c$	: Cutting speed
$f_t$	: Feed per tooth
$n_t$	: Number of cutting edges
$N$	: Spindle speed
$D$	: Tool diameter
$R$	: Tool radius
$Z_w$	: Metal removal rate
$S_h$	: Scallop height
$k$	: Number of factors
$\beta$	: Coefficients of linear regression model
$Z$	: Real geometrical error
$Z'$	: Predicted geometrical error
$A_p$	: Effective flute length
$L$	: Tool length
$H$	: Flute length

## **CHAPTER 1**

### **INTRODUCTION**

#### **1.1 Forging Process**

Forging is a metal forming process in which a piece of metal is shaped to the desired form by plastic deformation. The process usually includes sequential deformation steps to the final shape. In forging process, compressive force may be provided by means of manual or power hammers, mechanical, hydraulic or special forging presses. The process is normally but not always, performed hot by preheating the metal to a desired temperature before it is worked.

Compared to all manufacturing processes, forging technology has a special place because it helps to produce parts of superior mechanical properties with minimum waste of material. Forging process gives the opportunity to produce complex parts with desired directional strength, refining the grain structure and developing the optimum grain flow, which imparts desirable directional properties. Forging products are free from undesirable internal voids and have the maximum strength in the vital directions as well as a maximum strength to weight ratio [1].

Forging process can be classified into three groups as:

1. According to the forging temperature
  - Cold forging
  - Warm forging

- Hot forging
2. According to type of machine used
    - Mechanical presses
    - Hydraulic presses
    - Hammers
    - Screw presses
  3. According to the type of die set
    - Open die forging
    - Closed die forging

Descriptions, advantages and disadvantages of these can be found in several literatures [1].

## **1.2 Precision Forging**

Precision forging is a kind of closed die forging and normally means “close to final form” or “close tolerance” forging. It is not a special technology, but a refinement of existing techniques to a point where the forged part can be used with little or no subsequent machining. Some examples of precisely forged parts are given in Figure 1.1.

In precision forging process, improvements cover not only the forging method itself but also preheating, lubrication, and temperature control practices. Major advantages of precision forging can be summarized as:

- Reduction in material waste
- More uniform fiber orientation providing superior strength values

- Elimination of further operations i.e. machining, inducing less labor, material and production cost
- High efficiency due to the reduction in number of production processes



**Figure 1.1 Precisely forged parts [2]**

The decision to apply precision forging techniques depends on the relative economics of additional operations and tooling vs. elimination of machining. Because of higher tooling and development costs, precision forging is usually limited to high quality applications [3].

As the process name suggests, precision forging dies require better geometrical accuracy when compared with conventional forging processes. End products of precision forging are net-shape or near net-shape. Therefore, more attention should be paid to the manufacturing steps of precision die manufacturing.

The products of net-shape precision forging are used directly without any machining operations. A comparison can be made between a precision forged component and a conventionally forged component which are shown in Figure 1.2 to realize the quality of the end products.

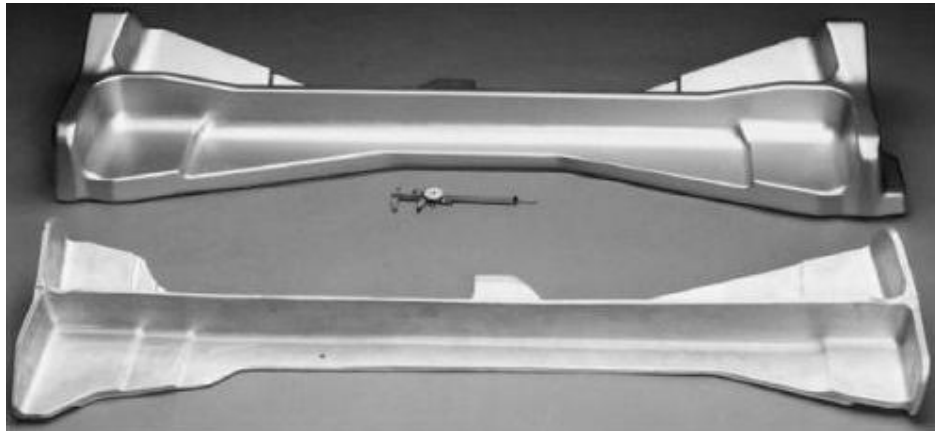


**Figure 1.2 Precision and conventionally forged components [3]**

In close die forging process, die surface characteristics are directly reflected on the forged component. Thus, the geometrical accuracy of the forging die influences the geometrical accuracy of the produced part. Geometrical inaccuracy, poor surface finish can be partially and/or fully eliminated by proper strategies in precision die manufacturing stages. For this reason, cutting parameters of the precision die production must be carefully determined to satisfy desired geometrical accuracy without excessive increase in cutting time.

Die manufacturers aim to obtain high geometrical accuracy and surface quality in die cavities by utilizing proper cutting strategies and parameters; however, there may exist geometrical discrepancy between surface profile of the designed and the manufactured die cavity. The effects of the cutting parameters on geometrical accuracy of a specific cavity profile can be analyzed to minimize this geometrical discrepancy.

### **1.3 Forging Die Manufacturing**

Forging die manufacturing requires various affiliated operations that should be separately considered. It would be beneficial to examine real applications of forging die manufacturing to acquire comprehensive information about processes. Thus, Aksan Steel Forging Company in Ankara is chosen as the reference company to investigate current practices in forging die manufacturing [4].

Die manufacturing process in Aksan Steel Forging Company commences with the analysis of forging part geometry. According to the geometrical features of the forging component, geometry of forging die cavity and copper electrode are determined. After examination of the forging part geometry, 3D solid models are prepared for both copper electrode and forging die. Then, these 3D models are transformed into a Computer Aided Manufacturing (CAM) system. Cutting parameters for the removal of unwanted volume are defined and tool paths are generated according to the selected volume removal strategy. These tool paths are converted into numerical codes by specific postprocessors relating to the CNC machine tool to be used. Die cavity and copper electrode are machined according to the generated NC codes. After rough machining of the die cavity, die is exposed to a proper heat treatment operation in accordance with the properties of the tool steel. Then finishing process is performed to remove excessive parts in the die cavity by the prepared copper electrode for electrical discharge machining (EDM). Finally, any defects on the surface are removed by manual polishing. Stepwise representation of die manufacturing processes in Aksan Steel Forging Company is given in Figure 1.3.

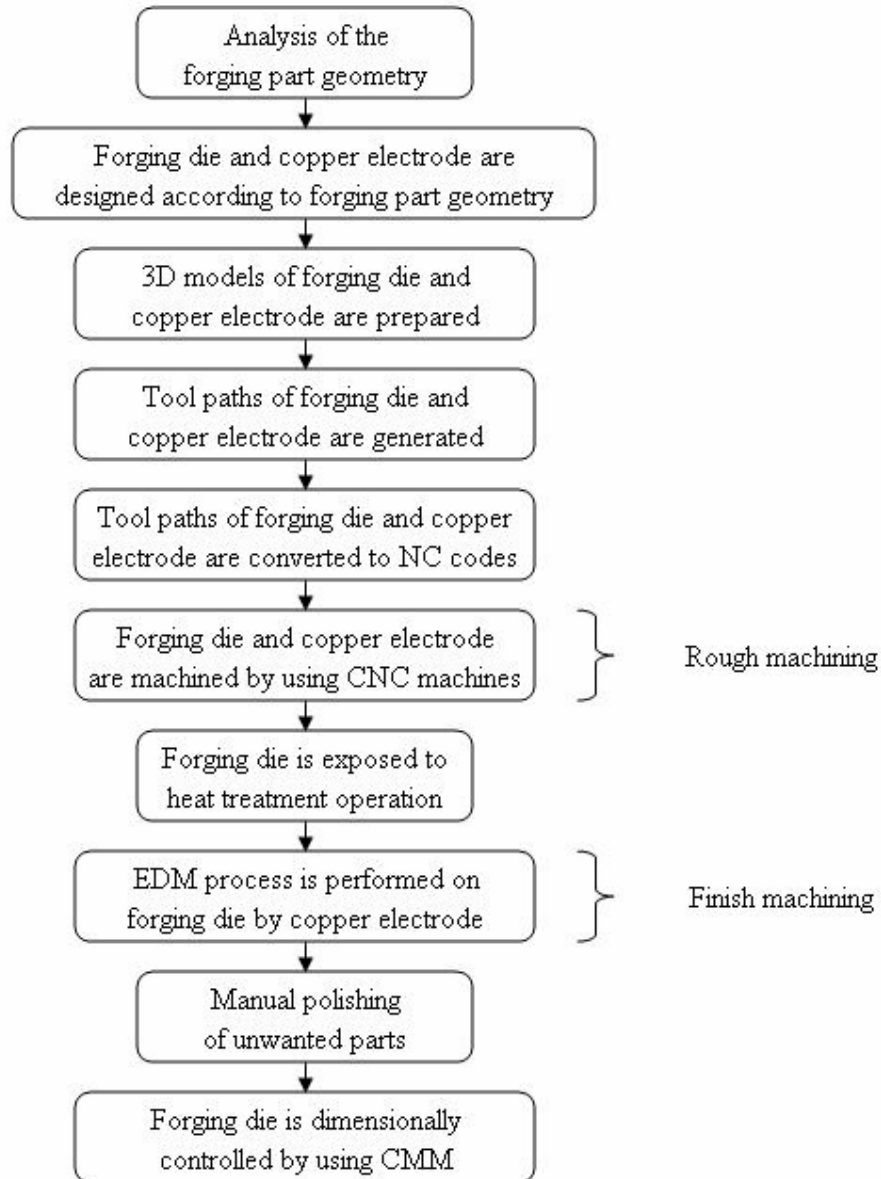


**Figure 1.3 Flow diagram of the die manufacturing processes of Aksan Steel Forging Company**

Application of EDM process necessitates manual polishing in the die cavities since micro cracks and nano cracks are formed at the surface layer which is produced by

the copper electrode. The formation of these cracks is exactly related with EDM in which electrically conductive material is removed by means of rapid and repetitive spark discharges resulting from local explosion of a dielectric liquid. These spark discharges are produced by applying a voltage between copper electrode and workpiece [5]. EDM process forms a layer as a result of the solidification of a melted zone. As a consequence of the rapid quenching process, micro cracks and nano cracks are formed at the surface of the layer [6]. As the hardness is higher in this layer, this layer becomes more brittle and the micro cracks may lead to crack propagation during forging process on die surfaces. As a result of these, polishing should be applied on die surfaces to remove this hardened layer after EDM process.

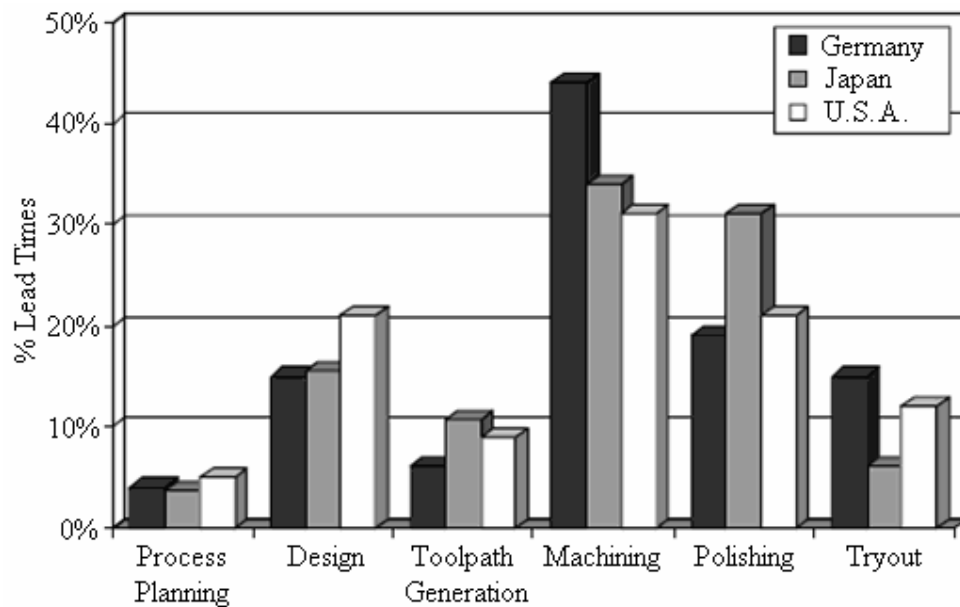


**Figure 1.4 Lead times in manufacturing of dies [7]**

It can be concluded from Figure 1.4 that, polishing time constitutes 20-30% of total manufacturing time of forging die production. It is obvious that reduction in any of

the steps of die manufacturing process, will improve efficiency of the whole operation in cost wise and time wise. For this reason, cutting strategies should be developed and numerical codes should be optimized in such a way that no additional application is required in the die cavity after CNC machining operation. At that point it should always be taken into account that a compromise must be achieved between machining times and final surface finish of the die cavity. As a consequence of this compromise, surface finish can be greatly improved, reducing and/or eliminating manual polishing, that may account for up to 20-30% of the total time spent in the die manufacturing process.

#### **1.4 CNC Milling vs. EDM Process in Die Manufacturing**

Nowadays CNC milling technology is a basic constituent part of every modern tool making company. According to the objective model for cavity manufacturing technology, where milling tool, die and product related parameters are considered, CNC milling technology is prevalently replacing classical die sinking EDM applications. As a consequence of these, for each die cavity, it has to be ascertain, which technology CNC milling plus EDM finishing or CNC milling alone is the most advantageous. In Table 1.1, advantages, disadvantages as well as limits of the EDM and CNC milling are presented.

For the selection of the most appropriate die cavity manufacturing technology, energy consumption and ecology are of a great importance too. It is well known that the EDM process has a very high level of energy consumption. Therefore, it should be used only in cases where, regarding product, milling tool shape or die related properties does not allow the CNC milling applications.

From ecology point of view CNC milling technology is prevailing EDM for the following reasons:

- Technology using less energy is much friendlier to the environment.
- Permanent decrease of cutting lubricants and coolants leads to dry machining.

- There must be constant monitoring of EDM electrolyte during the process as later on for waste treatment and disposal [8].

**Table 1.1 Comparison of EDM process with CNC milling application [8]**

Criterion	EDM	CNC Milling
Materials	All conductive materials	All cutting materials (steel up to 62 HRC)
Geometry	Free	Limited depth, radius
Sharped inner angles	Radius <0.1 mm reachable	Radius at the bottom >0.3 mm, radius at the wall >0.1 mm
Deep grooves	Depend on manufactured electrode	Up to $L/D < 10$ (L: Length of cutter, D: Diameter of cutter)
Polished surface	Always additional finish machining	Without additional finish machining
Cost of additional finish machining	High	Low
Geometric accuracy	Good	Better than EDM
Machining tool	Expensive (milled)	Simple, standard product

### **1.5 Importance of Geometric Accuracy and Manufacturing Time in Forging Die Manufacturing**

With the evolving demands on shape complexity and accuracy of the forged components, the dies play more critical role to minimize production costs with an acceptable surface quality. Forging die applications are increasing consistently since the requirements of leading industries dealing with forging industry; automotive, aerospace and agricultural industry, are minding the benefits of forged parts more and more. Forged products are found extensively in almost all industrial applications

requiring strength, reliability, toughness and quality. Forged components are economically attractive because of their inherent superior reliability, improved tolerance capability, and higher efficiency with which forging products can be machined and further processed by automated methods.

Nowadays, manufacturing of dies is more and more competitive, presenting greater requirements of dimensional precision and surface roughness as well as a decrease in costs and manufacturing times [9]. In order to achieve desired surface quality on forged components and to manufacture forging dies in tight tolerances without increasing production time significantly, cutting conditions and parameters must be determined diligently.

The current trend of die manufacturing is determination of cutting conditions to obtain the closest dimensional and geometrical accuracy resulted in minimization of further operations which is mostly manual polishing. However, variety in the geometry of produced components makes it difficult for die manufacturers to select the optimum operational conditions in a repetitive and reliable way. Great number of factors, which is necessary to take into account, makes it really difficult to select the optimum operational conditions properly. These factors can be summarized as, geometric specifications of the part, geometry of the part before being machined, material of the part, position of the part in the machine tool, fixture system of the part, method of machining, type of the tool holder, type of the cutting tool, cutting parameters (i.e. axial depth of cut, radial depth of cut, feed rate and spindle speed), cutting fluid and capability of CAM system [9]. Among these factors, only cutting parameters are fully numerically controlled and adjustable. Therefore, these parameters have substantial contribution to lessen the manufacturing times when compared with the effects of other factors. In order to minimize the cutting time of the manufacturing processes and obtain geometrical accuracy in accordance with product specifications, the most suitable manufacturing conditions for each operation must be carefully selected. While, only the cutting parameters (i.e. depth of cut, feed rate, cutting speed) are generally taken into account, each element involved in the machining process has a considerable influence on the final result of that process.

One can see that it is necessary to have a deeper knowledge about the optimum operation conditions, which will permit to assure a desired dimensional precision with an acceptable production time.

## **1.6 Some Previous Studies**

Various factors of CNC milling technology influence the quality of the final part and its manufacturing economy. Tool materials, type of the tool holder and control system of the machine tool, cutting parameters (depth of cut, feed and cutting speed) and axial capability of the machine tool are the key factors directly affecting the geometrical accuracy of the produced part. Among these factors, only cutting parameters are suitable for any kind of modifications without altering the current installation. Additional investments to increase performance of the machine tool (tool and axial capability wise) are generally less favorable by the manufacturers. Therefore, many research activities have been performed either to optimize current process or develop new approaches to maximize the process efficiency.

Individually analyzing the effects of each of these factors on the final result has generated much interest. Various research studies have been recently conducted in which one of the previously mentioned factors has been correlated with die surface quality. J. Vivancos et al [3], L.N. Lopez de Lacalle et al [11] have worked on steel machining and R.T. Coelho et al [12] dealt with aluminum alloys machining. However, only few researchers have analyzed the relationship between these factors and geometrical accuracy. Similarly, the influence of these factors on production time has been analyzed in very few cases.

Another key objective of the recent researches is the optimization of cutting parameters in high speed machining, and in this field a great variety of work can be found. A. Kaldos et al [13] based on optimization for aluminum alloys machining and W.T. Chien et al [14], H. Juan et al [15] and L.N. Lopez de Lacalle et al [16] studied optimization of cutting parameters for steel machining.

Many researchers have also worked on the optimization of feed rate and tool path strategy to achieve improvements on production time. R. Salami et al [17] dealt

with feed rate optimization for 3-axis ball-end milling of sculptured surfaces and Jenq Shyong By Chen et al [18] studied feed rate optimization and tool profile modification for the high efficiency ball-end milling process. Manuel Monreal and Ciro A. Rodriguez [19] focused on influence of tool path strategy on the cycle time of CNC milling operations.

To enhance die manufacturing capabilities of METU-BİLTİR Research and Application Center, a post processor with a simulation program for Mazak Variaxis 630-5x [20] and a methodology for prediction of surface roughness on curved cavities [21] have been developed so far by the members of the center.

### **1.7 Scope of the Thesis**

Recent requirements of die and mould manufacturing can be summarized as: maintaining geometrically accurate and high quality die surfaces as well as reduction in production time. In order to decrease production time of die manufacturing processes and achieve geometrical accuracy in accordance with product specifications, optimum cutting parameters for rough cutting and finish cutting operations must be accurately selected. By selecting a fixed feed rate based upon the maximum force, tool is saved but very often it results in extra machining time in rough cutting operations, which reduces productivity. By optimizing the feed rate, both objectives of saving the tool and also reducing machining time thereby increase in productivity can be achieved.

For the finish cutting operations, attaining geometrically accurate products with acceptable surface quality in a reasonable production time is the common objective of today's die manufacturers. Therefore, experimental analysis dealing with the effects of the cutting parameters on geometrical error and production time would be beneficial for the determination of these parameters. The main objective of this particular study is to find out geometrical discrepancy between CAD model of a die cavity and a manufactured die cavity by utilizing various cutting parameter values for the finish cut operation of precision forging dies.

In Chapter 1, brief information about forging die manufacturing and significance of geometrical accuracy in die manufacturing have been presented. Details of geometrical dimensioning and tolerancing will be examined and geometrical requirements of precision forging dies will be clarified in Chapter 2. According to these specifications, an experimental die cavity geometry covering major surface variations of forging dies will be defined for the experimental study.

In Chapter 3, optimum cutting strategy for rough machining of the defined experimental die cavity geometry will be investigated and feed rate optimization will be performed on the generated tool path. Details of the experimental analysis for finish cutting operation and geometrical error analysis for the manufactured die cavity will be explained in Chapter 4.

Effects of the cutting parameters on the geometrical error of the surface profile and the production time will be handled in Chapter 5. Prediction formula to estimate geometrical error in terms of the values of the cutting parameters will also be derived in this chapter. Verification experiments for the representative die cavity geometry and cavity geometry of a forging part used in industry will be performed to check the validity of the acquired formula.

Finally, conclusion and recommendations for future work will be presented in Chapter 6.

## **CHAPTER 2**

### **GEOMETRIC DIMENSIONING AND TOLERANCING IN FORGING DIES**

In this chapter, brief information about geometric dimensioning and tolerancing has been presented to provide background knowledge for the current study. The design considerations for forging die cavities have been given to relate geometric dimensioning and tolerancing with forging die cavity design. Finally, an experimental cavity profile which is required for the studies conducted in the following chapters has been determined.

#### **2.1 Definition of Geometric Dimensioning and Tolerancing**

Geometric dimensioning and tolerancing (GD&T) is a symbolic language. It is used to define the nominal geometry of parts and assemblies, to define the allowable variation in form and possibly size of individual features, and to define the allowable variation between features [22]. The features toleranced with GD&T reflect the actual relationship between mating parts. Drawings with properly applied geometric tolerancing provide the best opportunity for uniform interpretation and cost effective assembly [23].

GD&T is a design tool. Before designers can properly apply geometric tolerancing, they must carefully consider the fit and function of each feature of every part. GD&T, in effect, serves as a checklist to remind the designers to consider all aspects of each feature. Properly applied geometric tolerancing insures that every part will assemble every time. Geometric tolerancing allows the designers to specify the maximum available tolerance and consequently, design the most economical parts [23].

GD&T scheme identifies all applicable datums, which are reference surfaces, and the features being controlled to these datums. A properly toleranced drawing is not only a picture that communicates the size and shape of the part, but it also tells a story that explains the tolerance relationships between features [23].

Extensively used geometric tolerances with symbol identifiers are given in Table 2.1.

**Table 2.1 Tolerance symbols with their descriptions [22]**

Symbol	Description	Geometry
	ANGULARITY	ORIENTATION
	CONCENTRICITY	LOCATION
	CYLINDRICITY	FORM
	FLATNESS	FORM
	PARALLELISM	ORIENTATION
	PERPENDICULARITY	ORIENTATION
	POSITION	LOCATION
	PROFILE	PROFILE
	PROFILE OF A LINE	PROFILE
	CIRCULARITY	FORM
	STRAIGHTNESS	FORM
	SYMMETRY	LOCATION
	RUNOUT	RUNOUT
	TOTAL RUNOUT	RUNOUT

Geometric tolerances specify the maximum variation that is allowed in form or position from true geometry. The geometric tolerance is, in essence, width or diameter of tolerance zone within which a surface or axis of hole or cylinder can lie which results in resulting feature being acceptable for proper function and interchangeability [24].

If a tolerance of form is not specified on a drawing for a feature, then the feature will be accepted as regardless of form variation [24].

The tolerance zone for geometric dimensioning can be one of the following:

- The area within a circle
- The area between two circles
- The area between two equidistant lines or between two parallel straight lines
- The space within a cylinder
- The space between two coaxial cylinders
- The space between two equidistant surfaces or two parallel planes [24]

## **2.2 Feature Control Frame in GD&T**

The feature control frame in the GD&T language is like a sentence in any language. All of the geometric tolerancing for a feature, or pattern of features, is contained in one or more feature control frames [23].

One of the fourteen geometric characteristic symbols always appears in the first compartment of the feature control frame. The second compartment is the tolerance selection. In this compartment, tolerance can be followed by any appropriate modifiers. Figure 2.1 shows a feature control frame with the maximum material condition (MMC) modifier (i.e. circle M). The tolerance is preceded by a diameter symbol if the tolerance zone is cylindrical. If the tolerance zone is not cylindrical, then nothing precedes the tolerance. The final section is reserved for datums and any

appropriate material condition modifiers. If the datum is a size feature, then a material condition applies; if no material condition modifier is specified, then regardless of feature size (RFS) automatically applies. Datums are arranged in the order of importance. The first datum to appear in the feature control frame, the primary datum, is the most important datum. The second datum, the secondary datum, is the next most important datum, and the tertiary datum is the least important. Datums do not have to be specified in alphabetical order [23].

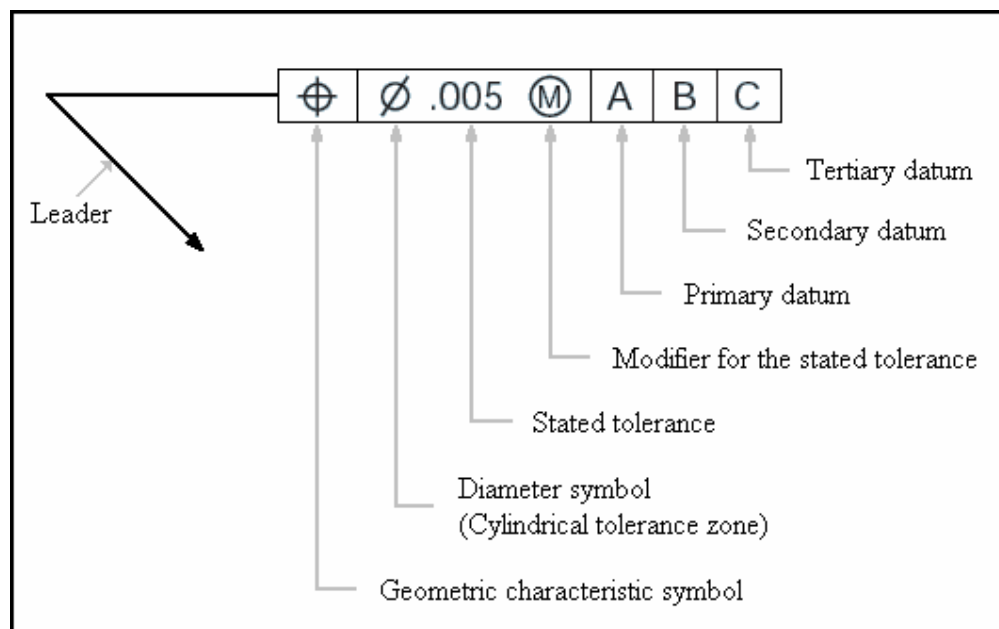


**Figure 2.1 Feature control frame [23]**

### **2.3 Advantages of GD&T over Coordinate Dimensioning and Tolerancing**

Since the middle of the nineteenth century, industry has been using the plus or minus tolerancing system for tolerancing drawings. The system has several limitations [23]. The plus or minus tolerancing system generates rectangular tolerance zones. A

tolerance zone, such as the example in Figure 2.2, is a boundary within which the axis of a feature that is in tolerance must lie. Rectangular tolerance zones do not have a uniform distance from the center to the outer edge. In Figure 2.2 from left to right and top to bottom, the tolerance is  $\pm 0.005$ ; across the diagonals, the tolerance is  $\pm 0.007$ . Therefore, when designers tolerance features with  $\pm 0.005$  tolerance, they must tolerance the mating parts to accept  $\pm 0.007$  tolerance, which exists across the diagonals of the tolerance zones.

Size features can only be specified at the regardless of feature size condition. Regardless of feature size means that the location tolerance remains the same no matter what size the feature happens to be within its size tolerance. If a hole, like the one in Figure 2.2, increases in size, it has more location tolerance, but there is no way to specify that additional tolerances with the plus or minus tolerancing system.

Datums are usually not specified where the plus or minus tolerancing system is used. Consequently, inspectors do not know which datums apply or in what order they apply.

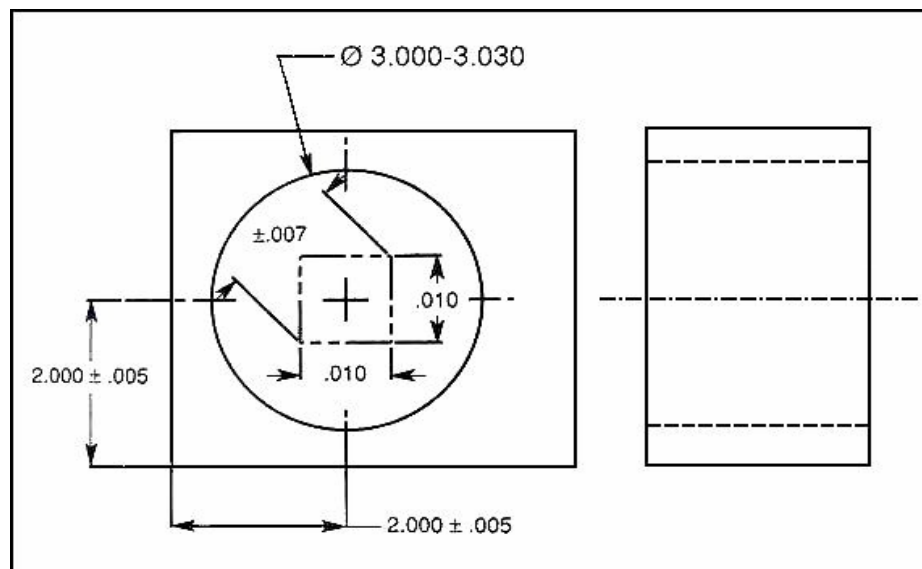


**Figure 2.2 Traditional plus or minus tolerancing system [23]**

## 2.4 Profile Tolerancing

A profile is the outline of an object. Specifically, the profile of a line is the outline of an object in a plane as the plane passes through the object. The profile of a surface is the result of projecting the profile of an object on a plane or taking cross sections through the object at various intervals.

Profile tolerancing is a powerful and versatile tolerancing tool which can be used to control just the size and shape of a feature or the size, shape, orientation, and location of an irregular shaped feature. The profile tolerance controls the orientation and location of features with unusual shapes.

Since acquiring desired geometrical accuracy and surface quality is quite important on the surface profile of die cavities, profile tolerancing is frequently utilized in the specifications of the die cavities.

A profile view or section view of a part is dimensioned with basic dimensions. A true profile may be dimensioned with basic size dimensions, basic coordinate dimensions, basic radii, basic angular dimensions, formulae. The feature control frame is always directed to the profile surface with a leader. Profile is a surface control; the association of a profile tolerance with an extension or a dimension line is inappropriate. The profile feature control frame contains the profile of a line or of a surface symbol and a tolerance. Since profile controls are surface controls, cylindrical tolerance zones and material conditions do not apply in the tolerance section of profile feature control frames. The shape of the tolerance is the shape of the profile not a cylinder, and material condition modifiers do not apply to surface controls.

When the leader from a profile tolerance points directly to the profile, the tolerance specified in the feature control frame is equally disposed about the true profile. In Figure 2.3, the 0.020 tolerance in the feature control frame is evenly divided, 0.010 outside and 0.010 inside true profile [23].

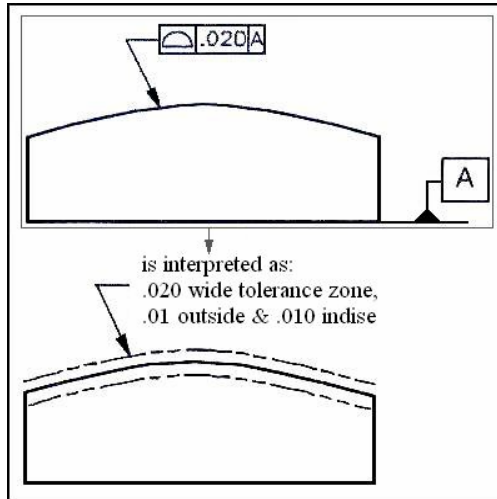


**Figure 2.3 Bilateral tolerance on a profile [23]**

If the leader from a profile tolerance points directly to a segment of a phantom line extending, outside or inside, parallel to the true profile, as shown in Figure 2.4-2.5, all the tolerance is outside or inside the true profile [23].

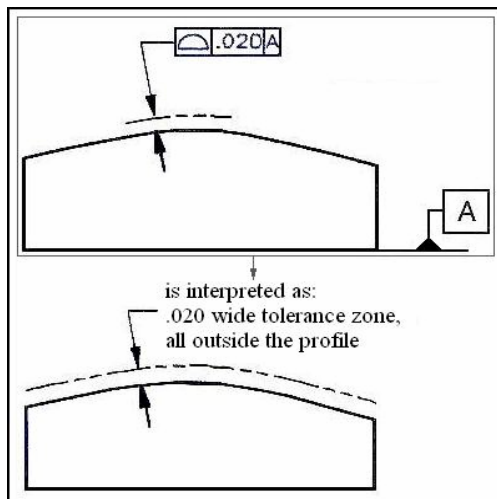


**Figure 2.4 Unilateral tolerance outside on a profile [23]**

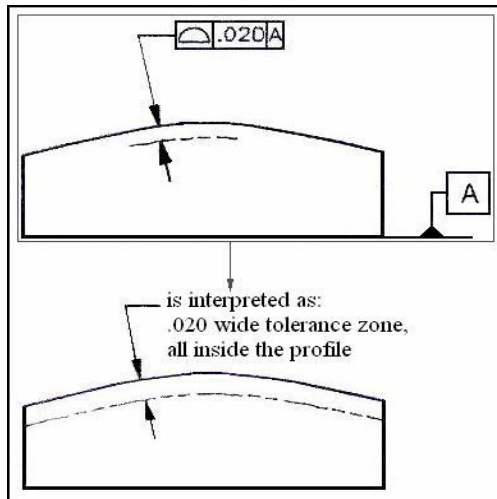


**Figure 2.5 Unilateral tolerance inside on a profile [23]**

The tolerance may even be specified as an unequal bilateral tolerance by drawing segments of phantom lines inside and outside parallel to the profile and specifying the outside tolerance with a basic dimension as shown in Figure 2.6 [23].

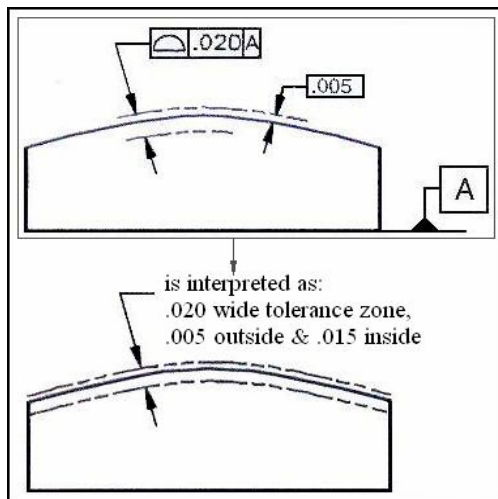


**Figure 2.6 Unequally distributed bilateral tolerance on a profile [23]**

Where a profile tolerance applies all around of a pointed feature, the “all around” symbol is specified, as shown in Figure 2.7. The “all around” symbol is indicated by a circle around the joint in the leader from the feature control frame to the profile.

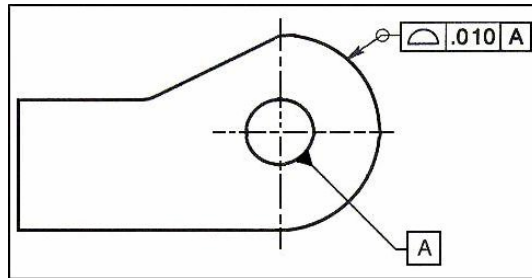


**Figure 2.7 All around tolerance symbol [23]**

If the profile is to extend between two points, as shown in Figure 2.8, the points are labeled, and a note using the “between” symbol is placed beneath the feature control frame. The profile tolerance applies to the portion of the profile between points X and Z where the leader is pointing.

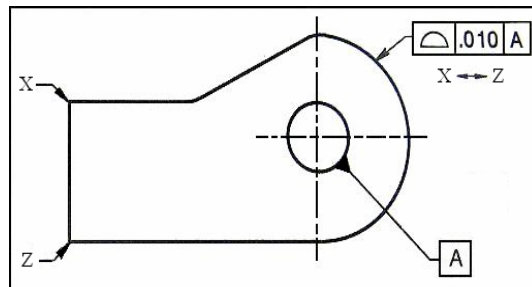


**Figure 2.8 Between tolerance symbol [23]**

If a part, such as a casting or forging, is to be controlled with a profile tolerance over its entire surface, the note “all over” is placed beneath the feature control frame, as shown in Figure 2.9. When an unusual profile tolerancing requirement occurs, one not covered by the notes and the symbols above, a local note clearly stating extent and application of the profile tolerance must be included [23].

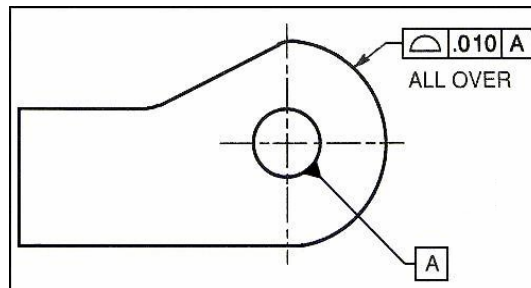


**Figure 2.9 All over tolerance symbol [23]**

## **2.5 Dimensional Tolerances of Dies**

The tolerances of conventional and precision forging dies are related to various kinds of dimension. When the categories of tolerances appearing on forging and precision dies are examined, they can be classified into four groups [25]:

1. First group of tolerances
  - Length, width, height
  - Mismatch
  - Residual flash
  - Pierced hole

2. Second group of tolerances
  - Thickness
  - Ejector marks
3. Third group of tolerances
  - Straightness and thickness
  - Center to center dimensions
4. Other categories of tolerance
  - Fillet and edge radii
  - Burr
  - Surface
  - Draft angle surfaces
  - Eccentricity for deep holes
  - Deformation of sheared ends
  - Deviation of form specified contour

The German standard for forging tolerances, DIN 7526 [25] gives comprehensive tolerance values for both normal and precision forgings. It is a well conceived standard that takes into account the weight of a forging, its complexity, and the difficulty of the material being forged. Table 2.2 illustrates the tolerances values from that standard for both simple and complex forgings. The tolerances in this table apply to dimensions of length, width, and height including diameters on one side of the parting line. All variations, including those due to die wear, die sinking, and shrinkage, are included in these tolerances [25].

**Table 2.2 Forging tolerances for length, width, and height [25]**

Forging weight (kg)	Dimension (mm)		
	30 - 100	100 - 160	160 - 250
<i>Standard tolerances for simple forgings</i>			
1.0 - 1.8	+1.07/-0.53	+1.20/-0.58	+1.37/-0.66
1.8 - 3.2	+1.20/-0.58	+1.37/-0.66	+1.52/-0.76
3.2 - 5.4	+1.37/-0.66	+1.52/-0.76	+1.70/-0.85
<i>Standard tolerances for complex forgings</i>			
1.0 - 1.8	+1.37/-0.66	+1.52/-0.76	+1.70/-0.85
1.8 - 3.2	+1.52/-0.76	+1.70/-0.85	+1.88/-0.91
3.2 - 5.4	+1.70/-0.85	+1.88/-0.91	+2.03/-1.02
<i>Precision tolerances for simple forgings</i>			
1.0 - 1.8	+0.69/-0.33	+0.76/-0.38	+0.86/-0.43
1.8 - 3.2	+0.76/-0.38	+0.86/-0.43	+0.97/-0.48
3.2 - 5.4	+0.86/-0.43	+0.97/-0.48	+1.07/-0.53
<i>Precision tolerances for complex forgings</i>			
1.0 - 1.8	+0.86/-0.43	+0.97/-0.48	+1.07/-0.53
1.8 - 3.2	+0.97/-0.48	+1.07/-0.53	+1.17/-0.58
3.2 - 5.4	+1.07/-0.53	+1.17/-0.58	+1.30/-0.64

The tolerances for length, diameter, step and thickness cover not only the differences of dimension, but also the deviations from specified contour. Therefore, profile tolerance of surfaces can be analyzed to explore the deviations from the specified contour. These deviations are not to exceed the limits given by the tolerances in Table 2.2. In extreme cases, they can cover the whole field of tolerances unless otherwise agreed between supplier and purchaser.

## **2.6 Design Considerations of Forging Dies**

Since die cavities basically consist of inclined/draft surfaces, corners and radii, a proper consistency between these geometries are always necessary to obtain smooth and continuous surfaces on the produced components. Therefore, values of these geometric entities must be precisely stated in accordance with the desired geometry.

Before determining the profile of the experimental study, design considerations of forging die cavities and current applications in Aksan Steel Forging Company have been investigated in detail.

### 2.6.1 Fillet and Corner Radii

One of the most important factor in the design of forging die cavities is the proper selection of fillet and corner radii. On closed die forgings, corners and fillets are the curved surfaces that unite smoothly the converging or intersecting sides of forged elements, such as ribs, bosses and webs. Corner radius on forging will be fillet radius on the die. This is same for the fillet radius of the part and the corner radius of the die as in illustrated in Figure 2.10.

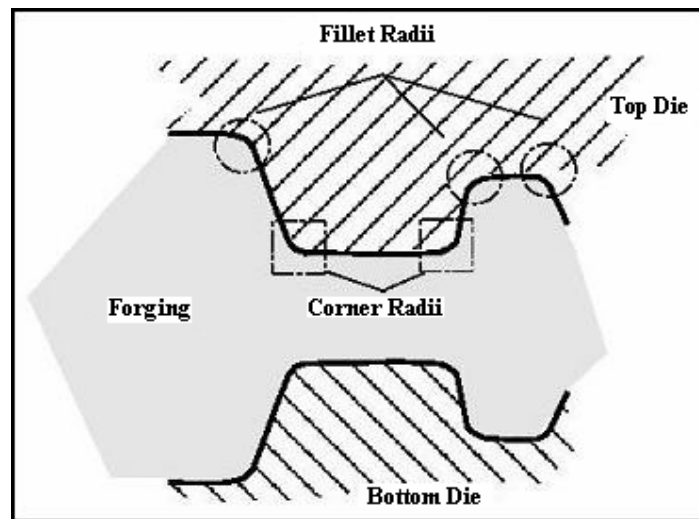


**Figure 2.10 Corner radii and fillet radii in forging dies [26]**

Recommended values of fillet and corner radii in forging die cavities are generally based on dominant features of the forged components. DIN 7523 Standard which is standard for design considerations for forging parts, fillet and corner radii are

determined according to height of the forged part. In Table 2.3 recommended values for minimum fillet and corner radii are presented.

**Table 2.3 Recommendations for minimum fillet and corner radii [27]**

<b>Forged part height (mm)</b>	<b>Fillet radius (mm)</b>	<b>Corner radius (mm)</b>
25	4	2
40	6	3
63	10	4
100	16	6
160	25	8
250	40	10
400	63	16

### **2.6.2 Draft Angle**

Axial projections on forging are usually tapered so that the forged part can be easily removed from the die cavity. This taper is usually called draft. Typical types of drafts existing in forging dies are shown in Figure 2.11. The most common draft angles are between  $5^\circ$  and  $7^\circ$ . For steel forgings, it is common to apply a smaller draft angles on the outside surface than on the inside because the outer surface will shrink away from die during cooling and permit removal of the forging. Forging designs with zero draft angles require dies with special knockouts [28].

It is difficult to apply hard and fast rules for selecting draft angles appropriate to individual forging designs.  $7^\circ$  is the most commonly used draft angle to reduce machining requirements.  $0^\circ$  and  $1^\circ$  draft angles are used on aluminum and magnesium forgings of extrusion types. Back extruded cylinders and shafts are frequently designed with  $1^\circ$  draft.  $3^\circ$  to  $5^\circ$  degree draft angle is suitable for most forgings of carbon, low-alloy and stainless steels, and for some of the nickel base

alloys.  $5^\circ$  draft angle is generally considered the minimum for titanium alloys because shallower drafts often lead to sizing problems.  $7^\circ$  or greater draft angle is generally required for forging of alloys requiring extreme pressures such as refractory metals, the nickel-based super alloys, and the hot-cold worked austenitic stainless steels [28].

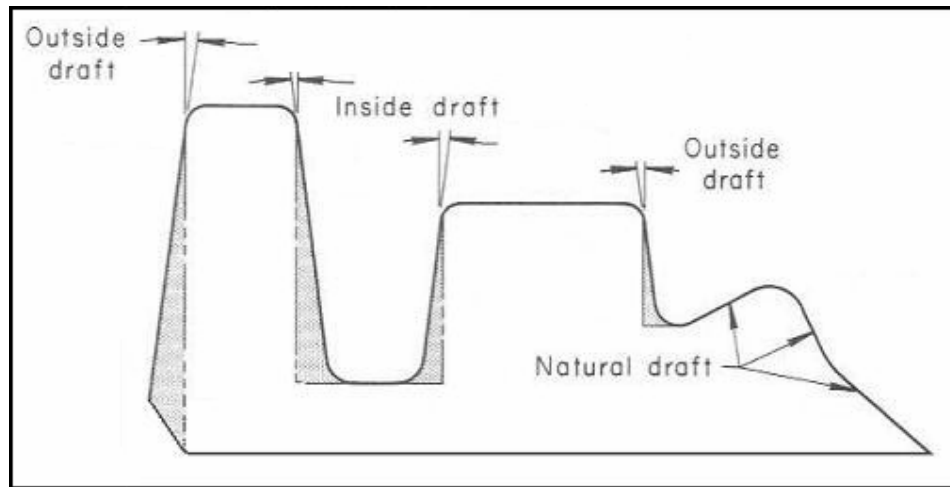


**Figure 2.11 Types of draft angles in forging dies**

## **2.7 Determination of the Experimental Geometry for the Study**

For the selection of the experimental die cavity geometry, it is aimed to form continuous surfaces combining various features of the forging die cavities. To determine the experimental die cavity geometry, many die cavities which are in use at Aksan Steel Forging Company are examined. When the solid models of the manufactured products are analyzed, it is observed that in the range of 0.12 to 2.41 kg products which 1000 ton press is capable of forging, value of the minimum corner radius and fillet radius is 2 mm and draft angles are varying in between  $3^\circ$  to  $7^\circ$ . Dimensional specifications of the products formed at Aksan Steel Forging Company

are presented in Table 2.4. In the table the minimum and the maximum values of the curved surfaces are also tabulated to visualize the dimensional range of these surfaces.

**Table 2.4 List of the parts forged by 1000 ton press  
at Aksan Steel Forging Company**

<b>Part No</b>	<b>Height (mm)</b>	<b>Width (mm)</b>	<b>Length (mm)</b>	<b>Net Weight (kg)</b>	<b>Radii (mm)</b>
020/10898F	18	60	124	0.83	R3-R5
8327945	26	40	40	0.13	R2
121-510-47626-4/1	14	30	70	0.12	R2-R5
132216/5089406V	48	123	146	0.61	R2-R8
RK50.02/6	58	166	39	0.55	R2-R9
182535/5117150V	24	44	83	0.33	R5-R16
129028/593675VA	103	65	124	0.54	R2-R10
560.0106DV	12	190	31	0.60	R4
182512/5154559V	28	38	132	0.38	R3-R20
3948-S-A DV	36	28	138	0.57	R3-R4
132215/567871V	38	84	167	0.51	R2-R15
182512/5126220V	40	28	117	0.37	R3-R20
DN32 D20 12854DV	32	65	63	0.72	R2-R15
129004/598293V	46	26	118	0.40	R2-R30
DN25 D20 12853DV	30	56	55	0.53	R2-R15
DN15 D10 11754DV	24	40	38	0.20	R2-R15
RK50.02/6	12	43	95	0.16	R2.5-R3
198-018.3	28	76	153	0.49	R2-R20
255153DV	30	90	95	0.72	R4-R15
DN40 D20 12841DV	34	70	68	0.91	R2-R15
255053DV	24	40	60	0.19	R3-R12
198-290.2	28	74	105	0.39	R4-R20
G36639	38	127	127	2.41	R5
PN320	58	84	64	1.13	R2-R8
158048/5085258V	79	86	86	1.38	R2-R5

According to the observations made in the company, it can be concluded that the experimental profile must involve three types of surfaces to represent forging die cavities. These surfaces are:

- Horizontal surfaces
- Surfaces of transitions (fillets and corner radii greater than 2 mm radius)
- Nearly vertical surfaces (draft surfaces with draft angles between  $3^\circ$  to  $7^\circ$ )

By keeping the considerations above in mind, a profile is designed to analyze the geometrical error between the CAD profile and the manufactured profile. The entities of the designed profile can be analyzed in Figure 2.12.

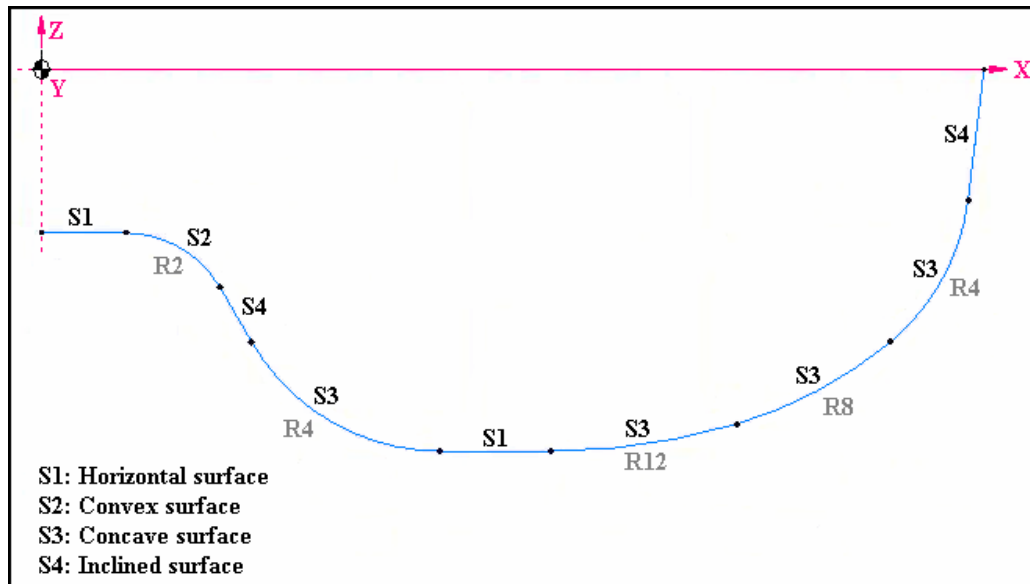


**Figure 2.12 Entities of the designed profile**

The dimensional values of the determined profile are given in Figure 2.13.

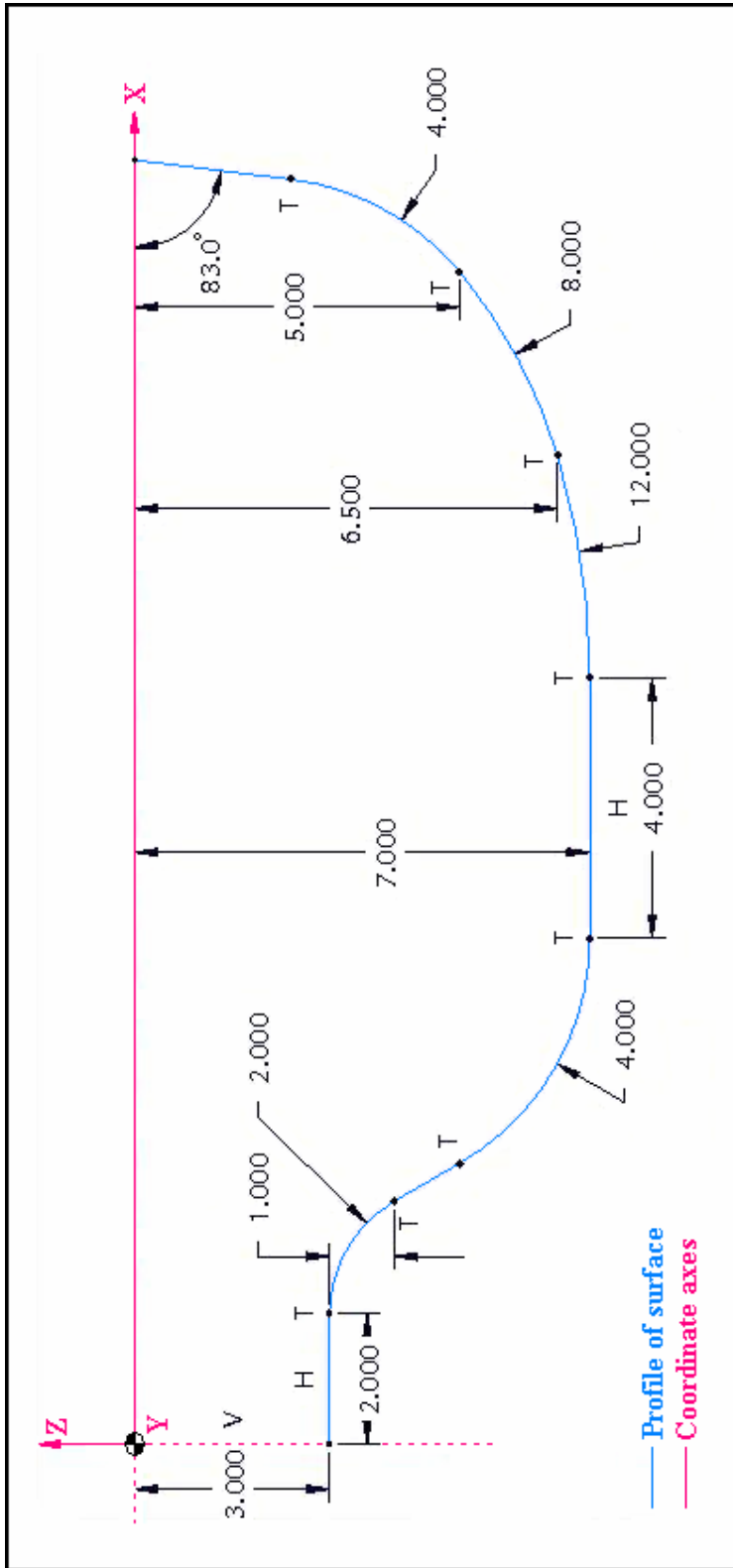
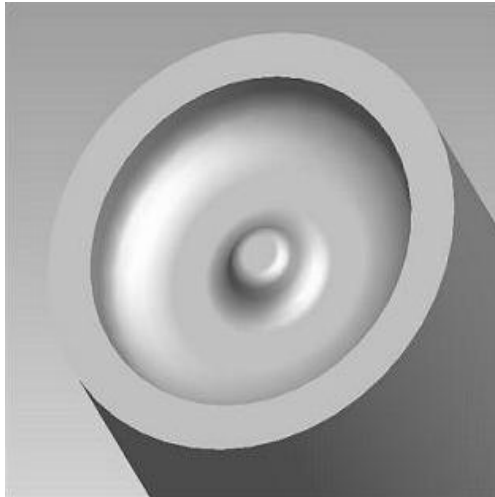


Figure 2.1.13 Profile used in the experiments

By rotating this experimental profile around Z axis, an axisymmetric die cavity geometry presented in Figure 2.14 is obtained.



**Figure 2.14 Experimental die cavity geometry**

As a final step, the profile tolerance of the experimental die cavity is defined according to the tolerance requirements of precision forging dies. The tolerances for length, diameter and thickness given in Table 2.2 can be utilized for tolerancing the specified profile. In Table 2.2, for the forging weight of 1.0-1.8 kg and dimension of 30-100 mm, it is recommended that upper tolerance value should be less than 0.69 mm, and lower tolerance value should be less than 0.33 mm. For the designed die cavity, dimension of the forged component is less than 30 mm. Therefore, the tolerance limits are tightened for the experimental die cavity. Additionally, when wear on the die surface is taken into account, it would be appropriate to give profile tolerancing to outside of the die cavity surface. As a result, tolerance value of 0.10 mm is assigned for the outside tolerance zone. Tolerance zone of the experimental die cavity is presented in Figure 2.15.

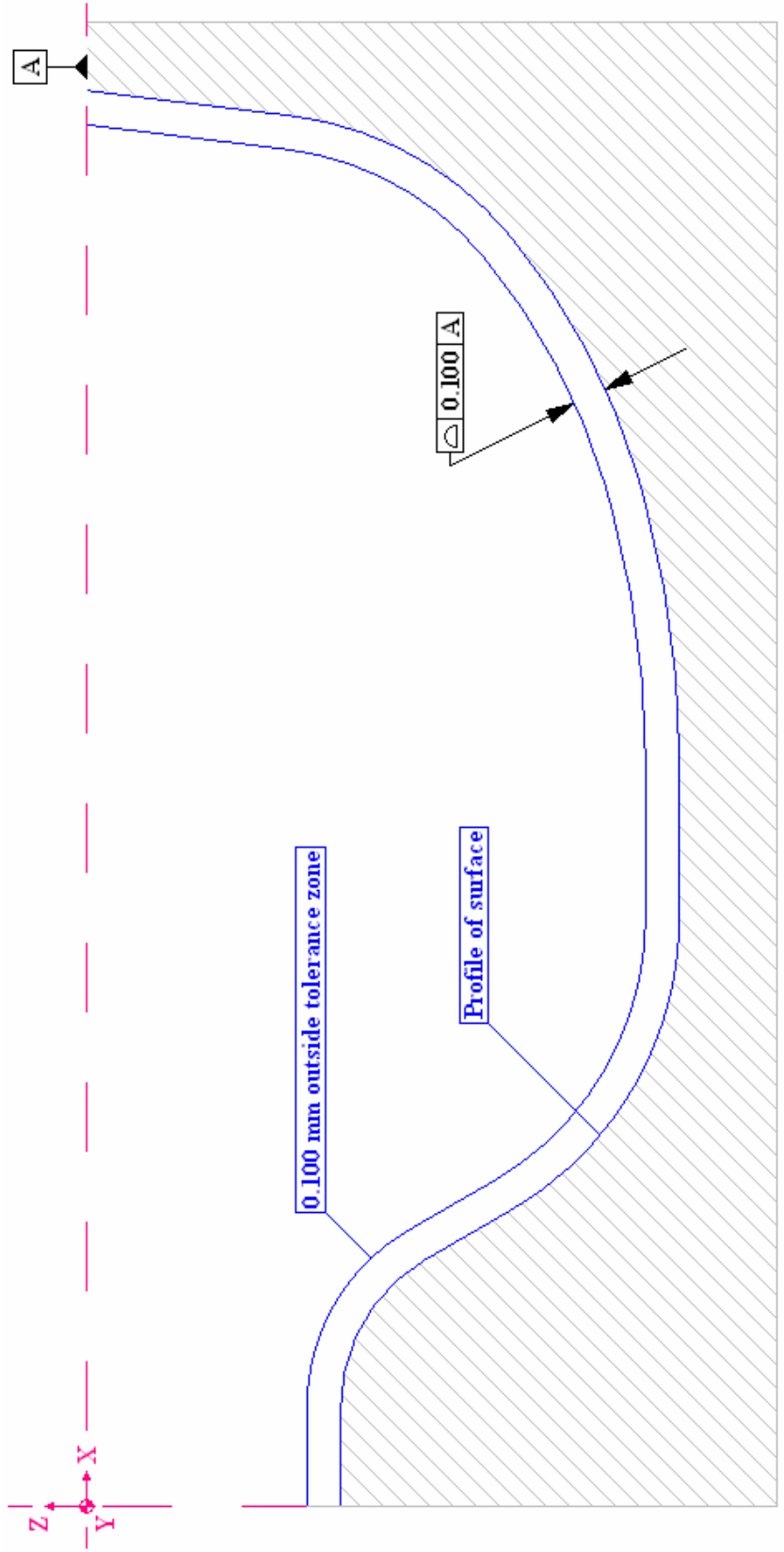


Figure 2.15 Profile tolerance of the experimental cavity

## CHAPTER 3

### ROUGH CUT MILLING OF EXPERIMENTAL DIE CAVITIES

In this chapter, details of rough cut milling have been presented and cutting strategies for the experimental die cavity have been analyzed. Feed rate optimization has been performed to satisfy constant metal removal rate along the tool path trajectory. Finally, optimized rough cut milling codes have been implemented to the die cavities which are required for the finish cut experiments.

#### **3.1 Importance of Rough Cutting Operations in Forging Die Manufacturing**

Nowadays, current trend in forging die manufacturing is to produce high quality surface with an accurate geometrical properties using high speed machining centers. With the introduction of new developments in CNC milling technology, higher feed rates and cutting speeds are more and more applicable. Advances in feed rate and cutting speed provide great reductions in the production time of forging die cavities. However, obtaining geometrical accuracy in accordance with the product specifications is still primary objective; therefore, the most suitable cutting parameters for each operation must be carefully selected.

Many researchers pay attention to optimizing finish parameters of the cutting operations but this is not completely sufficient to increase the efficiency of manufacturing processes of dies. As expected, a rough cutting operation is performed before each finishing operation. For this reason, proper strategies must be defined and applied for both rough cutting and finish cutting operations. A well done rough cutting operation not only provides a smoother surface before finish cutting but also increases tool life considerably.

In terms of rough machining of die cavities, the principal goals of the operation should be:

- Removing the same amount of material with the minimum cycle time
- Reducing number of plunge and retract motions of the tool
- Obtaining the minimum tool path length for the removal of the same amount of volume
- Providing a continuous contact of tool-workpiece to decrease the fluctuations of temperature on the cutting edge
- Decreasing nonproductive time

### **3.2 Cutting Parameters for Rough Machining**

There are many parameters influencing the characteristics of milling process. However, when the cutting parameters are considered, main parameters can be classified as:

- Axial depth of cut ( $a_p$ ) [mm]
- Radial depth of cut ( $a_e$ ) [mm]
- Feed rate ( $V_f$ ) [mm/min]
- Cutting speed ( $V_c$ ) [m/min]
- Type of milling i.e. down or up milling

Axial depth of cut is the axial engagement of the tool with respect to workpiece. Proper value of axial depth of cut should be determined to prevent excessive tool tip failure.

Radial depth of cut or radial engagement of the tool is also known as step over. For the milling process, maximizing metal removal rate is the basic goal in rough cutting

operations. Therefore, it should be logical to use 100% radial engagement of the cutting tool. However, choosing that amount of engagement substantially decreases tool life and tool performance. It would be better in terms of tool life and performance to use 66% radial engagement of the tool as a step over value [29].

As cutting tools are varying in terms of number of teeth on the tool tip, feed rate can be related with number of cutting flutes, spindle speed and feed per tooth according to the following equation:

$$V_f = f_t \cdot n_t \cdot N \quad (3.1)$$

where  $f_t$  is feed in mm per tooth,  $n_t$  is number of cutting flutes on the tool,  $N$  is spindle speed in rpm.

Cutting speed is the speed difference between cutting tool and surface of the workpiece it is operating on. It depends on tool diameter and spindle speed; and can be calculated according to the following equation:

$$V_c = \frac{\pi \cdot D \cdot N}{1000} \quad (3.2)$$

where  $D$  is tool diameter in mm,  $N$  is spindle speed in rpm.

In down milling the cutting edge is mainly exposed to compressive stresses, which are much more favorable for the properties of solid carbide cutters compared with the tensile stresses developed in up milling. When the cutting edge goes into cut in down milling, the chip thickness has its maximum value; on the contrary in up milling it has its minimum value. Up milling and down milling process are represented in Figure 3.1.

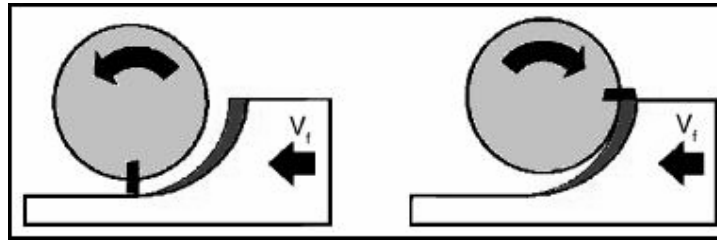


**Figure 3.1 Up and down milling**

Additionally, in up milling considerably more heat is generated than in down milling, because of higher friction on cutting edge. Therefore, in modern high speed milling, down milling is in use. It assures low milling tool wear although cutting process is more pretentious because of greater cutting forces. Modern machine tools are more rigid, that is why allowing use of down milling [8].

In the study, all machining operations related with rough and finish cutting have been carried out by Mazak Variaxis 630-5x vertical CNC milling machine which is currently in use at METU-BİLTİR Research and Application Center. Technical information about Mazak Variaxis 630-5x is presented in Appendix A.

Throughout the experiments, Dievar, high performance Chromium-Molybdenum-Vanadium alloyed hot work tool steel has been used as die material. Dievar tool steel is superior to DIN 1.2344 tool steel in terms of:

- Good dimensional stability throughout heat treatment and coating operations
- Good resistance to hot wear and plastic deformation
- Excellent toughness and ductility in all directions
- Good high temperature strength
- Improved die life

- Excellent hardenability

Properties of Dievar tool steel are given in Appendix B.

As rough cutting tool, Ø6 mm solid carbide end mill with two flutes is selected. Cutting speed and feed recommendations of the tool steel manufacturer and properties of the selected tool are presented in Appendix C.

In order to minimize vibrations of the tool, AA class collet has been used to mount cutters to HSK R32 tool holders [30].

Finally, throughout the experiments flood cooling has been applied to counteract excessive heat generation at the cutting edges of the tool.

### **3.3 Constant Metal Removal Rate in Rough Cut**

In the milling process, material removal rate is defined as the rate at which material is removed from an unfinished part, usually measured in cubic millimeters per minute. The main parameters that determine the metal removal rate are:

- Axial depth of cut ( $a_p$ ) [mm]
- Radial depth of cut ( $a_e$ ) [mm]
- Feed rate ( $V_f$ ) [mm/min]

According to these parameters which are demonstrated in Figure 3.2, metal removal rate,  $Z_w$ , can be defined as:

$$Z_w = a_p \cdot a_e \cdot V_f \quad (3.3)$$

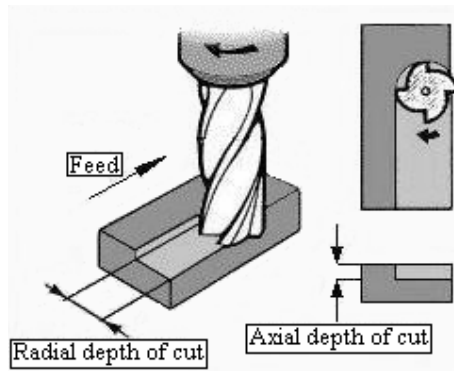


**Figure 3.2 Parameters of metal removal rate**

Maintaining a constant metal removal rate keeps the cutter at its maximum possible rate of advance into material for the varying cutting conditions. However, to keep material removal rate constant during any kind of operation, either radial depth of cut and feed rate must be kept constant or multiplication term of radial depth of cut and feed rate must be kept constant. Determining the exact and optimum feed rate selection for sculptured surface is very difficult and requires experience. By selecting a fixed feed rate based upon the maximum force, which is obtained during full length of machining, the tool is saved but it results in extra machining time, which reduces productivity. By optimizing the feed rate, both the objectives of saving the tool (more tool life) and also reducing machining time thereby increasing productivity can be achieved. Since rough machining operations are strongly geometrical feature dependent, feed rate adjustments are usually essential to maintain constant metal removal rate.

### **3.4 Tool Path Generation for Rough Machining**

For the generation of rough machining codes of the determined geometry, manufacturing module of Pro/Engineer Wildfire 3 [10] is extensively utilized. Features of the CAM module used throughout the process can be visualized in Figure 3.3.

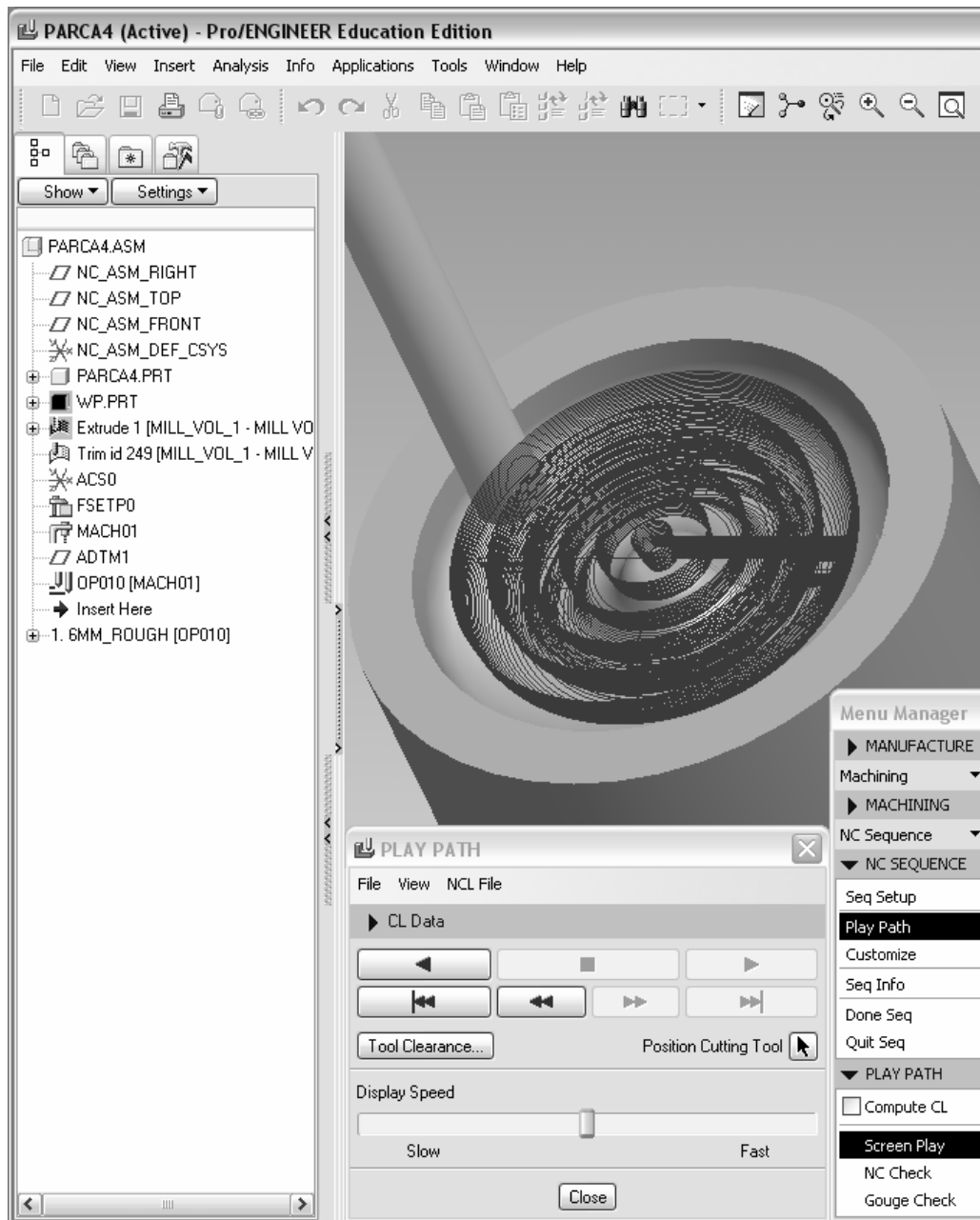


**Figure 3.3 NC programming [10]**

NC programming of the determined die cavity involves basically three main steps:

- Volume definition

- Cutting parameter selection
- Code generation

Initially, excess volume that is intended to be removed from the die cavity is defined. After that, tool and cutting parameters are determined by considering the cavity geometry. Cutter location data for the operation is then formed by taking the predefined cutting parameters and the tool data into consideration. This data file is then post processed and checked by NC simulation package of Pro/Engineer Wildfire 3 [10] whether code is collision free or not. Finally, transformed G-code file is fed to the CNC unit of Mazak Variaxis 630-5x.

In order to obtain the minimum tool path and minimize retract and plunge motions of the tool, various cutting strategies of Pro/Engineer Wildfire 3 library [10] seen in Figure 3.4, are examined.

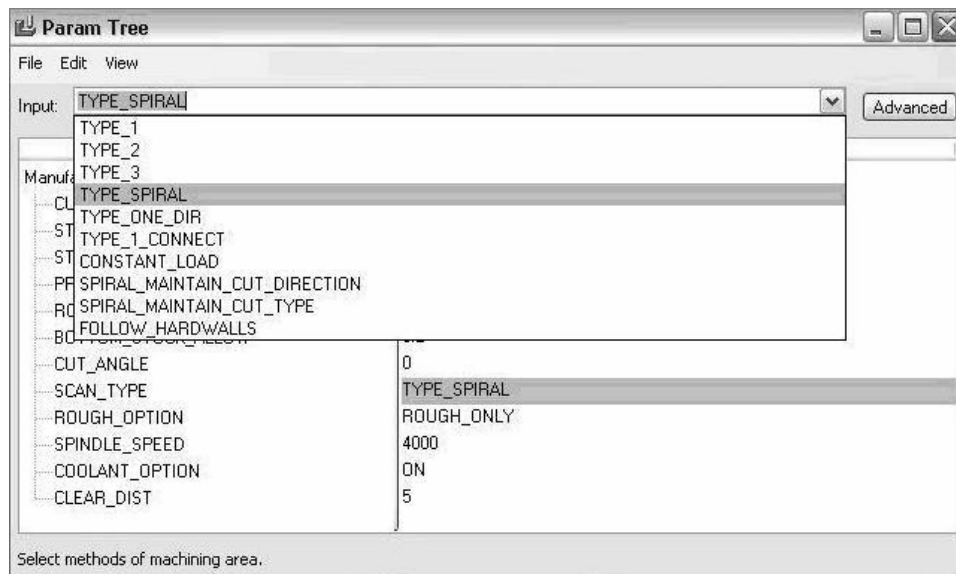


**Figure 3.4 Pro/Engineer Wildfire 3 cutting strategy library [10]**

When available cutting strategies of the Pro/Engineer Wildfire 3 library [10] are analyzed, it is realized that “Type\_1” produces a lace type tool path where the cutter retracts upon encountering an island. Similarly, “Type\_2” provides again a lace type tool path where the cutter would go around islands. “Type\_3” tool path is also a lace type tool path where the cutter would machine zone by zone. When “Type\_Spiral” tool path is selected, a spiral tool path which is more favorable than cutting strategies previously discussed is generated around all islands. Cutting tool locations of a typical spiral tool path are illustrated in Figure 3.5.

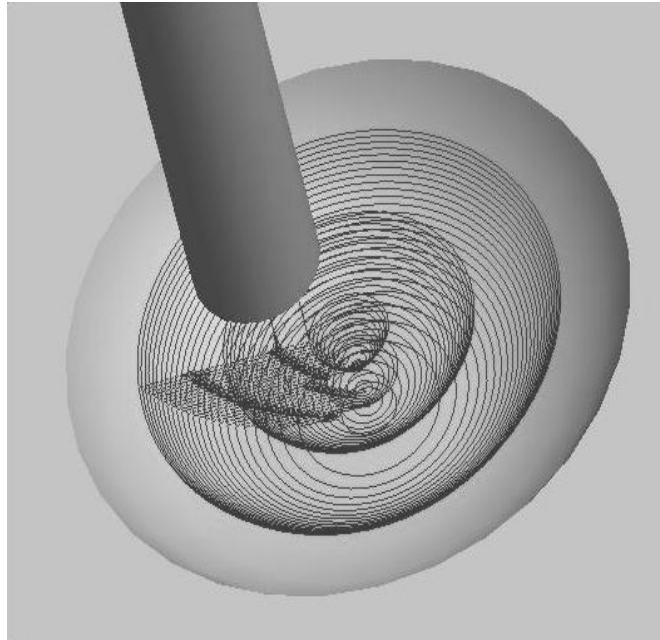


**Figure 3.5 Type spiral tool path**

As another cutting strategy, “Type\_One\_Dir” can be preferred to cut in one direction only, retracting and traversing to next cut. In order to maintain contour follow of the tool when entering and exiting from each cut, “Type\_1\_Connect” should be selected. “Constant\_Load” is used to create the slices with appropriate constant tool load.

However, in this approach radial depth of cut i.e. step over value is limited to half of the tool diameter which is undesirable. “Spiral\_Maintain\_Cut\_Direction” enables a spiral tool path maintaining cut direction and “Spiral\_Maintain\_Cut\_Type” enables spiral tool path maintaining cut type but again the radial depth of cut values are limited to half of tool diameter which is unacceptable. Finally in “Follow\_Hardwalls” each cut would follow hard walls of the feature.

Among all these cutting strategies, it is observed that the spiral motion of the tool is superior to other cutting strategies in terms of cycle time and tool-workpiece contact duration. Cycle time of the each cutting strategy for the removal of the same amount of volume can be examined in Table 3.1.

**Table 3.1 Cutting strategies vs. cycle time**

<b>Cutting Strategy</b>	<b>Cycle Time (min)</b>
Type_1	26.75
Type_2	20.73
Type_3	21.83
Type_Spiral	18.75
Type_One_Dir	62.71
Type_1_Connect	64.04
Constant_Load	40.21
Spiral_Maintain_Cut_Direction	22.08
Spiral_Maintain_Cut_Type	22.11
Follow_Hardwalls	19.40

### **3.5 Deficiencies of Spiral Tool Path**

Although the spiral motion of the tool can be accepted as the best alternative of Pro/Engineer Wildfire 3 library [10] to remove unwanted volume from the die cavity, there are still inadequacies of this cutting strategy to be considered and refined.

These deficiencies are not peculiar to spiral tool path only. Similar inefficiencies are observed for the other tool paths of the cutting strategies. At that point, it should be remembered that spiral tool path warrants excellent tool paths in terms of lessening plunge and retract motions of the tool, and obtaining the minimum tool path for the removal of the same amount of volume.

Insufficiencies of the spiral tool path can be summarized as:

- Lower metal removal rate due to lower step over value than the specified step over value at deep cavities of the geometry which is illustrated in Figure 3.6.
- Keeping constant feed rate for the return path of each plunge motion by not considering the removed volume on the return path which is illustrated in Figure 3.7.

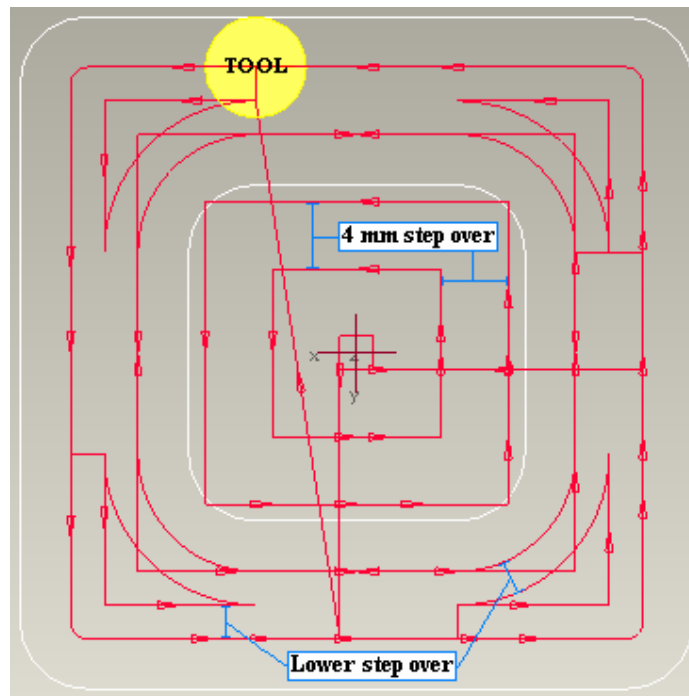


**Figure 3.6 First deficiency of spiral tool path**

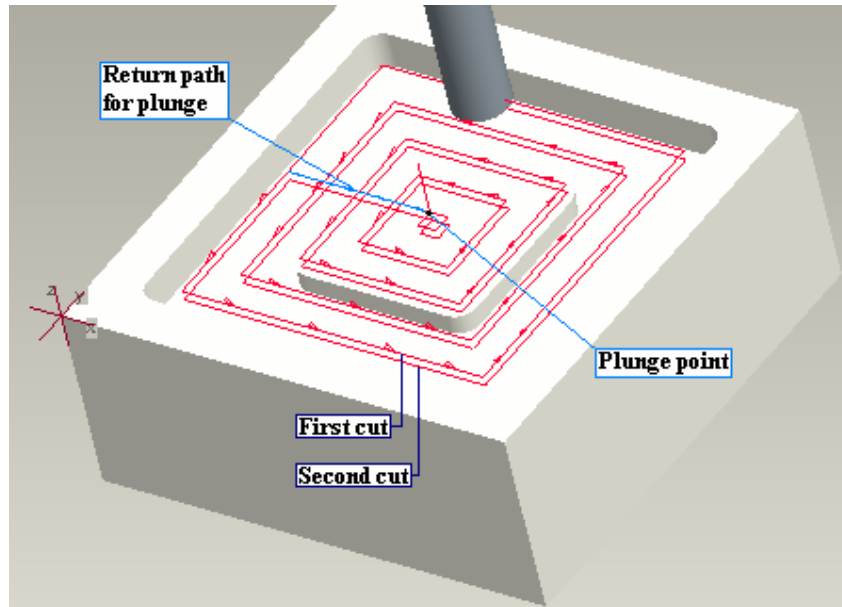


**Figure 3.7 Second deficiency of spiral tool path**

It is obvious that keeping feed rate constant along the cutting path does not always provide constant metal removal rate due to the deficiencies of the cutting strategies. To obtain constant metal removal rate in these inefficient regions of the cutting path, feed rate values should be modified. By adjusting feed rate along tool trajectory, metal removal rate can be kept always constant.

### **3.6 Rough Cutting Parameters for the Selected Geometry**

To define the proper diameter of the tool for the rough cutting operation, simulation package of Pro/Engineer Wildfire 3 [10] is utilized. Excess volume is removed by tools having diameter of 4 mm, 6 mm and 8 mm to compare the material left on the surface for the finish machining. It is observed that tool having diameter of 8 mm is not suitable for the material removal on the lower horizontal surface of the experimental die cavity. Ø8 mm tool selection results in excessive material remaining on the lower horizontal surface which is unacceptable. On the other hand, Ø4 mm tool properly removes material in the die cavity but this tool requires higher

production time when it is compared with Ø6 mm tool. According to these analyses, it is realized that Ø6 mm tool not only removes the excess volume efficiently but also provides a reasonable production time. Therefore, Ø6 mm solid carbide end mill with two cutting flutes is chosen for the rough cutting operations.

For the determination of the axial depth of cut value, tool properties and depth of cut value for the finishing operation are taken into consideration. Surfaces having staircase shape are generally obtained on the curved regions of the die cavities after rough cutting process. The height of these stairs can be minimized by selecting low axial depth of cut values for the rough cutting operations. However, taking a low axial depth of cut value definitely results in higher production time. Therefore, by keeping these considerations in mind, 0.2 mm is determined for the value of axial depth of cut.

Radial depth of cut or step over value is defined as 4.0 mm. For the Ø6 mm solid carbide end mill, step over value higher than 4.0 mm can be selected but this may yield substantial decrease in tool life and performance. Therefore, 66% radial engagement of the tool as step over value is utilized for the rough cutting operation [29].

By considering the recommended ranges of the feed and the cutting speed given in Table C.1 in Appendix C, the values of the cutting parameters for the rough cut operation are determined. Cutting speed of 140 m/min and feed of 0.04 mm/tooth are selected as the rough cutting parameters. All parameters for the rough cutting operation of the experimental die cavities are presented in Table 3.2.

**Table 3.2 Rough cutting parameters**

Cutting Speed, $V_c$ (m/min)	Feed, $f_t$ (mm/tooth)	Axial Depth of Cut, $a_p$ (mm)	Step Over, $a_e$ (mm)
140	0.04	0.2	4

Feed in mm per tooth value given in Table 3.2 can be converted to mm/min by using Equations 3.1-3.2 respectively. For the Ø6 mm tool with cutting speed ( $V_c$ ) of 140 m/min, spindle speed ( $N$ ) is calculated as 7427 rpm. By multiplying this spindle speed value with the number of cutting flutes ( $n_t = 2$ ) and feed ( $f_t$ ) of 0.04 mm/tooth, feed rate ( $V_f$ ) can be found as 594 mm/min.

### 3.7 Rough Cut Optimization

Due to the deficiencies mentioned in Section 3.5, rough machining codes of the experimental die cavity are subjected to feed rate optimization to achieve substantial amount of cycle time reduction. Optimized codes are generated for the rough machining process by revising the feed rates along the cutting trajectory to maintain constant metal removal rate. In the performed optimization, the programmed tool path is not altered. Instead, optimization ensures that the tool path has the optimum feed rate values to produce high quality parts in the least amount of time.

In the optimized tool path, these common inefficiencies of the original tool path are eliminated:

- Excessively conservative feed rates
- Cutting feed rate used for motions in air
- No feed rate compensation for milling less (or more) material than expected
- No feed rate compensation for changing cutting conditions, such as: changing axial and radial depth of cut

In the optimization process, original code is initially examined to find out the regions where metal removal rate is lower than the predefined value. Predefined metal removal rate can be computed by Equation 3.3. By multiplying axial depth of cut ( $a_p$ ) of 0.2 mm with step over ( $a_e$ ) of 4.0 mm and feed rate ( $V_f$ ) of 594 mm/min, metal removal rate can be found as 475.2 mm<sup>3</sup>/min.

It is definite that metal removal rate is not  $475.2 \text{ mm}^3/\text{min}$  in the regions where step over value is less than 4 mm. Therefore, the original code is analyzed step by step and lines where step over value is less than 4 mm are found out. For these regions, a new feed rate value is computed to satisfy  $475.2 \text{ mm}^3/\text{min}$  of metal removal rate. Additionally, a new feed rate which is named as air cut feed rate at 2000 mm/min is defined on the return path of the tool for each plunge motion. Sample of an optimized segment is illustrated in Figure 3.8.

In Figure 3.8, it can be observed that there is a line segment where step over value is 2.461 mm which is less than 4 mm. To keep metal removal rate constant at this line segment, a new feed rate value must be applied. By dividing the metal removal rate ( $Z_w$ ) of  $475.2 \text{ mm}^3/\text{min}$  to axial depth of cut ( $a_p$ ) of 0.2 mm and step over ( $a_e$ ) of 2.461 mm, optimized feed rate ( $V_f'$ ) is found as 965 mm/min.

<u>Original codes</u>	<u>Optimized codes</u>
G1Y16.242	G1Y16.242
G3X0.Y16.242I0.J-16.242	G3X0.Y16.242I0.J-16.242
G1Y12.185	G1Y12.185 <u>F2000.</u> — <b>Air cut feed rate</b>
Z-3.1F50.	Z-3.1F50.
G3X12.185Y0.I0.J-12.185F594.	G3X12.185Y0.I0.J-12.185F594.
G1X9.724	G1X9.724 — <b>~2.5 mm Step over</b>
G2X9.724Y0.I-9.724J0.	G2X9.724Y0.I-9.724J0.F965.— <b>Computed feed rate</b>
G1X5.724	G1X5.724 <u>F594.</u> — <b>Original feed rate</b>
G2X0.Y5.724I-5.724J0.	
X5.724Y0.I0.J-5.724	<u>G2X5.724Y0.I-5.724J0.</u>
G1X12.185	G1X12.185 <u>F2000.</u> — <b>Air cut feed rate</b>
G3X0.Y12.185I-12.185J0.	G3X0.Y12.185I-12.185J0.F594.
G1Y16.185	G1Y16.185
G3X0.Y16.185I0.J-16.185	G3X0.Y16.185I0.J-16.185
G1Y12.117	G1Y12.117 <u>F2000.</u> — <b>Air cut feed rate</b>
Z-3.3F50.	Z-3.3F50.
G3X12.117Y0.I0.J-12.117F594.	G3X12.117Y0.I0.J-12.117F594.
G1X10.154	G1X10.154

**Figure 3.8 Sample of optimized code**

The feed rate value is replaced by 965 mm/min for the particular line segment. Then, next line is checked whether the step over value is 4 mm or not. In this case  $\Delta X = 9.724 - 5.724 = 4$  mm which is the predefined step over value. Therefore, the original feed rate value which is 594 mm/min is applied for the next line. Similarly, the same procedure is carried out for the whole rough machining codes.

It should be kept in mind that, with this performed feed rate optimization; the rapid motions and the programmed path of the tool are not changed. The original codes can be compared with the optimized codes in Appendix D.

As a result of these, a reduction is achieved in the production time of each die cavity. With the original codes, it is requiring 18.75 min. to remove excess material in the die cavity. When the optimized codes are implemented for the rough machining, it takes only 14.22 min. 24.2% time reduction is extremely significant reduction when the objectives of die manufacturers are taken into account.

By utilizing the optimized rough cutting codes to CNC unit of Mazak Variaxis 630-5x, die cavities which are requisite for the experimental study are manufactured. Required number of die cavities is determined according to  $3^2$  factorial design which will be discussed in Chapter 4 in detail. Geometrical distribution of these die cavities is presented in Figure 3.9.

To minimize measurement errors and to settle reference coordinate axis accurately, flat planes illustrated in Figure 3.10 are machined to the sides of the workpiece as datum surfaces. These machined planes generate X and Y axis of the reference coordinates. Positions of the experimental cavities are computed with respect to this reference coordinate and directly these values are applied to yield precise measurements on the coordinate measurement machine.

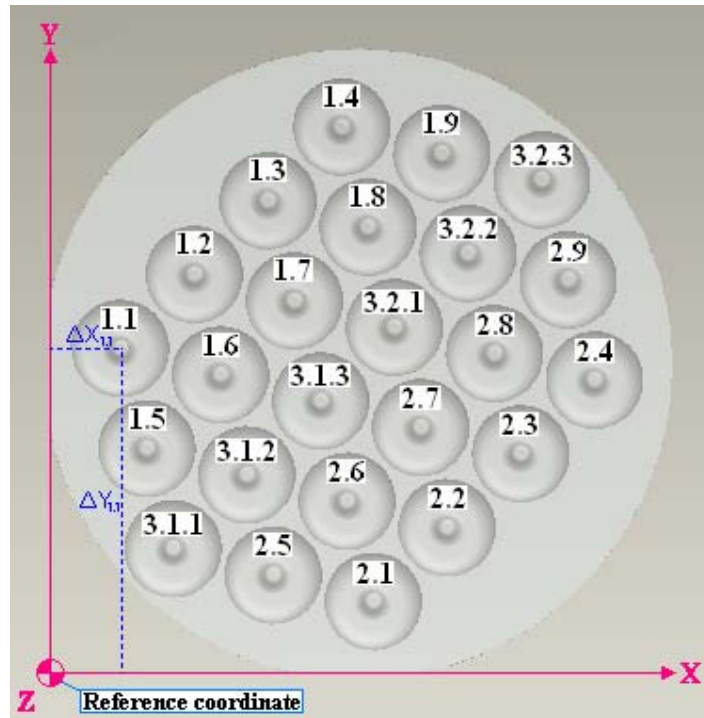


Figure 3.9 Geometrical distribution of the die cavities with experiment numbers

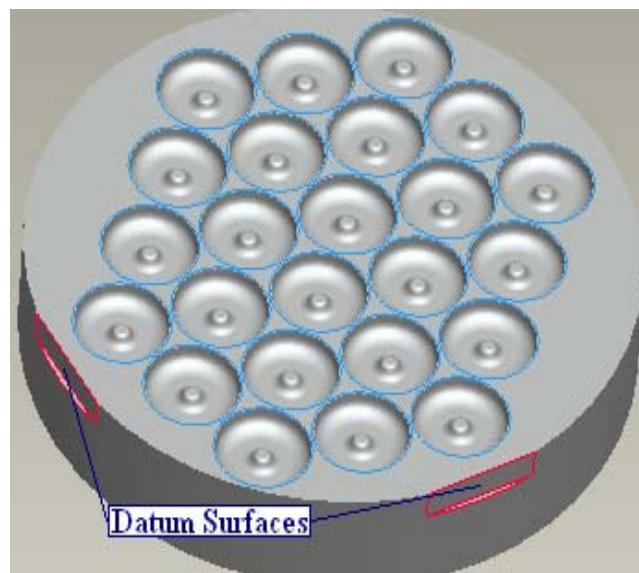


Figure 3.10 Datum surfaces for reference coordinate

Offset values of the die cavities,  $\Delta X$  and  $\Delta Y$ , (i.e. distance between the center point of each die cavity and the reference coordinate system) and numeration of each die cavity are presented in Table 3.3.

**Table 3.3 Cutting coordinates of die cavities wrt reference coordinate**

<b>Experiment Number</b>	<b><math>\Delta X</math> (mm)</b>	<b><math>\Delta Y</math> (mm)</b>
1.1	29.056	130.879
1.2	58.754	160.578
1.3	88.453	190.276
1.4	118.151	219.974
1.5	39.662	90.574
1.6	69.361	120.272
1.7	99.059	149.971
1.8	128.758	179.669
1.9	158.456	209.368
2.1	130.879	29.056
2.2	160.578	58.754
2.3	190.276	88.453
2.4	219.974	118.151
2.5	90.574	39.662
2.6	120.272	69.361
2.7	149.971	99.059
2.8	179.669	128.758
2.9	209.368	158.456
3.1.1	50.269	50.269
3.1.2	79.967	79.967
3.1.3	109.666	109.666
3.2.1	139.364	139.364
3.2.2	169.063	169.063
3.2.3	198.761	198.761

## CHAPTER 4

### FINISH CUT MILLING OF EXPERIMENTAL DIE CAVITIES

In this chapter, three level factorial design for the experimental study has been initially defined. Then, details of the finish cut parameter selection and experimental levels are presented. Finally, geometrical error measurement technique for the manufactured experimental cavity profile has been explained.

#### 4.1 Three Level Factorial Design

$3^k$  design is a factorial design, that is, a factorial arrangement with  $k$  factors each at three levels. Three levels of the factors are referred as low, intermediate, and high. Each treatment in the  $3^k$  design are denoted by  $k$  digits, where the first digit indicates the level of factor A, the second digit indicates the level of factor B and the  $k^{\text{th}}$  digit indicates the level of factor  $k$ . Geometry of  $3^2$  design is shown in Figure 4.1.

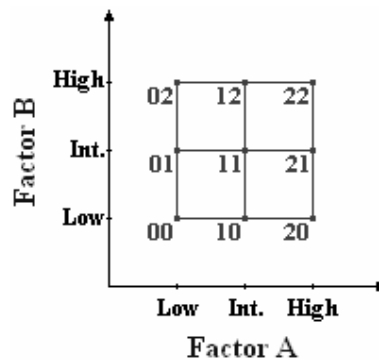


Figure 4.1 Treatment combinations in  $3^2$  design

In the  $3^k$  system of designs, when the factors are quantitative, low, intermediate, and high levels are denoted by -1, 0, and +1 respectively. This facilitates fitting a regression model relating the response to the factor levels. When  $3^2$  design in Figure 4.1 is considered and let  $x_1$  represent factor A and  $x_2$  represent factor B, a regression model relating the response  $y$  to  $x_1$  and  $x_2$  that is supported by this design is:

$$y = \beta_0 + \beta_1 x_1 + \beta_2 x_2 + \beta_{12} x_1 x_2 + \beta_{11} x_1^2 + \beta_{22} x_2^2 \quad (4.1)$$

Second order response model in two variables given above can be transformed into linear regression model to evaluate the unknown parameters.

Supposing that  $x_3 = x_1 x_2$ ,  $x_4 = x_1^2$ ,  $x_5 = x_2^2$  and  $\beta_3 = \beta_{12}$ ,  $\beta_4 = \beta_{11}$ ,  $\beta_5 = \beta_{22}$  then Equation 4.1 becomes:

$$y = \beta_0 + \beta_1 x_1 + \beta_2 x_2 + \beta_3 x_3 + \beta_4 x_4 + \beta_5 x_5 \quad (4.2)$$

In general, any regression model that is linear in the parameters is a linear regression model, regardless of the shape of the response surface that it generates. In this chapter, details of parameter estimation in linear regression models are not derived however all calculations related with the parameter estimation are presented in Appendix E.

In this study, the simplest design in the  $3^k$  system,  $3^2$  design, which has two factors, each at three levels is performed. Since there are  $3^2 = 9$  treatment combinations, there are eight degrees of freedom between these treatment combinations. Main effects of A and B each have two degrees of freedom, and AB interaction has four degrees of freedom. [31].

## 4.2 Finish Cut Experiments and Experimental Details

In order to examine the effects of the cutting parameters; step over, feed and cutting speed to the geometric error during finish cut of the forging die cavities, the factorial design method has been utilized. The design consists of running tests with all the possible combinations of variables at each of three levels, thereby obtaining most of

the information required for a multilevel experiment. In that way, the factorial design does an excellent job relating the experimental effort to the information obtained.

The input parameters; step over, feed and cutting speed are all quantitative factors that level values of each should be properly defined. Improper selection of the level values and/or determination of level limits may result in incompatible results of the response variable which is undesirable.

By considering the recommended ranges of the feed and the cutting speed given in Table C.1 in Appendix C, three levels for the step over and the feed; two levels for the cutting speed are selected. Thus, two sets of  $3^2$  factorial test have been performed and number of experiments is enhanced from  $3^2 = 9$  to  $2 \times 3^2 = 18$  by introducing the second level of the cutting speed to the factorial design. The cutting parameter values in Table C.1 are presented in Table 4.1 as a matter of convenience.

**Table 4.1 Cutting data recommendations for end milling [34]**

<b>Cutting Parameters</b>	<b>Solid Carbide</b>	<b>Carbide Indexable Insert</b>	<b>High Speed Steel</b>
Cutting Speed $V_c$ (m/min)	130-170	120-160	25-30
Feed $f_t$ (mm/tooth)	0.03-0.20	0.08-0.20	0.05-0.35

At that point it should also be kept in mind that radius of the ball cutter must always be less than the radius of any concave surfaces and corners in the die cavity to ensure tool contact throughout the tool path. Since the minimum curved section of the experimental die cavity has dimension of R4 mm, ball nose solid carbide end mill having radius of 3 mm is utilized for the finish cutting operations.

The first input parameter, step over, is very significant factor to achieve desired quality and accuracy on the surface of the forging die cavities. The radial motion (step over) of the ball nose cutter always leads up to scallop formation on the surface of the die cavity which is illustrated in Figure 4.2.

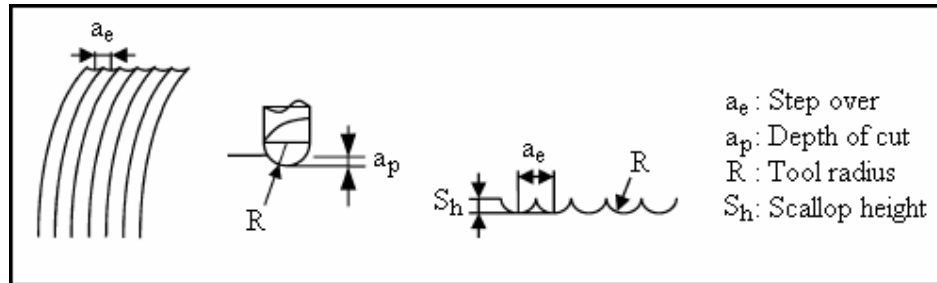


**Figure 4.2 Scallop formations during ball nose finishing [8]**

Elimination of these formations during finish cut operation is directly related with the defined step over value. For this reason, a systematic approach is implemented to decide on the first input parameter values. The level values of step over are determined by taking a certain percentage of the cutter diameter. The first level of step over value 0.10 mm constitutes 1.67% of the  $\text{Ø}6$  mm solid carbide ball nose cutter seeming quite small value for the application. Keeping the step over value low guarantees excellent geometrical accuracy and surface quality but causes substantially longer production time. Therefore, the second level of step over is chosen as 0.20 mm which is 3.33% of the tool diameter and double of the first level. This step over value should present good geometric accuracy and surface quality with a reasonable production time. Finally, third level is selected as 0.30 mm which is triple of low level value and 5.00% of the cutter diameter. Tool paths for the three levels of step over are represented in Figure 4.3-4.5.

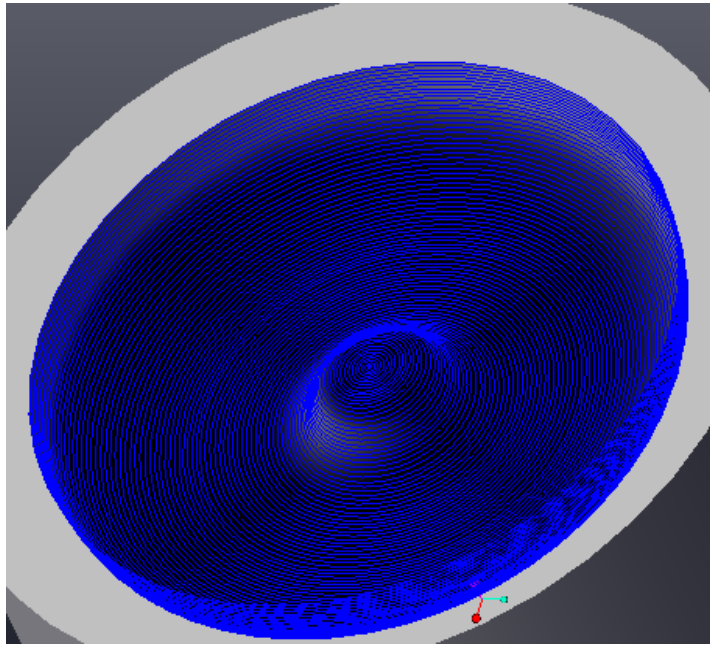


**Figure 4.3 Tool path with 0.10 mm step over**

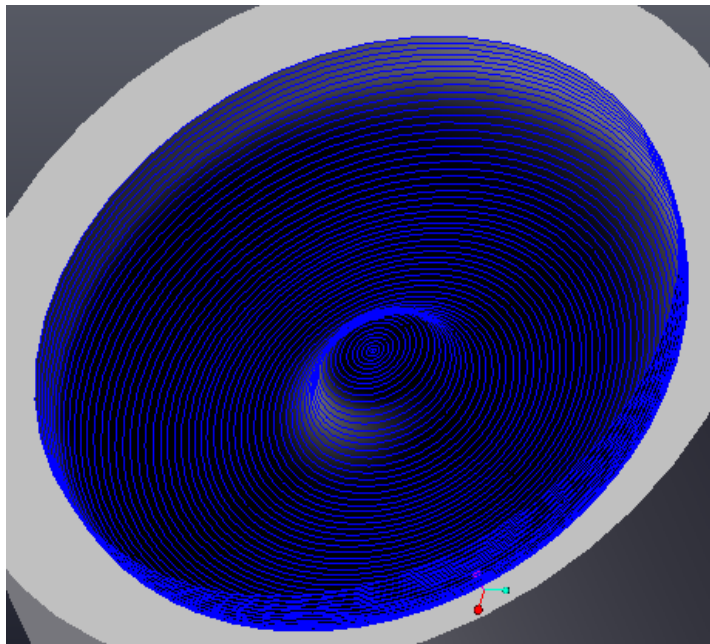


**Figure 4.4 Tool path with 0.20 mm step over**

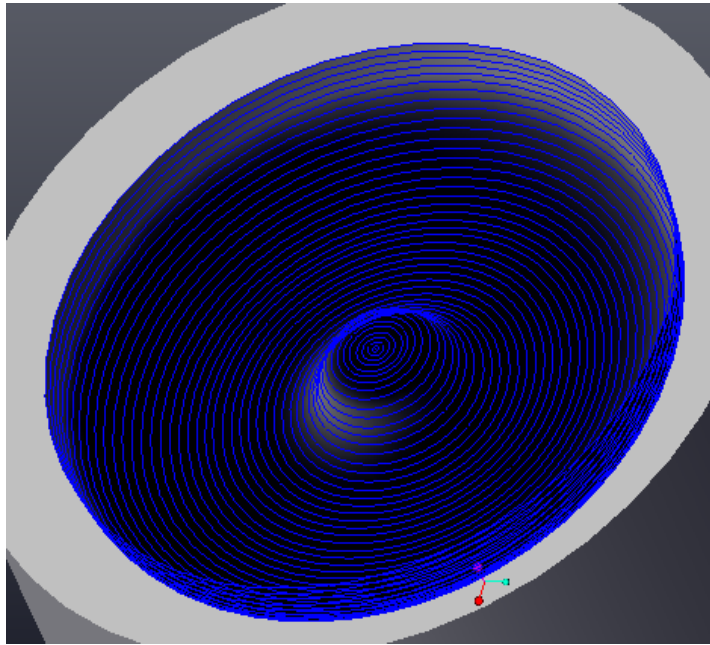


**Figure 4.5 Tool path with 0.30 mm step over**

The cutting data recommendations of tool steel manufacturer's presented in Table 4.1 have been used to determine low, intermediate and high level values of the second input parameter, the feed. According to the cutting recommendations for solid carbide cutters, level values of the feed are selected as 0.03, 0.04 and 0.05 mm/tooth respectively.

When the reference values for the solid carbide cutters given in Table 4.1 are examined, it is observed that proposed range for the cutting speed is in between 130 m/min and 170 m/min. As mentioned previously, two levels are decided to be practical for the third input parameter. Therefore, low level i.e. 130 m/min and high level i.e. 170 m/min are chosen for the cutting speed. Variable factors considered in the finish cut experiments and the selected levels are summarized in Table 4.2-4.3.

**Table 4.2 Selected factors and levels for the first set of finish cut experiments**

Levels	Step over, $a_e$ (mm)	Feed, $f_t$ (mm/tooth)	Cutting speed, $V_c$ (m/min)
Low Level	0.10	0.030	130
Intermediate Level	0.20	0.040	-
High Level	0.30	0.050	-

**Table 4.3 Selected factors and levels for the second set of finish cut experiments**

Levels	Step over, $a_e$ (mm)	Feed, $f_t$ (mm/tooth)	Cutting speed, $V_c$ (m/min)
Low Level	0.10	0.030	-
Intermediate Level	0.20	0.040	-
High Level	0.30	0.050	170

Within this setup, 18 experiments are performed to analyze the geometrical discrepancy between the CAD model of the die cavity and the manufactured die cavity. Additionally, 6 verification experiments are held to check out the validity of the prediction formula which will be derived in Chapter 5. All experimental details, levels and factors are presented in Table 4.4.

After determination of the cutting parameters, proper cutting strategies for the generation of finish machining codes are investigated. In finish machining, volume is not removed like in the case of rough machining. Therefore, cutting strategies for finish machining differ from the cutting strategies for rough machining. A strategy suitable for rough machining would be less favorable for finish machining. For the finish machining of the experimental die cavities, it is aimed to obtain the minimum tool path having one directional continuous motion of the tool providing smooth transitions between radial movements.

When the available cutting strategies of Pro/Engineer Wildfire 3 library are examined, it is realized that “Type\_One\_Dir” cutting strategy corresponds the objectives better than the other cutting strategies for the finish machining of the experimental die cavities. Therefore, “Type\_One\_Dir” cutting strategy is utilized for the finish machining of the experimental die cavities.

**Table 4.4 Design matrix for the experiments**

	<b>Experiment No</b>	<b>Step Over (mm)</b>	<b>Feed (mm/tooth)</b>	<b>Cutting Speed (m/min)</b>
<b>1<sup>st</sup> set of experiments</b>	1.1	0.10	0.030	130
	1.2	0.10	0.040	130
	1.3	0.10	0.050	130
	1.4	0.20	0.030	130
	1.5	0.20	0.040	130
	1.6	0.20	0.050	130
	1.7	0.30	0.030	130
	1.8	0.30	0.040	130
	1.9	0.30	0.050	130
<b>2<sup>nd</sup> set of experiments</b>	2.1	0.10	0.030	170
	2.2	0.10	0.040	170
	2.3	0.10	0.050	170
	2.4	0.20	0.030	170
	2.5	0.20	0.040	170
	2.6	0.20	0.050	170
	2.7	0.30	0.030	170
	2.8	0.30	0.040	170
	2.9	0.30	0.050	170
<b>Verification experiments</b>	3.1.1	0.15	0.030	130
	3.1.2	0.20	0.035	130
	3.1.3	0.25	0.050	130
	3.2.1	0.15	0.030	170
	3.2.2	0.20	0.045	170
	3.2.3	0.25	0.050	170

### 4.3 Geometrical Measurement

#### 4.3.1 Measurement Setup

Precision measurement of the manufactured products in Cartesian coordinate system can be performed by using a coordinate measuring machine (CMM). DEA Brown&Sharpe GLOBALSTATUS777 coordinate measuring machine, which is available at METU-BİLTİR Research and Application Center, is utilized for the dimensional examination of the experimental die cavities. The available CMM at the Center which is presented in Figure 4.6 uses digital readouts, air bearings, computer controls to achieve accuracies in the order of 1  $\mu\text{m}$  over spans of 100 mm.



**Figure 4.6 CMM used in the study**

For the geometrical error measurement, the experimental workpiece is initially fixed on granite plate of the CMM by two mounting clamps to prevent movement of the part on the granite surface. The reference coordinate which is used throughout the machining operations is recreated by forming reference planes on the flat surfaces of the product. By intersecting these two planes, reference coordinate of the machined part is defined and fixed. After converting the CMM coordinate system to the part coordinate system, measuring probe becomes aware of the reference coordinate and angular position of the each axis. For instance,  $\Delta X = 29.056$  and  $\Delta Y = 130.879$  movement of the measuring probe from reference coordinate turns out to be exact position of the probe on center of the experimental cavity number 1.1 which was illustrated in Figure 3.9.

#### **4.3.2 Scanning Technique on CMM**

The dimensions of sculptured surfaces along a directional path can be measured by using scanning technique of CMMs. By introducing boundary points and measurement increments on the directional path, a scanning trajectory for the measurement can be defined. Geometrical variations, positive and negative slopes on the path are taken into account by the computer routines of the CMM. Therefore, there is no need to concern about the diversity of the surface. A sample measurement representing the scanning technique can be visualized in Figure 4.7.

At that point, it should be kept in mind that, values of the measurement increments directly influence the number of points taken on the surface and the fitted curve on these points. As a consequence of this, the measurement interval must be settled to a reasonable value to maintain contact to all surfaces through the trajectory. In this particular study, the maximum incremental value for the measuring probe movement is taken as 0.10 mm since the minimum step over value is predefined as 0.10 mm. The minimum incremental value is chosen as 0.05 mm which is quite safe value for the measurements taken on the curved sections of the surfaces. According to these measurement intervals, measuring probe definitely moves 0.10 mm increments on the flat surfaces of the trajectory; and measuring increments reduce from 0.10 mm to 0.05 mm for the curved regions of the trajectory.

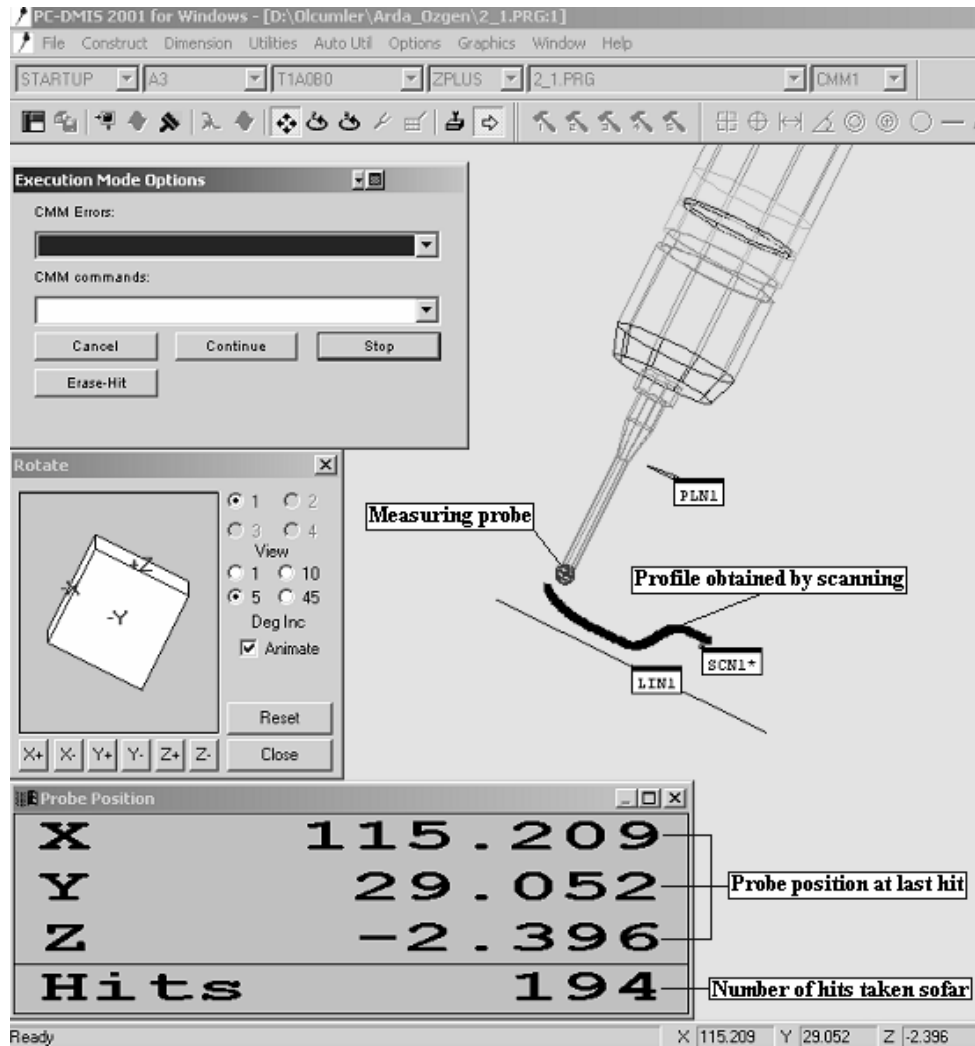


**Figure 4.7 Scanning technique on CMM**

Since the experimental cavity geometry is axisymmetric, measurement along a profile would be sufficient to represent the characteristics of the whole die cavity. For the geometrical error analysis of the experimental die cavity, scanning is performed in two directions which are orthogonal to each other. Scanning directions of the experimental die cavity is represented in Figure 4.8.

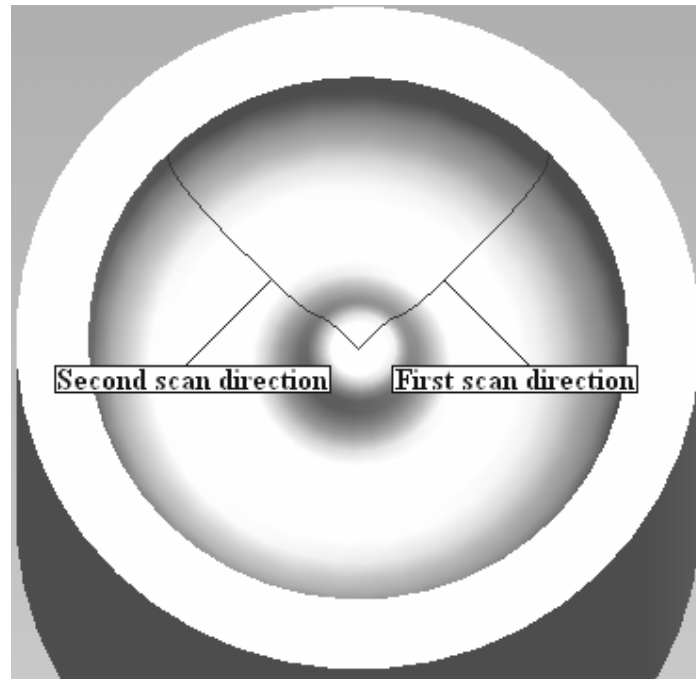


**Figure 4.8 Scanning directions**

### **4.3.3 Geometrical Error Analysis**

In order to measure the geometrical error on the profile of the surface, fitted curve is transformed into Pro/Engineer Wildfire 3 [10] with the reference coordinate system formed during CMM measurements. By coupling the original profile of the die cavity with the fitted curve on top of each other, dimensional discrepancies on the profile are analyzed. These discrepancies are the major geometrical errors along the profile that must be carefully examined. To determine the maximum error region, a line which is normal to the original profile along the profile trajectory is created. By dragging the created line along the profile trajectory, dimensional variation between the original profile and the fitted curve is observed. The maximum dimension of the dragged line yields the maximum deviation between the CAD and the manufactured profile. The process for the analysis of the geometrical error is represented in Figure 4.9.

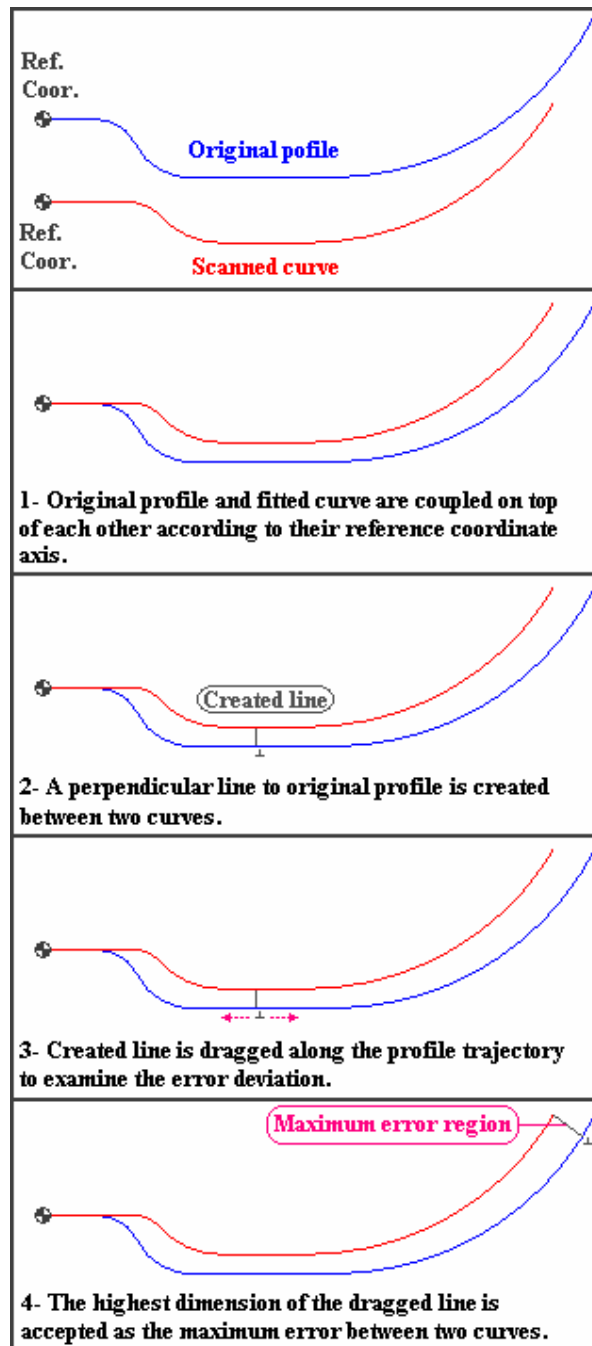


Figure 4.9 Geometrical error analysis process

Sample matching of the two profiles can be visualized in Figure 4.10.

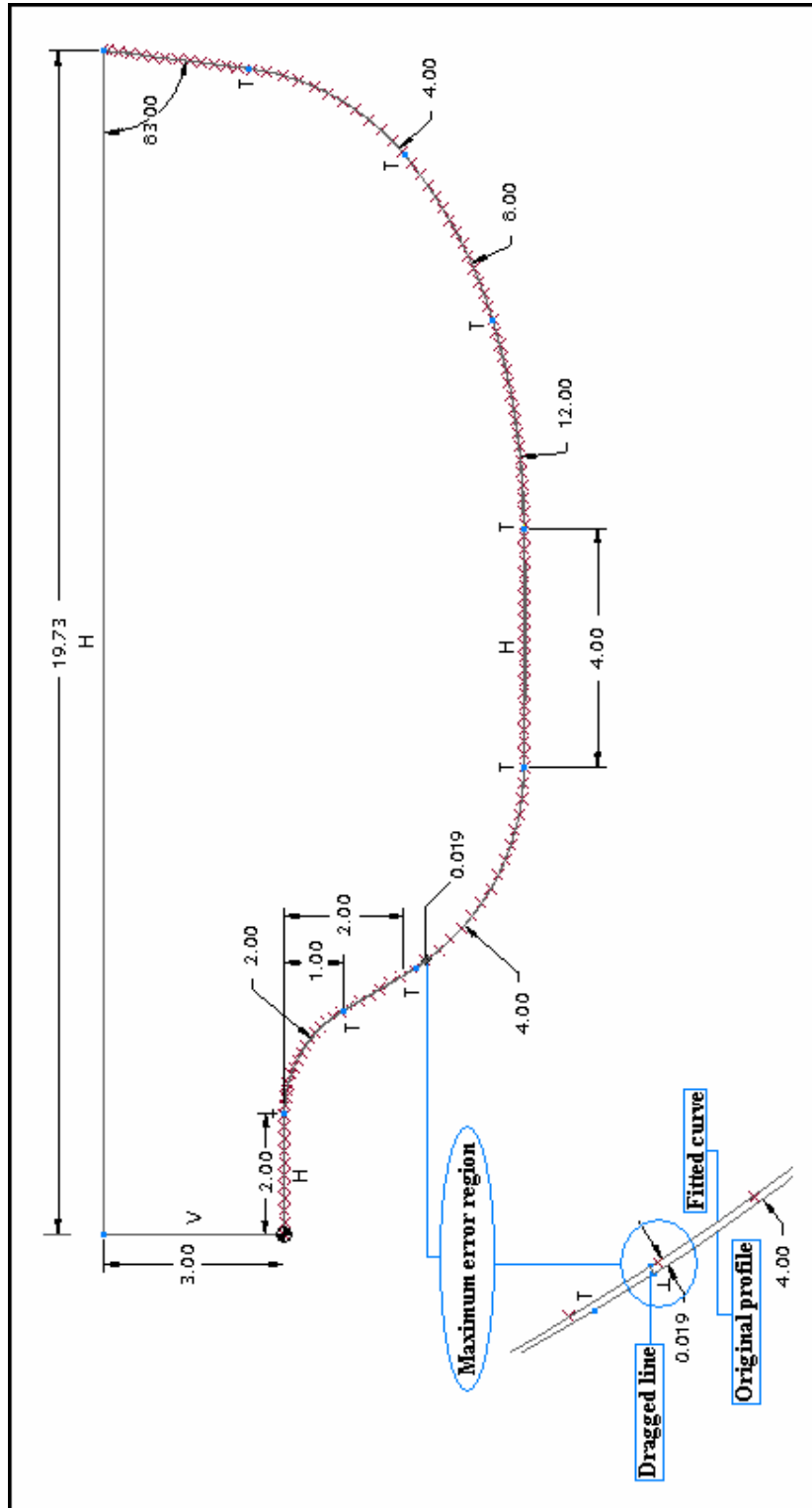


Figure 4.10 Geometrical error measurement

The measurement procedure is applied to the all die cavities manufactured in the finish cut experiments. Analysis and results of the finish cut experiments will be evaluated in Chapter 5.

## CHAPTER 5

### ANALYSIS OF THE EXPERIMENTS AND DERIVATION OF GEOMETRICAL ERROR PREDICTION FORMULA

In this chapter, effects of the cutting parameters i.e. step over, feed and cutting speed on geometrical accuracy of the surface profile have been examined by utilizing  $3^2$  factorial design. Geometrical error analysis for the finish cut experiments has been given initially. Then, geometrical error prediction formula and verification analysis for the prediction formula have been presented.

#### 5.1 Geometrical Error Analysis of the First Set of Experiments

The design matrix for the first set is shown in Figure 5.1.

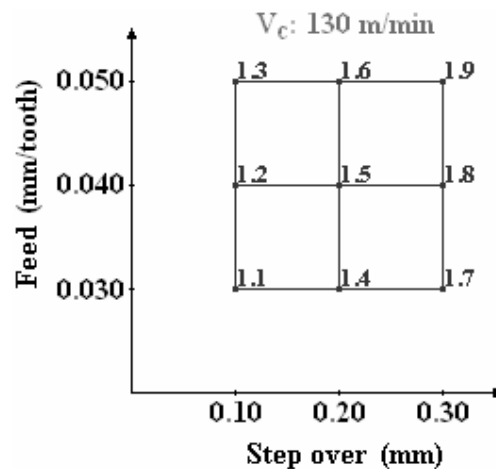
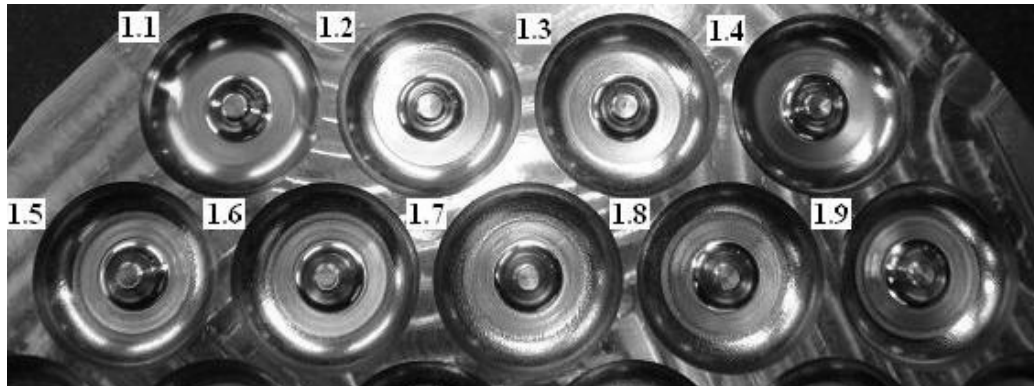


Figure 5.1 Design matrix for the first set of experiments

With the application of the cutting parameter values described in Figure 5.1, experimental die cavities involving surface and geometrical diversities are attained. Manufactured die cavities in the first set of experiments are shown in Figure 5.2.



**Figure 5.2 Photograph of the first set of experiments**

The procedure for the geometrical error measurement between the CAD profile and the manufactured profile was discussed in Section 4.3.3. According to this procedure, the error measurements are performed and geometrical error variations of the first set are obtained. Results of the geometrical error analysis for the first set of experiments are presented in Table 5.1. The error measurements are performed in two scan directions. Therefore, averages of the geometrical error measurements are also tabulated in Table 5.1.

It can be observed from Table 5.1 that all geometrical error values are lower than 100  $\mu\text{m}$  which is the predefined profile tolerance value for the experimental die cavity. Therefore, all die cavities can be accepted as geometrically accurate in the defined tolerance limits. However, when surface quality is taken into account, die cavities having step over value of 0.10 mm are superior to the others. Depending on visual

inspection, these die cavities can be directly utilized for forging applications without any requirement of polishing operation.

**Table 5.1 Results of the first set of experiments**

Exper. No	Cutting Parameters			Geometrical Error		
	Step Over (mm)	Feed (mm/tooth)	Cutting Speed (m/min)	1 <sup>st</sup> Scan Dir. Error Meas. (µm)	2 <sup>nd</sup> Scan Dir. Error Meas. (µm)	Average Error (µm)
1.1	0.10	0.030	130	22	19	20.5
1.2	0.10	0.040	130	25	29	27.0
1.3	0.10	0.050	130	34	31	32.5
1.4	0.20	0.030	130	34	35	34.5
1.5	0.20	0.040	130	39	39	39.0
1.6	0.20	0.050	130	43	42	42.5
1.7	0.30	0.030	130	44	46	45.0
1.8	0.30	0.040	130	52	47	49.5
1.9	0.30	0.050	130	54	57	55.5

By examining the main effect plots given in Figure 5.3-5.4, one can decide on the parameter having major influence on the geometrical error. These plots are just representation of marginal response averages at the three levels of two factors. Main effects of the step over and the feed for the first set of experiments are represented in Figure 5.3-5.4 respectively.

When the main effect of the step over is analyzed, it is realized that change in the input variable from 0.10 mm to 0.30 mm is resulted with a change in the response variable i.e. geometrical error from 26.7 µm to 50.0 µm. Response line characterizes a linear behavior in the range of the step over values. On the other hand, variation in the second input parameter, feed, causes again increase in the response value similar to the step over but rate of increase is milder than the first input parameter. Linear

tendency of the response curve of the feed is another point observed in the main effect plot of the second input parameter.

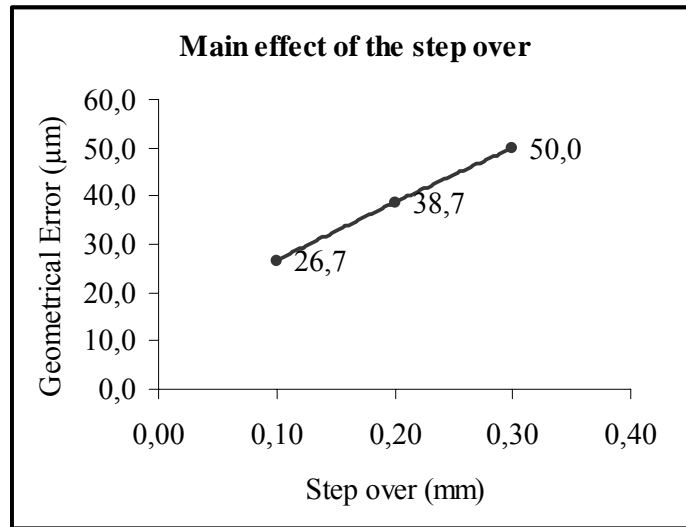


**Figure 5.3 Main effect plot of the first input parameter**

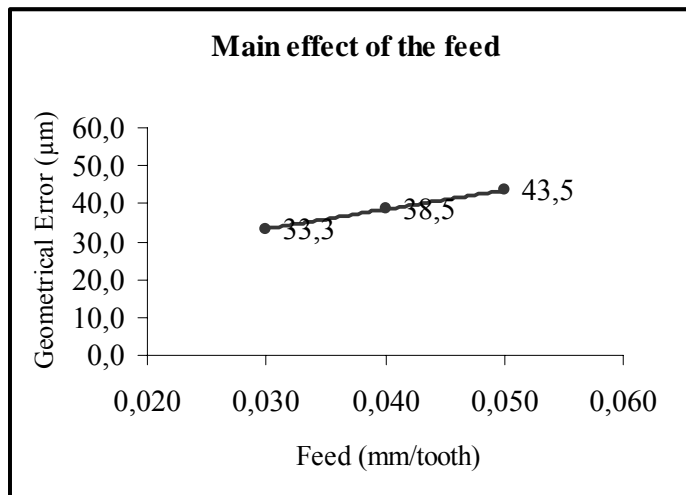


**Figure 5.4 Main effect plot of the second input parameter**

When the interaction effect plot of the input parameters is analyzed, it can be concluded that interaction between the step over and the feed is quite low due to the similar shape of the response curves attained from the three levels of the parameters. The interaction effect plot of the input parameters is shown in Figure 5.5.

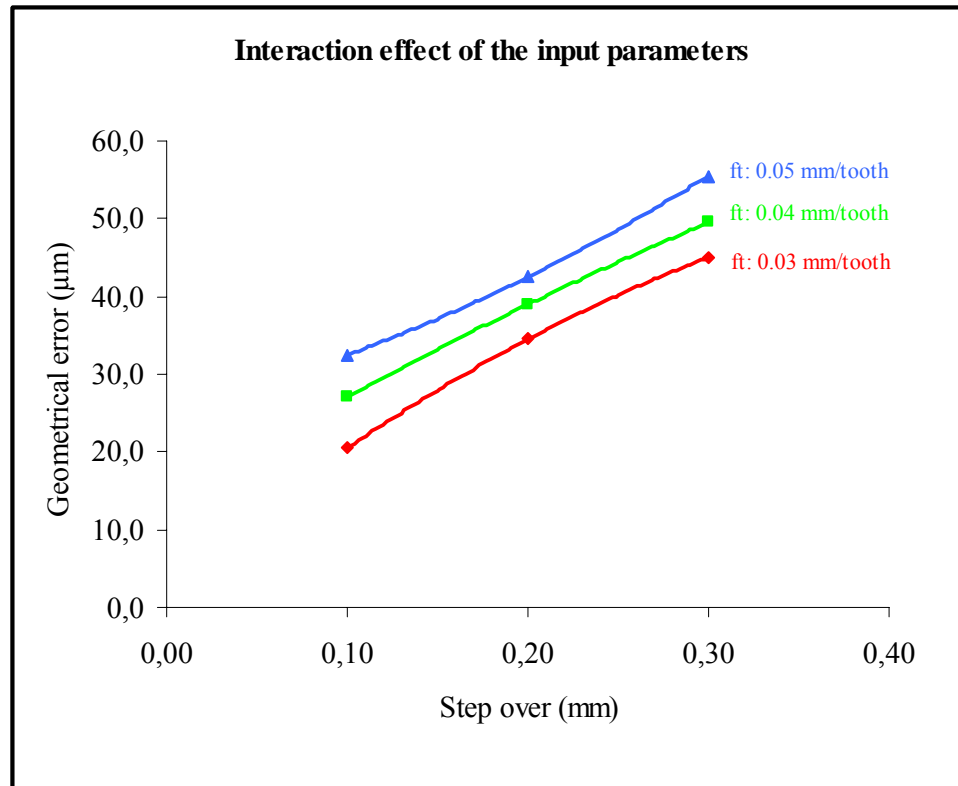


**Figure 5.5 Interaction effect plot of the input parameters**

Since the factors in this factorial experiment are quantitative, a response surface may be used to model the relationship between geometrical error, step over and feed. 3D surface plot for the results of the first set of experiments is presented in Figure 5.6.

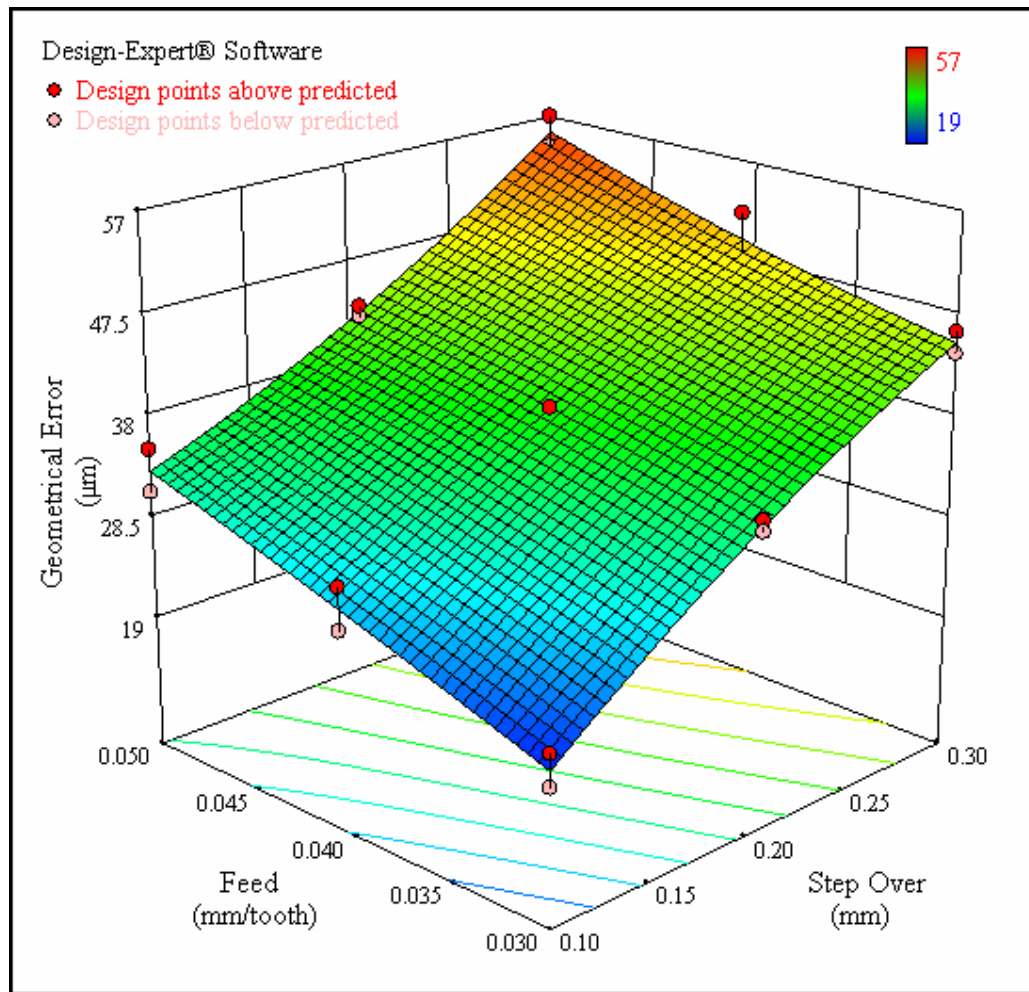


**Figure 5.6 Surface plot of the response variable geometrical error [32]**

It is obvious from the first set of experiments that lower step over and feed values provide excellent geometrical accuracy and surface quality; however, lowering these cutting parameters causes higher production time which is undesirable in competitive market conditions. Therefore, a compromise is essential for the determination of cutting parameters by regarding geometrical accuracy and production time together. For this reason, further analysis is performed to clarify the relation between the geometrical error and the production time of the experimental die cavities. Time and error wise comparison of the first set of experiments is given in Table 5.2.

**Table 5.2 Comparison of geometrical error values with production time values**

Exper. No	Cutting Speed (m/min)	Feed (mm/tooth)	Step Over (mm)	Average Geom. Error ( $\mu\text{m}$ )	Production Time (min)
1.1	130	0.030	0.10	20.5	44.4
1.2	130	0.040	0.10	27.0	33.5
1.3	130	0.050	0.10	32.5	26.9
1.4	130	0.030	0.20	34.5	22.8
1.5	130	0.040	0.20	39.0	17.3
1.6	130	0.050	0.20	42.5	14.0
1.7	130	0.030	0.30	45.0	15.6
1.8	130	0.040	0.30	49.5	11.9
1.9	130	0.050	0.30	55.5	9.7

## 5.2 Geometrical Error Analysis of the Second Set of Experiments

The design matrix for the second set of experiments is given in Figure 5.7.

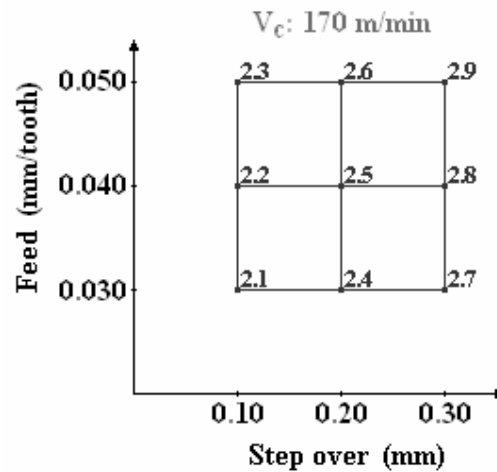


**Figure 5.7 Design matrix for the second set of experiments**

By applying the cutting parameter values given in Figure 5.7, die cavities for the second set of experiments are manufactured. Visual diversities of the manufactured die cavities can be observed in Figure 5.8.

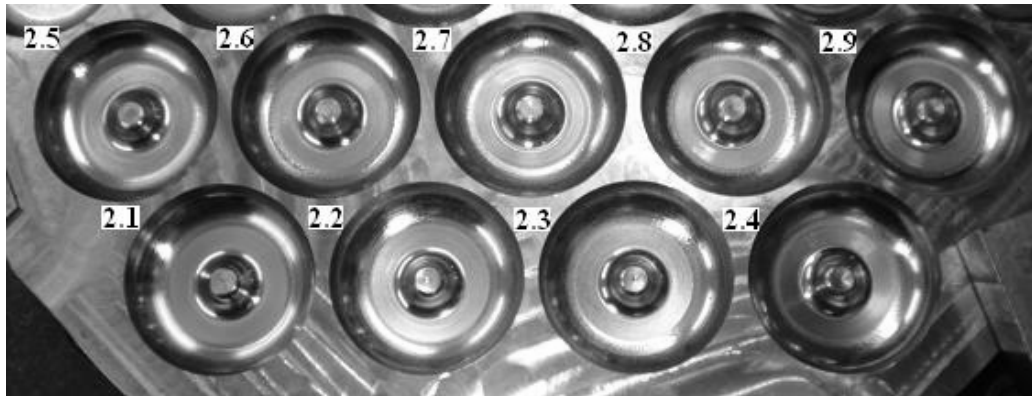


**Figure 5.8 Photograph of the second set of experiments**

At that point it should be remembered that main difference between the first and the second set of experiments is the cutting speed of the ball nose cutter. Geometrical error analysis for the second set of experiments is given in Table 5.3.

When the results of the first and the second set of experiments are examined, it can be concluded that increase in the cutting speed causes slightly higher geometrical error values on the surface profile of the die cavities. All of the measured geometrical error values for the second set are again lower than the defined profile tolerance value. Similar with the results of the first set of experiments, die cavities manufactured with step over value of 0.10 mm have better surface properties than the other die cavities.

**Table 5.3 Results of the second set of experiments**

Exper. No	Cutting Parameters			Geometrical Error		
	Step Over (mm)	Feed (mm/tooth)	Cutting Speed (m/min)	1 <sup>st</sup> Scan Dir. Error Meas. ( $\mu\text{m}$ )	2 <sup>nd</sup> Scan Dir. Error Meas. ( $\mu\text{m}$ )	Average Error ( $\mu\text{m}$ )
2.1	0.10	0.030	170	20	23	21.5
2.2	0.10	0.040	170	29	28	28.5
2.3	0.10	0.050	170	34	33	33.5
2.4	0.20	0.030	170	38	35	36.5
2.5	0.20	0.040	170	41	42	41.5
2.6	0.20	0.050	170	46	42	44.0
2.7	0.30	0.030	170	44	47	45.5
2.8	0.30	0.040	170	49	53	51.0
2.9	0.30	0.050	170	58	56	57.0

By analyzing the main effect plots of the second set of experiments, the input parameters having major influence on the response variable can be found out. Main effects of the step over and the feed on the geometrical error are presented in Figure 5.9-5.10 respectively.

According to the main effect plot of the step over, it can be observed that variation from 0.10 mm to 0.30 mm is resulted with an increase in geometrical error from 27.8  $\mu\text{m}$  to 51.2  $\mu\text{m}$ . Response line characterizes a linear behavior in the range of the step over values. Additionally, variation in the feed induces increase in the geometrical error value similar to the step over but rate of increase is less than the first input parameter. Final observation from the main effect plot of the feed is, response curve has a linear tendency in the range of the second input variable.

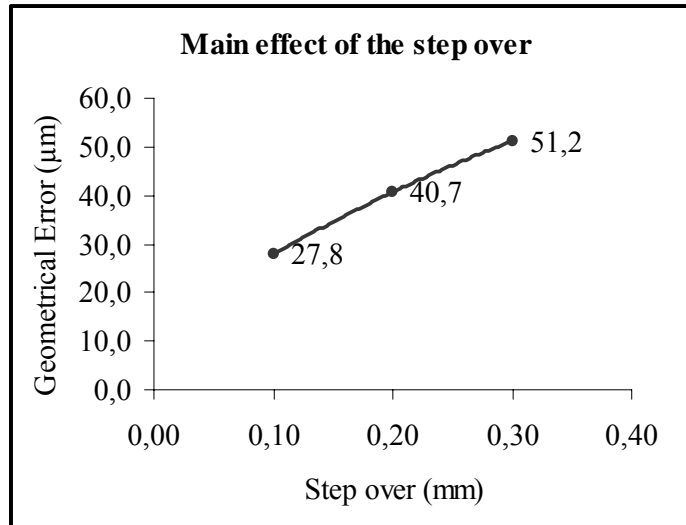


**Figure 5.9 Main effect plot of the first input parameter**

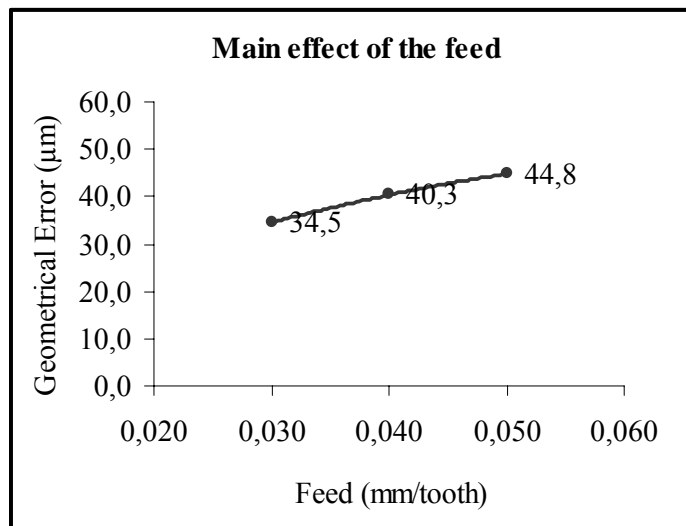


**Figure 5.10 Main effect plot of the second input parameter**

When the interaction effect plot of the input parameters is analyzed for the second set of experiments, it is definite that interaction between the step over and the feed is fairly low due to the similar tendencies of the response curves obtained from the three levels of the parameters. The interaction effect plot of the input parameters is presented in the Figure 5.11.

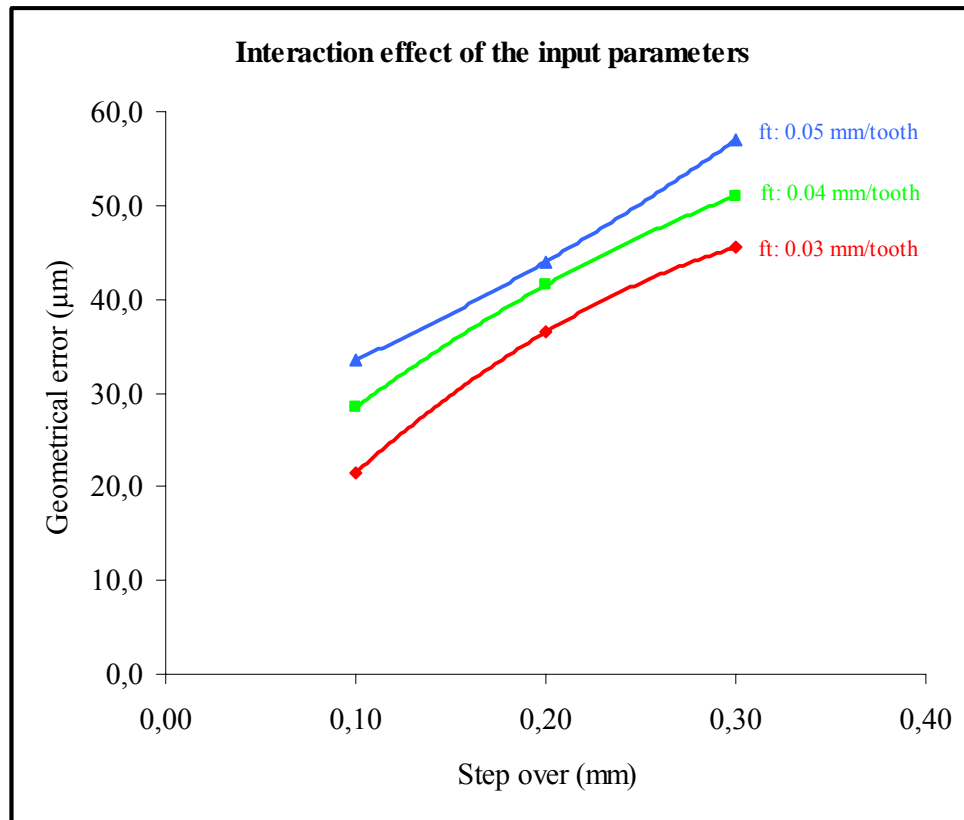


**Figure 5.11 Interaction effect plot of the input parameters**

In Figure 5.12, 3D surface plot for the second set of experiments is presented to relate the cutting parameters with the geometrical error.

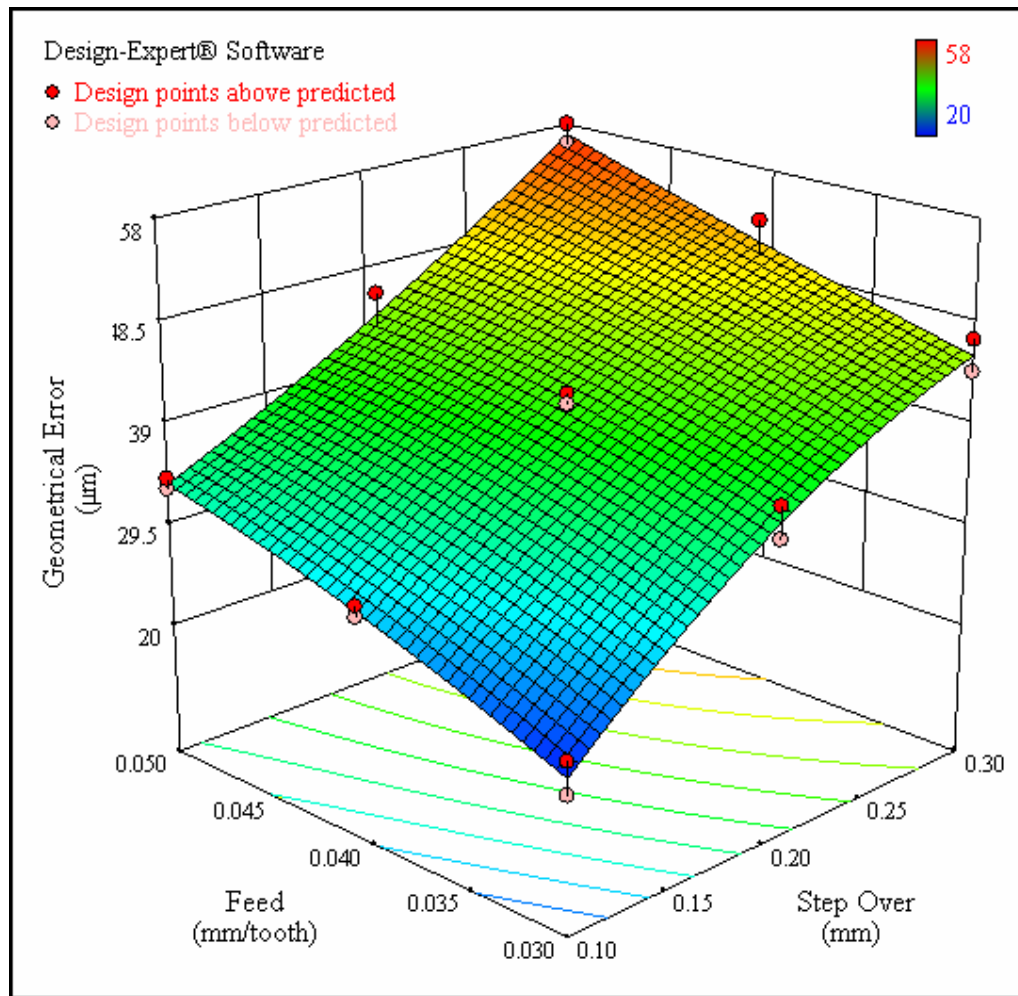


**Figure 5.12** Surface plot of the response variable geometrical error [32]

As a result of these experimental analyses, it is clear that the cutting parameters proportionally influence characteristics of the surface profile in terms of geometrical error and surface quality. Keeping these parameters at lower recommended values provides not only excellent geometrical accuracy and surface quality for the forging die cavities but also elimination of manual polishing utilized in forging die production. At that point it should be kept in mind that, higher surface quality and geometrical accuracy necessitate longer production time for the removal of the same amount of volume. Therefore, optimum cutting parameters for an acceptable

geometrical and surface quality with a reasonable production time should be determined beforehand. For the second set of experiments, again further analysis is performed to clarify the relation between the geometrical error and the production time. Time and error wise comparison of the second set of experiments is presented in Table 5.4.

**Table 5.4 Comparison of geometrical error values with production time values**

Exper. No	Cutting Speed (m/min)	Feed (mm/tooth)	Step Over (mm)	Average Geom. Error ( $\mu\text{m}$ )	Production Time (min)
2.1	170	0.030	0.10	21.5	33.5
2.2	170	0.040	0.10	28.5	25.1
2.3	170	0.050	0.10	33.5	20.1
2.4	170	0.030	0.20	36.5	17.0
2.5	170	0.040	0.20	41.5	12.7
2.6	170	0.050	0.20	44.0	10.2
2.7	170	0.030	0.30	45.5	11.4
2.8	170	0.040	0.30	51.0	8.6
2.9	170	0.050	0.30	57.0	7.0

### 5.3 Geometrical Error Prediction Formula

In order to predict geometrical error values for various applications, a prediction formula is derived. Regression analysis is performed and coefficients of linear regression model mentioned in Chapter 4 are computed.

The least square estimate of  $\beta$  is as follows:

$$\beta = (X^T X)^{-1} X^T y \quad (5.1)$$

where X is the matrix obtained from the input parameters, step over, feed, cutting speed and y is the vector of the response variable, geometrical error. The variable

coefficients are computed by applying the least square method to the experimental data. Details of the coefficient calculations are presented in Appendix E. For the range of cutting speed of 130-170 m/min, feed of 0.030-0.050 mm/tooth, step over of 0.10-0.30 mm; the geometrical error can be predicted in  $\mu\text{m}$  by using the equation:

$$\begin{aligned} \text{Geom\_error} = & -19.083 + 156.67a_e + 831.25f_t + 0.0278V_c \\ & - 250a_e f_t + 2.016 \cdot 10^{-13} a_e V_c + 0.2083 f_t V_c - 75a_e^2 - 3750f_t^2 \end{aligned} \quad (5.2)$$

where  $a_e$  is the step over in mm,  $f_t$  is the feed in mm/tooth and  $V_c$  is the cutting speed in m/min.

In the regression analysis, quadratic term for the cutting speed is excluded from the prediction formula since only two levels are selected for the cutting speed. As mentioned in Section 4.2, three levels are determined for the step over and the feed. Thus, the prediction formula involves quadratic terms for these parameters.

#### 5.4 Verification Analysis for the Finish Cut Experiments

To check for the validity of the prediction formula given in Equation 5.2, additional experiments are performed with different cutting parameter values. Results of the verification experiments are presented in Table 5.5.

**Table 5.5 Results of the verification experiments**

Exper. No	Cutting Parameters			Geometrical Error		
	Step Over (mm)	Feed (mm/tooth)	Cutting Speed (m/min)	1 <sup>st</sup> Scan Dir. Error Meas. ( $\mu\text{m}$ )	2 <sup>nd</sup> Scan Dir. Error Meas. ( $\mu\text{m}$ )	Average Error ( $\mu\text{m}$ )
3.1.1	0.15	0.030	130	27	28	27.5
3.1.2	0.20	0.035	130	38	36	37.0
3.1.3	0.25	0.050	130	48	49	48.5
3.2.1	0.15	0.030	170	28	29	28.5
3.2.2	0.20	0.045	170	43	43	43.0
3.2.3	0.25	0.050	170	52	48	50.0

Visual diversities of the verification cavities can be examined in Figure 5.13.

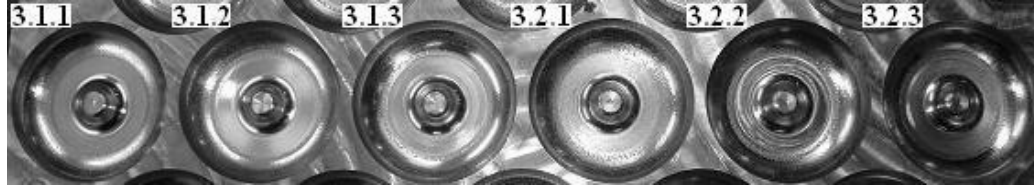


**Figure 5.13 Photograph of the verification experiments**

Comparison of the real geometrical error value with the predicted geometrical error value indicates conformity of the prediction formula for the various cutting parameters. The deviation between these two error values can be calculated as:

$$\%Error = \left| \frac{Z - Z'}{Z} \right| \times 100 \quad (5.3)$$

where  $Z$  is the real geometrical error measured by CMM and  $Z'$  is the predicted geometrical error computed by the prediction formula.

The parameters used in the verification experiments are substituted into Equation 5.2 and the geometrical error values for the verification experiments are calculated. The results of the calculations are given in Table 5.6.

It can be observed from Table 5.6 that the maximum error between the measured error value and the predicted one is 2.00% which is an acceptable error percentage for geometrical error prediction on surface profile of forging die cavities. These results verify that the prediction formula is suitable for geometrical error estimation in forging die cavities when  $\text{Ø}6$  mm ball nose cutter is used in the defined limits of the cutting parameters i.e.  $a_e = 0.10\text{-}0.30$  mm,  $f_t = 0.030\text{-}0.050$  mm/tooth and  $V_c = 130\text{-}170$  m/min.

**Table 5.6 Comparison of predicted error values with measured error values**

<b>Exper. No</b>	<b>Average of the Measured Geometrical Error (<math>\mu\text{m}</math>)</b>	<b>Predicted Geometrical Error (<math>\mu\text{m}</math>)</b>	<b>Error %</b>
3.1.1	27.5	27.6	0.36
3.1.2	37.0	36.6	1.08
3.1.3	48.5	49.4	1.86
3.2.1	28.5	29.0	1.75
3.2.2	43.0	43.1	0.24
3.2.3	50.0	51.0	2.00

## **5.5 Case Study**

Although the experimental profile is defined to analyze the geometrical error on surface profile of the die cavities, a real case application would be beneficial to evaluate validity of the experimental study. For this reason, a case study is conducted to investigate geometrical error on the surface profile of the forging die for a real part geometry which is taken from Aksan Steel Forging Company. Die and forging part geometries are shown in Figure 5.14.

To remove the excess volume in the die cavity, available cutting strategies in the Pro/Engineer Wildfire 3 library [10] are again analyzed. It is realized that “Type\_Spiral” cutting strategy is better than the other cutting strategies in terms of cycle time and tool-workpiece contact duration. Cycle time of the each cutting strategy for the removal of the same amount of volume can be examined in Table 5.7.

The finish cut experiments indicates that increase in the step over and the feed is resulted in linear advance of the geometrical error. Additionally, it is concluded that influence of the step over on the geometrical error is considerably higher than influence of the feed. Therefore, by considering these facts, step over of 0.10 mm, feed of 0.045 mm/tooth and cutting speed of 130 mm/min are selected as values of the finish cut parameters for the case study.

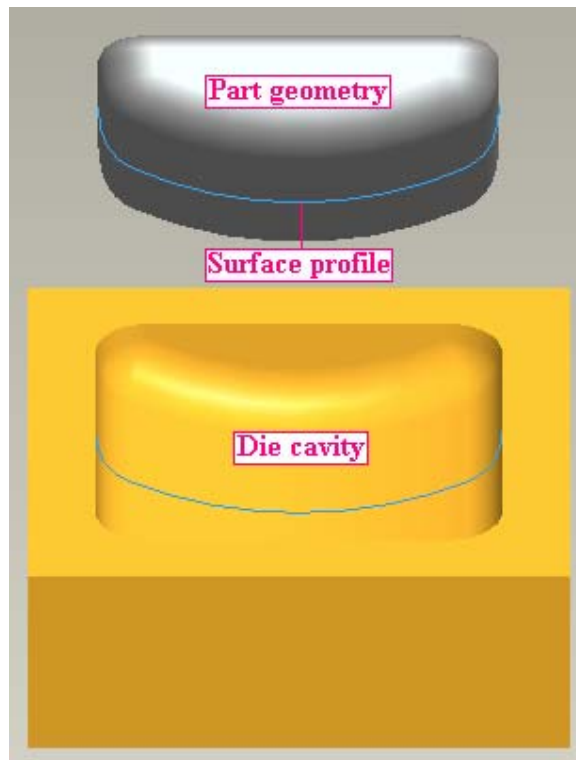


**Figure 5.14 Die and forging part geometries for the case study**

**Table 5.7 Cutting strategies vs. cycle time**

Cutting Strategy	Cycle Time (min)
Type_1	17.92
Type_2	16.73
Type_3	14.00
Type_Spiral	9.92
Type_One_Dir	18.94
Type_1_Connect	18.28
Constant_Load	20.69
Spiral_Maintain_Cut_Direction	12.61
Spiral_Maintain_Cut_Type	12.73
Follow_Hardwalls	11.38

Surface attained after performing finish machining can be visualized in Figure 5.15.

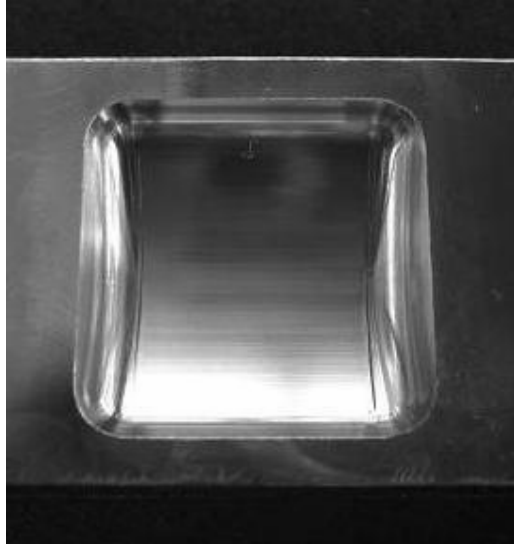


**Figure 5.15 Photograph of the case study**

The geometrical error measurement is performed in a similar way described in Section 4.3.3. The results of the geometrical error measurements for the case study are presented in Table 5.8.

**Table 5.8 Results of the case study**

Experiment	Cutting Parameters			Geometrical Error		
	Step Over (mm)	Feed (mm/tooth)	Cutting Speed (m/min)	1 <sup>st</sup> Scan Dir. Error Meas. (μm)	2 <sup>nd</sup> Scan Dir. Error Meas. (μm)	Average Error (μm)
Case_study	0.10	0.045	130	29	32	30.5

When the input parameters are substituted in Equation 5.2, the geometrical error for the case study is computed as 29.4  $\mu\text{m}$ . The error between the predicted geometrical error and the measured geometrical error is given in Table 5.9.

**Table 5.9 Comparison of predicted error values with measured error values**

<b>Experiment</b>	<b>Average of the Measured Geometrical Error (<math>\mu\text{m}</math>)</b>	<b>Predicted Geometrical Error (<math>\mu\text{m}</math>)</b>	<b>Error %</b>
Case_study	30.5	29.4	3.61

It can be observed from Table 5.9 that the predicted value for the geometrical error is close to the measured average error value. Verification results indicates that the prediction formula is suitable for error estimation on sculptured surfaces of Dievar tool steel when  $\text{Ø}6$  mm ball nose cutter is used for finish cut operations of forging die production. As a result, it can be concluded that Equation 5.2 predicts the geometrical error on surface profile of the die cavities well in the range of the cutting parameters.

## CHAPTER 6

### CONCLUSION

#### 6.1 Conclusions

Geometrical discrepancies may exist between the CAD model of die cavities and the manufactured die cavities. In this study, it is aimed to find out the effects of the cutting parameters i.e. step over, feed and cutting speed on geometrical accuracy of the surface profile of forging die cavities. For this purpose, a representative die cavity profile involving major design features of the forging die cavities is initially determined. The geometrical discrepancy between CAD model of the representative die cavity profile and the manufactured profile is examined by utilizing design of experiment approach. The factorial design is implemented to investigate the influence of the step over, the feed and the cutting speed on the geometrical error. Then, a methodology is developed for the prediction of geometrical error on sculptured surfaces of forging die cavities. Additionally, feed rate optimization is performed for the rough cutting operation of die cavity production by satisfying metal removal rate constant along the tool path trajectory.

Conclusions for the rough cutting process can be summarized as follows:

- In order to obtain the minimum tool path and minimize retract and plunge motions of the tool, various cutting strategies available in Pro/Engineer Wildfire 3 library [10] are analyzed and it is realized that a spiral tool path is more favorable than any other strategy for the rough machining of forging die cavities in terms of cycle time and the tool-workpiece contact duration.

- Lower metal removal rate in some sections of the tool path due to lower step over value than the specified step over value, is common deficiency of the cutting strategies available in the CAM module of Pro/Engineer Wildfire 3 [10]. This problem exists also for the application of the spiral tool path. The spiral tool path for the experimental die cavity geometry is refined by the feed rate optimization to provide the constant metal removal rate along the tool path trajectory. Instead of using a single feed rate value which is 594 mm/min, different and higher feed rate values are utilized along the tool path trajectory. Depending on the geometrical considerations, feed rate values are increased up to 1500 mm/min for cutting process. For the motions of the tool in air, feed rate value of 2000 mm/min is applied. As a consequence of the performed optimization, the metal removal rate is kept at 475.2 mm<sup>3</sup>/min by introducing higher feed rate values in the surface regions of the die cavity where step over value is less than 4 mm. As expected, increase in the feed rate values results in a reduction in the production time of the rough cutting operation. It takes 18.75 min. when the original tool path is used to remove the same amount of volume but with the implementation of higher feed rate values to the machining code, the time required has been reduced to 14.22 min. As a result of this optimization, approximately 24.2% time reduction is attained for the rough machining of the experimental die cavity geometry.

The following conclusions have been reached as results of the finish cut experiments:

- In the first set of experiments where the cutting speed is 130 m/min, it is observed that the variation in the step over is more influential than the variation in the feed to the geometrical error. When the main effect plot of the step over is examined, it is realized that the geometrical error averages are 26.7 μm, 38.7 μm and 50.0 μm. The geometrical error averages due to the feed variation are close to each other and observed as 33.3 μm, 38.5 μm and 43.5 μm indicating that feed variation is less effective on the geometrical error than the step over variation.

- The second set of experiments is performed to analyze the effect of the cutting speed as the third input parameter on the geometrical error. According to the tool steel manufacturer's recommendations [34], the cutting speed is taken as 170 m/min for the second set of experiments. The geometrical error averages as a result of the step over change are 27.8  $\mu\text{m}$ , 40.7  $\mu\text{m}$  and 51.2  $\mu\text{m}$ . The geometrical error averages due to feed variation are again quite close to each other i.e. 34.5  $\mu\text{m}$ , 40.3  $\mu\text{m}$  and 44.8  $\mu\text{m}$ .
- Time wise analysis is also performed for the defined cutting parameters of finish cut experiments to evaluate geometrical error vs. production time relationship. It is realized that the production time is almost inversely proportional to the input parameters. By keeping the feed constant, doubling the step over value lowers production time to half of its value. The opposite is also true since variation of the step over and/or the feed results in similar tendency in the time response.
- As a consequence of the first and the second set of experiments, it is clear that increasing the cutting speed results in reduction of ~26% in production time with slightly higher geometrical error values. It is also realized that change in the step over is more effective on the geometrical error than the change in the feed. From these observations, it is concluded that low step over values together with slightly high feed values would provide excellent geometrical accuracy and surface quality in a reasonable production time.
- In order to estimate the geometrical error on sculptured surfaces of forging die cavities, the geometrical error prediction formula has been derived. When Dievar tool steel is considered as die material and  $\text{\O}6$  mm solid carbide ball nose cutter is utilized for finishing operations, the geometrical error can be estimated by the following equation:

$$\begin{aligned} \text{Geom\_error} = & -19.083 + 156.67a_e + 831.25f_t + 0.0278V_c \\ & - 250a_e f_t + 2.016 \cdot 10^{-13} a_e V_c + 0.2083f_t V_c - 75a_e^2 - 3750f_t^2 \end{aligned} \quad (6.1)$$

where  $a_e$  is the step over in mm,  $f_t$  is the feed in mm/tooth and  $V_c$  is the cutting speed in m/min.

- Validity of the prediction formula is tested by performing verification experiments for the representative die geometry and a die cavity geometry of a forging part used in industry. The maximum prediction error is observed as 3.61% indicating that the prediction formula is good enough for the error estimation on sculptured surfaces of Dievar tool steel. Therefore, it is concluded that the derived mathematical model is promising to be applicable for geometrical error prediction on the surface profile of the forging die cavities in the chosen range of the cutting parameters i.e.  $a_e = 0.10-0.30$  mm,  $f_t = 0.030-0.050$  mm/tooth and  $V_c = 130-170$  m/min.

## **6.2 Recommendations for Future Work**

- The cutting strategies of other CAM software systems may be analyzed and compared with Pro/Engineer Wildfire 3 library. In case of superior strategy than the spiral tool path, this strategy may be exposed to optimization for the rough machining process of forging dies.
- This work may be extended for different type and size of milling cutters.
- Cutting parameter values higher than the recommended values may be utilized for the finish cut experiments to investigate the geometrical error variation in the outside of the proposed range of the parameters.
- Similar study may be conducted to analyze the effects of cutting parameters on surface roughness of the die cavities.
- The effects of cutting parameters on tool life may be studied and the ways to improve the tool life may be investigated.
- Cutting forces may be calculated for various positions of the cutter during machining of sculptured surfaces.

## REFERENCES

- [1] Boyer H., "Metals Handbook Forging and Casting", (1971) ASM Handbook Committee, 8<sup>th</sup> Edition.
- [2] Strecon, web site: "<http://www.strecon.com>", last accessed: September 2007.
- [3] Forging Industry Association, web site: "<http://www.forging.org/facts>", last accessed: August 2007.
- [4] Aksan Steel Forging Company, web site: "<http://www.aksanforging.com>", last accessed: October 2007.
- [5] Ghanem F., Braham C., Sidhom H., "Influence of steel type on electrical discharge machined surface integrity", *Journal of Materials Processing Technology*, 142 (2003) 163-173.
- [6] Cusanelli G., Hessler Wyser A., Bobard F., Demellayer R., Perez R., Flükiger R., "Microstructure at submicron scale of the white layer produced by EDM technique", *Journal of Materials Processing Technology*, 149 (2004) 289-295.
- [7] P. FallboEhmer, C.A. RodroAguéz, T. Ozel, T. Altan, "High speed machining of cast iron and alloy steels for die and mold manufacturing", *Journal of Materials Processing Technology*, 98 (2000) 104-115.
- [8] B. Kecelj, J. Kopac, Z. Kampus, K. Kuzman, "Speciality of HSC in manufacturing of forging dies", *Journal of Materials Processing Technology* 157-158 (2004) 536-542.

- [9] J. Vivancos, C.J. Lui, L. Costa, J.A. Ortiz, "Optimal machining parameters selection in high speed milling of hardened steels for injection moulds", *Journal of Materials Processing Technology*, 155-156 (2004) 1505-1512.
- [10] Manufacturing Module of Pro/Engineer Wildfire 3.
- [11] L.N. Lopez de Lacalle, A. Lamikiz, J.A. Sanchez, J.L. Arana, "Improving the surface finish in high speed milling of stamping dies", *Journal of Materials Processing Technology* 123 (2002) 292-302.
- [12] R.T. Coelho, L.R. Silva, A. Braghini, A.A. Bezerra, "Some effects of cutting edge preparation and geometric modifications when turning INCONEL 718TM at high cutting speeds", *Journal of Materials Processing Technology* 148 (2004) 147-153.
- [13] A. Kaldos, I.F. Dagiloke, A. Boyle, "Computer aided cutting process parameter selection for high speed milling", *Journal of Materials Processing Technology* 61 (1996) 219-224.
- [14] W.T. Chien, C.S. Tsai, "The investigation on the prediction of tool wear and the determination of optimum cutting conditions in machining 17-4PH stainless steel", *Journal of Materials Processing Technology* 140 (2003) 340-345.
- [15] H. Juan, S.F. Yu, B.Y. Lee, "The optimal cutting-parameter selection of production cost in HSM for SKD61 tool steels", *International Journal of Machine Tools & Manufacture. Design, Research and Application* 43 (2003) 679-686.
- [16] L.N. Lopez de Lacalle, A. Lamikiz, M.A. Salgado, S. Herranz, A. Rivero, "Process planning for reliable high-speed machining of moulds", *International Journal of Production Research* 40 (12) (2002) 2789-2809.

[17] R. Salami, M.H. Sadeghi, B. Motakef, "Feed rate optimization for 3-axis ball-end milling of sculptured surfaces", *International Journal of Machine Tools & Manufacture* 47 (2007) 760-767.

[18] Jenq Shyong By Chen, Yung Kuo Huang, Mao-Son Chen, "Feed rate optimization and tool profile modification for the high-efficiency ball end milling process", *International Journal of Machine Tools & Manufacture* 45 (2005) 1070-1076.

[19] M. Monreal, C.A. Rodriguez, "Influence of tool path strategy on the cycle time of high-speed milling", *Computer Aided Design* 35 (2003) 395-401.

[20] Cengiz Ender, "Development of postprocessor simulation and verification software for a five-axis CNC milling machine" M. S. Thesis, Middle East Technical University, Ankara, Turkey, 2005.

[21] Kazım Arda Çelik, "Development of a methodology for prediction of surface roughness of curved cavities manufactured by 5-axes CNC milling" M. S. Thesis, Middle East Technical University, Ankara, Turkey, 2007.

[22] Wikipedia, web site: "[http://en.wikipedia.org/wiki/Geometric\\_Dimensioning\\_and\\_Tolerancing](http://en.wikipedia.org/wiki/Geometric_Dimensioning_and_Tolerancing)", last accessed: October 2007.

[23] Gene R. Cogorno, "Geometric Dimensioning and Tolerancing for Mechanical Design", (2006) McGraw Hill Mechanical Engineering.

[24] Roymech, web site: "[http://www.roymech.co.uk/Useful\\_Tables/Drawing](http://www.roymech.co.uk/Useful_Tables/Drawing)", last accessed: September 2007.

[25] DIN 7526, German standard for forging die tolerances.

[26] “Development of Modeling Tools for the Forging Industry”, (1999) School of Mechanical Engineering, University of Bath.

[27] DIN 7523, German standard for forging die design.

[28] A. M. Sabroff, F. W. Boulger, H. J. Henning, “Forging Materials and Practices”, (1968) Reinhold Book Corporation.

[29] Fitzpatric Michael, “Machining and CNC technology”, (2005) MC Graw Hill.

[30] Iscar, “The Catalog of Metal Working Tools”, (2004) Complete Machining Solutions.

[31] Montgomery D.C., “Design and Analysis of Experiments”, (2001) New York Wiley.

[32] General Factorial Design Section of Design-Expert Statistical Software Program.

[33] Mazak Variaxis 630-5X Operating Manual.

[34] Assab Korkmaz Dievar Tool Steel Catalog.

## APPENDIX A

### MAZAK VARIAXIS 630-5X CNC MILLING CENTER

The 5-axis vertical machining center, Mazak Variaxis 630-5x, shown in Figure A.1 is designed targeting high speed and high accuracy machining of products. In the production of wide variety of parts in small to medium lot size, shorter cycle time is achieved by reduced idle time which is made possible by applying high speed operation up to 25000 rpm [33]. Linear guides are used for the X, Y and Z axis slide ways to provide high rigidity to ensure high accuracy in high speed operation. Positioning accuracy is  $\pm 3 \mu\text{m}$  and repeatability  $\pm 1 \mu\text{m}$  [33]. In this 5-axis machine tool; X, Y and Z axes are the linear axes. A axis denotes rotational axis around X axis and C axis denotes rotational axis around Z axis.



**Figure A.1 Mazak Variaxis 630-5x milling center**

Machine properties are:

- Maximum feed rate is 50 m/min
- Maximum speed of spindle 25000 rpm
- Maximum spindle power 30 Hp
- Maximum workpiece weight 500 kg
- Magazine of 30 tool capacity
- X axis stroke 630 mm
- Y axis stroke 765 mm
- Z axis stroke 510 mm
- C axis rotation 360°
- A axis rotation 150° (-120° / +30°)

## APPENDIX B

### DIEVAR PREMIUM HOT WORK TOOL STEEL

#### B.1 General

Dievar is a premium hot work tool steel developed by Uddeholm [34]. It is manufactured utilizing latest production and refining techniques. Dievar development has yielded a die steel with the ultimate resistance to heat checking, gross cracking, hot wear and plastic deformation. The unique properties profile for Dievar makes it one of the best choice for die casting, forging and extrusion [34]. Information about chemical composition of Dievar and hardness value at delivery stage can be analyzed from Table B.1.

**Table B.1 General characteristics of Dievar [34]**

Standard specification	Cr-Mo-V alloyed hot work tool steel
Delivery condition	Soft annealed to approx. 160 HB
Colour code	Grey/yellow

## B.2 Hot Work Applications

Heat checking is one of the most common failure mechanism e.g. in die casting and nowadays also in forging applications. Dievar's superior ductility yields the highest possible level of heat checking resistance. With Dievar's outstanding toughness and hardenability the resistance to heat checking can further be improved. If gross cracking is not a factor then a higher working hardness can be utilized (i.e. +2 HRC). Regardless of the dominant failure mechanism; e.g. heat checking, gross cracking, hot wear or plastic deformation. Dievar offers the potential for significant improvements in die life and then resulting in better tooling economy [34].

## B.3 Properties

The reported properties are representative of samples which have been taken from the centre of a 610 x 203 mm bar. Unless otherwise is indicated all specimens have been hardened at 1025°C, quenched in oil and tempered twice at 625°C for two hours; yielding a working hardness of 44-46 HRC [34]. Physical and mechanical properties of tool steel Dievar are presented in Table B.2-B.3.

**Table B.2 Physical properties of Dievar [34]**

Temperature	20°C	400°C	600°C
Density, kg/m <sup>3</sup>	7 800	7 700	7 600
Modulus of elasticity MPa	210 000	180 000	145 000
Coefficient of thermal expansion per °C from 20°C	–	12,7 x 10 <sup>-6</sup>	13,3 x 10 <sup>-6</sup>
Thermal conductivity W/m °C	–	31	32

**Table B.3 Mechanical properties of Dievar [34]**

Hardness	44 HRC	48 HRC	52 HRC
Tensile strength, $R_m$	1480 MPa	1640 MPa	1900 MPa
Yield strength, $R_{p0,2}$	1210 MPa	1380 MPa	1560 MPa
Elongation, $A_5$	13 %	13 %	12,5 %
Reduction of area, $Z$	55 %	55 %	52 %

## APPENDIX C

### PROPERTIES OF THE CUTTING TOOLS USED IN ROUGH AND FINISH CUT MILLING

#### C.1 General

For the rough cutting operation, Grayson branded  $\text{Ø}6$  mm flat carbide end mill with two flutes has been used. Dimensional properties of the rough cutting tool are given in Figure C.1.

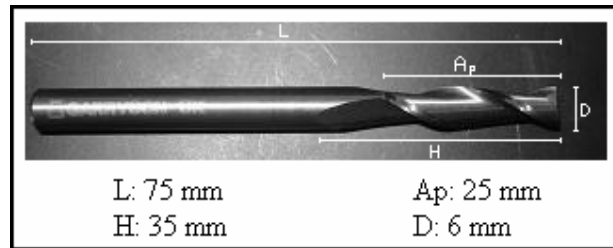


**Figure C.1 Dimensional properties of the rough cutter**

For the finishing operation, again Grayson branded  $\text{Ø}6$  mm ball nose carbide mill with two flutes has been used throughout the experiments. Dimensional properties of the finish cutting tool are given in Figure C.2.

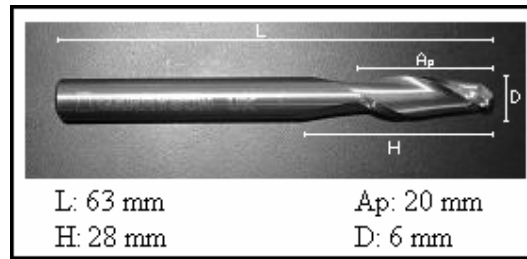


**Figure C.2 Dimensional properties of the finish cutter**

## C.2 Cutting Data Recommendations of Dievar Tool Steel for Carbide Tools

The cutting data given in Table C.1 are to be considered as guiding values which must be adapted to existing local condition.

**Table C.1 Cutting data recommendations for end milling [34]**

End milling			
Cutting data parameters	Type of milling		
	Solid carbide	Carbide indexable insert	High speed steel
Cutting speed ( $v_c$ ) m/min	130–170	120–160	25–30 <sup>1)</sup>
Feed ( $f_z$ ) mm/tooth	0,03–0,20 <sup>2)</sup>	0,08–0,20 <sup>2)</sup>	0,05–0,35 <sup>2)</sup>
Carbide designation ISO US	–	P20–P30 C6–C5	– –

<sup>1)</sup> For coated HSS end mill  $v_c$  45–50m/min. (150–160 f.p.m.).  
<sup>2)</sup> Depending on radial depth of cut and cutter diameter.

## APPENDIX D

### ORIGINAL TOOL PATH VS. OPTIMIZED TOOL PATH

The original tool path obtained from CAM module of Pro/Engineer Wildfire 3 [10] and the optimized tool path in which metal removal rate is kept constant are given as follows:

<u>Original Codes</u>	<u>Optimized Codes</u>
T1M6	T1M6
S7427M3	S7427M3
M8	M8
G94	G94
G90	G90
G54	G54
G0X0.Y.605	G0X0.Y.605
Z5.	Z5.
G1Z-.2F50.	G1Z-.2F50.
G3X0.Y.605I0.J-.605F594.	G3X0.Y.605I0.J-.605F594.
G1Y4.605	G1Y4.605
G3X0.Y4.605I0.J-4.605	G3X0.Y4.605I0.J-4.605
G1Y8.605	G1Y8.605
G3X0.Y8.605I0.J-8.605	G3X0.Y8.605I0.J-8.605
G1Y12.605	G1Y12.605
G3X0.Y12.605I0.J-12.605	G3X0.Y12.605I0.J-12.605
G1Y16.605	G1Y16.605
G3X0.Y16.605I0.J-16.605	G3X0.Y16.605I0.J-16.605
G1Y.581	G1Y.581F2000.
Z-.4F50.	Z-.4F50.
G3X0.Y.581I0.J-.581F594.	G3X0.Y.581I0.J-.581F594.
G1Y4.581	G1Y4.581
G3X0.Y4.581I0.J-4.581	G3X0.Y4.581I0.J-4.581
G1Y8.581	G1Y8.581
G3X0.Y8.581I0.J-8.581	G3X0.Y8.581I0.J-8.581
G1Y12.581	G1Y12.581
G3X0.Y12.581I0.J-12.581	G3X0.Y12.581I0.J-12.581
G1Y16.581	G1Y16.581
G3X0.Y16.581I0.J-16.581	G3X0.Y16.581I0.J-16.581
G1Y.556	G1Y.556F2000.

Original Codes

G1Y.556  
Z-.6F50.  
G3X0.Y.556I0.J-.556F594.  
G1Y4.556  
G3X0.Y4.556I0.J-4.556  
G1Y8.556  
G3X0.Y8.556I0.J-8.556  
G1Y12.556  
G3X0.Y12.556I0.J-12.556  
G1Y16.556  
G3X0.Y16.556I0.J-16.556  
G1Y.531  
Z-.8F50.  
G3X0.Y.531I0.J-.531F594.  
G1Y4.531  
G3X0.Y4.531I0.J-4.531  
G1Y8.531  
G3X0.Y8.531I0.J-8.531  
G1Y12.531  
G3X0.Y12.531I0.J-12.531  
G1Y16.531  
G3X0.Y16.531I0.J-16.531  
G1Y.507  
Z-1.F50.  
G3X0.Y.507I0.J-.507F594.  
G1Y4.507  
G3X0.Y4.507I0.J-4.507  
G1Y8.507  
G3X0.Y8.507I0.J-8.507  
G1Y12.507  
G3X0.Y12.507I0.J-12.507  
G1Y16.507  
G3X0.Y16.507I0.J-16.507  
G1Y.482  
Z-1.2F50.  
G3X0.Y.482I0.J-.482F594.  
G1Y4.482  
G3X0.Y4.482I0.J-4.482  
G1Y8.482  
G3X0.Y8.482I0.J-8.482  
G1Y12.482  
G3X0.Y12.482I0.J-12.482  
G1Y16.482  
G3X0.Y16.482I0.J-16.482  
G1Y.458  
Z-1.4F50.  
G3X0.Y.458I0.J-.458F594.  
G1Y4.458  
G3X0.Y4.458I0.J-4.458  
G1Y8.458  
G3X0.Y8.458I0.J-8.458  
G1Y12.458

Optimized Codes

G1Y.556F2000.  
Z-.6F50.  
G3X0.Y.556I0.J-.556F594.  
G1Y4.556  
G3X0.Y4.556I0.J-4.556  
G1Y8.556  
G3X0.Y8.556I0.J-8.556  
G1Y12.556  
G3X0.Y12.556I0.J-12.556  
G1Y16.556  
G3X0.Y16.556I0.J-16.556  
G1Y.531F2000.  
Z-.8F50.  
G3X0.Y.531I0.J-.531F594.  
G1Y4.531  
G3X0.Y4.531I0.J-4.531  
G1Y8.531  
G3X0.Y8.531I0.J-8.531  
G1Y12.531  
G3X0.Y12.531I0.J-12.531  
G1Y16.531  
G3X0.Y16.531I0.J-16.531  
G1Y.507F2000.  
Z-1.F50.  
G3X0.Y.507I0.J-.507F594.  
G1Y4.507  
G3X0.Y4.507I0.J-4.507  
G1Y8.507  
G3X0.Y8.507I0.J-8.507  
G1Y12.507  
G3X0.Y12.507I0.J-12.507  
G1Y16.507  
G3X0.Y16.507I0.J-16.507  
G1Y.482F2000.  
Z-1.2F50.  
G3X0.Y.482I0.J-.482F594.  
G1Y4.482  
G3X0.Y4.482I0.J-4.482  
G1Y8.482  
G3X0.Y8.482I0.J-8.482  
G1Y12.482  
G3X0.Y12.482I0.J-12.482  
G1Y16.482  
G3X0.Y16.482I0.J-16.482  
G1Y.458F2000.  
Z-1.4F50.  
G3X0.Y.458I0.J-.458F594.  
G1Y4.458  
G3X0.Y4.458I0.J-4.458  
G1Y8.458  
G3X0.Y8.458I0.J-8.458  
G1Y12.458

Original Codes

G3X0.Y12.458I0.J-12.458  
G1Y16.458  
G3X0.Y16.458I0.J-16.458  
G1Y.433  
Z-1.6F50.  
G3X0.Y.433I0.J-.433F594.  
G1Y4.433  
G3X0.Y4.433I0.J-4.433  
G1Y8.433  
G3X0.Y8.433I0.J-8.433  
G1Y12.433  
G3X0.Y12.433I0.J-12.433  
G1Y16.433  
G3X0.Y16.433I0.J-16.433  
G1Y.409  
Z-1.8F50.  
G3X0.Y.409I0.J-.409F594.  
G1Y4.409  
G3X0.Y4.409I0.J-4.409  
G1Y8.409  
G3X0.Y8.409I0.J-8.409  
G1Y12.409  
G3X0.Y12.409I0.J-12.409  
G1Y16.409  
G3X0.Y16.409I0.J-16.409  
G1Y.384  
Z-2.F50.  
G3X0.Y.384I0.J-.384F594.  
G1Y4.384  
G3X0.Y4.384I0.J-4.384  
G1Y8.384  
G3X0.Y8.384I0.J-8.384  
G1Y12.384  
G3X0.Y12.384I0.J-12.384  
G1Y16.384  
G3X0.Y16.384I0.J-16.384  
G1Y.36  
Z-2.2F50.  
G3X0.Y.36I0.J-.36F594.  
G1Y4.36  
G3X0.Y4.36I0.J-4.36  
G1Y8.36  
G3X0.Y8.36I0.J-8.36  
G1Y12.36  
G3X0.Y12.36I0.J-12.36  
G1Y16.36  
G3X0.Y16.36I0.J-16.36  
G1Y.335  
Z-2.4F50.  
G3X0.Y.335I0.J-.335F594.  
G1Y4.335  
G3X0.Y4.335I0.J-4.335

Optimized Codes

G3X0.Y12.458I0.J-12.458  
G1Y16.458  
G3X0.Y16.458I0.J-16.458  
G1Y.433F2000.  
Z-1.6F50.  
G3X0.Y.433I0.J-.433F594.  
G1Y4.433  
G3X0.Y4.433I0.J-4.433  
G1Y8.433  
G3X0.Y8.433I0.J-8.433  
G1Y12.433  
G3X0.Y12.433I0.J-12.433  
G1Y16.433  
G3X0.Y16.433I0.J-16.433  
G1Y.409F2000.  
Z-1.8F50.  
G3X0.Y.409I0.J-.409F594.  
G1Y4.409  
G3X0.Y4.409I0.J-4.409  
G1Y8.409  
G3X0.Y8.409I0.J-8.409  
G1Y12.409  
G3X0.Y12.409I0.J-12.409  
G1Y16.409  
G3X0.Y16.409I0.J-16.409  
G1Y.384F2000.  
Z-2.F50.  
G3X0.Y.384I0.J-.384F594.  
G1Y4.384  
G3X0.Y4.384I0.J-4.384  
G1Y8.384  
G3X0.Y8.384I0.J-8.384  
G1Y12.384  
G3X0.Y12.384I0.J-12.384  
G1Y16.384  
G3X0.Y16.384I0.J-16.384  
G1Y.36F2000.  
Z-2.2F50.  
G3X0.Y.36I0.J-.36F594.  
G1Y4.36  
G3X0.Y4.36I0.J-4.36  
G1Y8.36  
G3X0.Y8.36I0.J-8.36  
G1Y12.36  
G3X0.Y12.36I0.J-12.36  
G1Y16.36  
G3X0.Y16.36I0.J-16.36  
G1Y.335F2000.  
Z-2.4F50.  
G3X0.Y.335I0.J-.335F594.  
G1Y4.335  
G3X0.Y4.335I0.J-4.335

Original Codes

G1Y8.335  
 G3X0.Y8.335I0.J-8.335  
 G1Y12.335  
 G3X0.Y12.335I0.J-12.335  
 G1Y16.335  
 G3X0.Y16.335I0.J-16.335  
 G1Y.305  
 Z-2.6F50.  
 G3X0.Y.305I0.J-.305F594.  
 G1Y4.305  
 G3X0.Y4.305I0.J-4.305  
 G1Y8.305  
 G3X0.Y8.305I0.J-8.305  
 G1Y12.305  
 G3X0.Y12.305I0.J-12.305  
 G1Y16.305  
 G3X0.Y16.305I0.J-16.305  
 G1Y.266  
 Z-2.8F50.  
 G3X0.Y.266I0.J-.266F594.  
 G1Y4.266  
 G3X0.Y4.266I0.J-4.266  
 G1Y8.266  
 G3X0.Y8.266I0.J-8.266  
 G1Y12.266  
 G3X0.Y12.266I0.J-12.266  
 G1Y16.266  
 G3X0.Y16.266I0.J-16.266  
 G1Y.242  
 Z-2.9F50.  
 G3X0.Y.242I0.J-.242F594.  
 G1Y4.242  
 G3X0.Y4.242I0.J-4.242  
 G1Y8.242  
 G3X0.Y8.242I0.J-8.242  
 G1Y12.242  
 G3X0.Y12.242I0.J-12.242  
 G1Y16.242  
 G3X0.Y16.242I0.J-16.242  
 G1Y12.185  
 Z-3.1F50.  
 G3X12.185Y0.I0.J-12.185F594.  
 G1X9.724  
 G2X9.724Y0.I-9.724J0.  
 G1X5.724  
 G2X0.Y5.724I-5.724J0.  
 X5.724Y0.I0.J-5.724  
 G1X12.185  
 G3X0.Y12.185I-12.185J0.  
 G1Y16.185  
 G3X0.Y16.185I0.J-16.185  
 G1Y12.117

Optimized Codes

G1Y8.335  
 G3X0.Y8.335I0.J-8.335  
 G1Y12.335  
 G3X0.Y12.335I0.J-12.335  
 G1Y16.335  
 G3X0.Y16.335I0.J-16.335  
 G1Y.305F2000.  
 Z-2.6F50.  
 G3X0.Y.305I0.J-.305F594.  
 G1Y4.305  
 G3X0.Y4.305I0.J-4.305  
 G1Y8.305  
 G3X0.Y8.305I0.J-8.305  
 G1Y12.305  
 G3X0.Y12.305I0.J-12.305  
 G1Y16.305  
 G3X0.Y16.305I0.J-16.305  
 G1Y.266F2000.  
 Z-2.8F50.  
 G3X0.Y.266I0.J-.266F594.  
 G1Y4.266  
 G3X0.Y4.266I0.J-4.266  
 G1Y8.266  
 G3X0.Y8.266I0.J-8.266  
 G1Y12.266  
 G3X0.Y12.266I0.J-12.266  
 G1Y16.266  
 G3X0.Y16.266I0.J-16.266  
 G1Y.242F2000.  
 Z-2.9F50.  
 G3X0.Y.242I0.J-.242F1188.  
 G1Y4.242  
 G3X0.Y4.242I0.J-4.242  
 G1Y8.242  
 G3X0.Y8.242I0.J-8.242  
 G1Y12.242  
 G3X0.Y12.242I0.J-12.242  
 G1Y16.242  
 G3X0.Y16.242I0.J-16.242  
 G1Y12.185F2000.  
 Z-3.1F50.  
 G3X12.185Y0.I0.J-12.185F594.  
 G1X9.724  
 G2X9.724Y0.I-9.724J0.F965.  
 G1X5.724F594.  
 G2X5.724Y0.I-5.724J0.  
 G1X12.185F2000.  
 G3X0.Y12.185I-12.185J0.F594.  
 G1Y16.185  
 G3X0.Y16.185I0.J-16.185  
 G1Y12.117F2000.

Original Codes

Z-3.3F50.  
G3X12.117Y0.I0.J-12.117F594.  
G1X10.154  
G2X0.Y10.154I-10.154J0.  
X10.154Y0.I0.J-10.154  
G1X6.154  
G2X0.Y6.154I-6.154J0.  
X6.154Y0.I0.J-6.154  
G1X12.117  
G3X0.Y12.117I-12.117J0.  
G1Y16.117  
G3X0.Y16.117I0.J-16.117  
G1Y6.154  
G2X0.Y-6.154I0.J-6.154  
G1Y-12.038  
Z-3.5F50.  
G3X-12.038Y0.I0.J12.038F594.  
G1X-10.423  
G2X-10.423Y0.I10.423J0.  
G1X-6.423  
G2X-6.423Y0.I6.423J0.  
G1X-12.038  
G3X0.Y-12.038I12.038J0.  
G1Y-16.038  
G3X0.Y-16.038I0.J16.038  
G1Y-11.945  
Z-3.7F50.  
G3X-11.945Y0.I0.J11.945F594.  
G1X-10.62  
G2X-10.62Y0.I10.62J0.  
G1X-6.62  
G2X-6.62Y0.I6.62J0.  
G1X-11.945  
G3X0.Y-11.945I11.945J0.  
G1Y-15.945  
G3X0.Y-15.945I0.J15.945  
G1Y-11.838  
Z-3.9F50.  
G3X-11.838Y0.I0.J11.838F594.  
G1X-10.77  
G2X-10.77Y0.I10.77J0.  
G1X-6.77  
G2X-6.77Y0.I6.77J0.  
G1X-11.838  
G3X0.Y-11.838I11.838J0.  
G1Y-15.838  
G3X0.Y-15.838I0.J15.838  
G1Y-11.716  
Z-4.1F50.  
G3X-11.716Y0.I0.J11.716F594.  
G1X-10.89  
G2X-10.89Y0.I10.89J0.  
G1X-6.89

Optimized Codes

Z-3.3F50.  
G3X12.117Y0.I0.J-12.117F594.  
G1X10.154  
G2X10.154Y0.I-10.154J0.F1210.  
G1X6.154F594.  
G2X6.154Y0.I-6.154J0.  
G1X12.117F2000.  
G3X0.Y12.117I-12.117J0.F594.  
G1Y16.117  
G3X0.Y16.117I0.J-16.117  
G1Y6.154F2000.  
G2X0.Y-6.154I0.J-6.154  
G1Y-12.038  
Z-3.5F50.  
G3X-12.038Y0.I0.J12.038F594.  
G1X-10.423  
G2X-10.423Y0.I10.423J0.F1471.  
G1X-6.423F594.  
G2X-6.423Y0.I6.423J0.  
G1X-12.038F2000.  
G3X0.Y-12.038I12.038J0.F594.  
G1Y-16.038  
G3X0.Y-16.038I0.J16.038  
G1Y-11.945F2000.  
Z-3.7F50.  
G3X-11.945Y0.I0.J11.945F594.  
G1X-10.62  
G2X-10.62Y0.I10.62J0.F1500.  
G1X-6.62F594.  
G2X-6.62Y0.I6.62J0.  
G1X-11.945F2000.  
G3X0.Y-11.945I11.945J0.F594.  
G1Y-15.945  
G3X0.Y-15.945I0.J15.945  
G1Y-11.838F2000.  
Z-3.9F50.  
G3X-11.838Y0.I0.J11.838F594.  
G1X-10.77  
G2X-10.77Y0.I10.77J0.F1500.  
G1X-6.77F594.  
G2X-6.77Y0.I6.77J0.  
G1X-11.838F2000.  
G3X0.Y-11.838I11.838J0.F594.  
G1Y-15.838  
G3X0.Y-15.838I0.J15.838  
G1Y-11.716F2000.  
Z-4.1F50.  
G3X-11.716Y0.I0.J11.716F594.  
G1X-10.89  
G2X-10.89Y0.I10.89J0.F1500.  
G1X-6.89F594.

Original Codes

G2X-6.89Y0.I6.89J0.  
 G1X-11.716  
 G3X0.Y-11.716I11.716J0.  
 G1Y-15.716  
 G3X0.Y-15.716I0.J15.716  
 G1Y-6.89  
 G3X0.Y6.89I0.J6.89  
 G1Y11.577  
 Z-4.3F50.  
 G3X11.577Y0.I0.J-11.577F594.  
 G1X11.005  
 G2X11.005Y0.I-11.005J0.  
 G1X7.005  
 G2X7.005Y0.I-7.005J0.  
 G1X11.577  
 G3X0.Y11.577I-11.577J0.  
 G1Y15.577  
 G3X0.Y15.577I0.J-15.577  
 G1Y7.005  
 G2X0.Y-7.005I0.J-7.005  
 G1Y-11.418  
 Z-4.5F50.  
 G3X-11.418Y0.I0.J11.418F594.  
 G1X-11.121  
 G2X-11.121Y0.I11.121J0.  
 G1X-7.121  
 G2X-7.121Y0.I7.121J0.  
 G1X-11.418  
 G3X0.Y-11.418I11.418J0.  
 G1Y-15.418  
 G3X0.Y-15.418I0.J15.418  
 G1Y-11.237  
 Z-4.7F50.  
 G3X0.Y-11.273I0.J11.237F594.  
 G2X-11.237Y0.I0.J11.237  
 G1X-7.236  
 G2X-7.236Y0.I7.236J0.  
 G1X-11.236  
 G3X0.Y-11.237I11.237J0.  
 G1Y-15.237  
 G3X0.Y-15.237I0.J15.237  
 G1Y-7.236  
 G2X0.Y7.236I0.J7.236  
 G1Y13.029  
 Z-4.9F50.  
 G3X13.029Y0.I0.J-13.029F594.  
 G1X9.352  
 G2X9.352Y0.I-9.352J0.  
 G1X7.352  
 G2X7.352Y0.I-7.352J0.  
 G1X13.029  
 G3X0.Y13.029I-13.029J0.

Optimized Codes

G2X-6.89Y0.I6.89J0.  
 G1X-11.716F2000.  
 G3X0.Y-11.716I11.716J0.F594.  
 G1Y-15.716  
 G3X0.Y-15.716I0.J15.716  
 G1Y-6.89F2000.  
 G3X0.Y6.89I0.J6.89  
 G1Y11.577  
 Z-4.3F50.  
 G3X11.577Y0.I0.J-11.577F594.  
 G1X11.005  
 G2X11.005Y0.I-11.005J0.F1500.  
 G1X7.005F594.  
 G2X7.005Y0.I-7.005J0.  
 G1X11.577F2000.  
 G3X0.Y11.577I-11.577J0.F594.  
 G1Y15.577  
 G3X0.Y15.577I0.J-15.577  
 G1Y7.005F2000.  
 G2X0.Y-7.005I0.J-7.005  
 G1Y-11.418  
 Z-4.5F50.  
 G3X-11.418Y0.I0.J11.418F594.  
 G1X-11.121  
 G2X-11.121Y0.I11.121J0.F1500.  
 G1X-7.121F594.  
 G2X-7.121Y0.I7.121J0.  
 G1X-11.418F2000.  
 G3X0.Y-11.418I11.418J0.F594.  
 G1Y-15.418  
 G3X0.Y-15.418I0.J15.418  
 G1Y-11.237F2000.  
 Z-4.7F50.  
 G3X0.Y-11.237I0.J11.237F594.  
 G2X-11.237Y0.I0.J11.237F2000.  
 G1X-7.236F594.  
 G2X-7.236Y0.I7.236J0.  
 G1X-11.236F2000.  
 G3X0.Y-11.237I11.237J0.F594.  
 G1Y-15.237  
 G3X0.Y-15.237I0.J15.237  
 G1Y-7.236F2000.  
 G2X0.Y7.236I0.J7.236  
 G1Y13.029  
 Z-4.9F50.  
 G3X13.029Y0.I0.J-13.029F594.  
 G1X9.352  
 G2X9.352Y0.I-9.352J0.  
 G1X7.352  
 G2X7.352Y0.I-7.352J0.F1188.  
 G1X13.029F2000.  
 G3X0.Y13.029I-13.029J0.F594.

Original Codes

G1Y15.029  
 G3X0.Y15.029**I0.J-15.029**  
 G1Y12.789  
 Z-5.1F50.  
 G3X12.789Y0.I0.J-12.789F594.  
 G1X9.469  
 G2X9.469Y0.**I-9.469J0.**  
 G1X7.469  
 G2X7.469Y0.**I-7.469J0.**  
 G1X12.789  
 G3X0.Y12.789**I-12.789J0.**  
 G1Y14.789  
 G3X0.Y14.789**I0.J-14.789**  
 G1Y12.526  
 Z-5.3F50.  
 G3X12.526Y0.I0.J-12.526F594.  
 G1X9.601  
 G2X9.601Y0.**I-9.601J0.**  
 G1X7.601  
 G2X7.601Y0.**I-7.601J0.**  
 G1X12.526  
 G3X0.Y12.526**I-12.526J0.**  
 G1Y14.526  
 G3X0.Y14.526**I0.J-14.526**  
 G1Y12.238  
 Z-5.5F50.  
 G3X12.238Y0.I0.J-12.238F594.  
 G1X9.751  
 G2X9.751Y0.**I-9.751J0.**  
 G1X7.751  
 G2X7.751Y0.**I-7.751J0.**  
 G1X12.238  
 G3X0.Y12.238**I-12.238J0.**  
 G1Y14.238  
 G3X0.Y14.238**I0.J-14.238**  
 G1Y11.921  
 Z-5.7F50.  
 G3X11.921Y0.I0.J-11.921F594.  
 G1X9.922  
 G2X9.922Y0.**I-9.922J0.**  
 G1X7.922  
 G2X7.922Y0.**I-7.922J0.**  
 G1X11.921  
 G3X0.Y11.921**I-11.921J0.**  
 G1Y13.921  
 G3X0.Y13.921**I0.J-13.921**  
 G1Y11.566  
 Z-5.9F50.  
 G3X11.566Y0.I0.J-11.566F594.  
 G1X10.119  
 G2X10.119Y0.**I-10.119J0.**  
 G1X8.119

Optimized Codes

G1Y15.029  
 G3X0.Y15.029**I0.J-15.029F1188.**  
 G1Y12.789**F2000.**  
 Z-5.1F50.  
 G3X12.789Y0.I0.J-12.789F594.  
 G1X9.469  
 G2X9.469Y0.**I-9.469J0.F715.**  
 G1X7.469**F594.**  
 G2X7.469Y0.**I-7.469J0.F1188.**  
 G1X12.789**F2000.**  
 G3X0.Y12.789**I-12.789J0.F594.**  
 G1Y14.789  
 G3X0.Y14.789**I0.J-14.789F1188.**  
 G1Y12.526**F2000.**  
 Z-5.3F50.  
 G3X12.526Y0.I0.J-12.526F594.  
 G1X9.601  
 G2X9.601Y0.**I-9.601J0.F812.**  
 G1X7.601**F594.**  
 G2X7.601Y0.**I-7.601J0.F1188.**  
 G1X12.526**F2000.**  
 G3X0.Y12.526**I-12.526J0.F594.**  
 G1Y14.526  
 G3X0.Y14.526**I0.J-14.526F1188.**  
 G1Y12.238**F2000.**  
 Z-5.5F50.  
 G3X12.238Y0.I0.J-12.238F594.  
 G1X9.751  
 G2X9.751Y0.**I-9.751J0.F955.**  
 G1X7.751**F594.**  
 G2X7.751Y0.**I-7.751J0.F1188.**  
 G1X12.238**F2000.**  
 G3X0.Y12.238**I-12.238J0.F594.**  
 G1Y14.238  
 G3X0.Y14.238**I0.J-14.238F1188.**  
 G1Y11.921**F2000.**  
 Z-5.7F50.  
 G3X11.921Y0.I0.J-11.921F594.  
 G1X9.922  
 G2X9.922Y0.**I-9.922J0.F1188.**  
 G1X7.922**F594.**  
 G2X7.922Y0.**I-7.922J0.F1188.**  
 G1X11.921**F2000.**  
 G3X0.Y11.921**I-11.921J0.F594.**  
 G1Y13.921  
 G3X0.Y13.921**I0.J-13.921F1188.**  
 G1Y11.566**F2000.**  
 Z-5.9F50.  
 G3X11.566Y0.I0.J-11.566F594.  
 G1X10.119  
 G2X10.119Y0.**I-10.119J0.F1500.**  
 G1X8.119**F594.**

Original Codes

G2X8.119Y0.I-8.119J0.  
 G1X11.566  
 G3X0.Y11.566I-11.566J0.  
 G1Y13.566  
 G3X0.Y13.566I0.J-13.566  
 G1Y11.162  
 Z-6.1F50.  
 G3X11.162Y0.I0.J-11.162F594.  
 G1X10.346  
 G2X10.346Y0.I-10.346J0.  
 G1X8.346  
 G2X8.346Y0.I-8.346J0.  
 G1X11.162  
 G3X0.Y11.162I-11.162J0.  
 G1Y13.162  
 G3X0.Y13.162I0.J-13.162  
 G1Y10.688  
 Z-6.3F50.  
 G3X10.688Y0.I0.J-10.688F594.  
 G1X10.613  
 G2X10.613Y0.I-10.613J0.  
 G1X8.613  
 G2X8.613Y0.I-8.613J0.  
 G1X10.688  
 G3X0.Y10.688I-10.688J0.  
 G1Y12.688  
 G3X0.Y12.688I0.J-12.688  
 G1Y12.101  
 Z-6.5F50.  
 G3X12.101Y0.I0.J-12.101F594.  
 G1X8.937  
 G2X8.937Y0.I-8.937J0.  
 G1X12.101  
 G3X0.Y12.101I-12.101J0.  
 G1Y11.34  
 Z-6.7F50.  
 G3X11.34Y0.I0.J-11.34F594.  
 G1X9.354  
 G2X9.354Y0.I-9.354J0.  
 G1X11.34  
 G3X0.Y11.34I-11.34J0.  
 G1Y10.219  
 Z-6.9F50.  
 G3X10.219Y0.I0.J-10.219F594.  
 G1X9.985  
 G2X9.985Y0.I-9.985J0.  
 G1X10.219  
 G3X0.Y10.219I-10.219J0.  
 G1Z5.  
 M9  
 M5  
 M2

Optimized Codes

G2X8.119Y0.I-8.119J0.F1188.  
 G1X11.566F2000.  
 G3X0.Y11.566I-11.566J0.F594.  
 G1Y13.566  
 G3X0.Y13.566I0.J-13.566F1188.  
 G1Y11.162F2000.  
 Z-6.1F50.  
 G3X11.162Y0.I0.J-11.162F594.  
 G1X10.346  
 G2X10.346Y0.I-10.346J0.F1500.  
 G1X8.346F594.  
 G2X8.346Y0.I-8.346J0.F1188.  
 G1X11.162F2000.  
 G3X0.Y11.162I-11.162J0.F594.  
 G1Y13.162  
 G3X0.Y13.162I0.J-13.162F1188.  
 G1Y10.688F2000.  
 Z-6.3F50.  
 G3X10.688Y0.I0.J-10.688F594.  
 G1X10.613  
 G2X10.613Y0.I-10.613J0.F1500.  
 G1X8.613F594.  
 G2X8.613Y0.I-8.613J0.F1188.  
 G1X10.688F2000.  
 G3X0.Y10.688I-10.688J0.F594.  
 G1Y12.688  
 G3X0.Y12.688I0.J-12.688F1188.  
 G1Y12.101F2000.  
 Z-6.5F50.  
 G3X12.101Y0.I0.J-12.101F594.  
 G1X8.937  
 G2X8.937Y0.I-8.937J0.F750.  
 G1X12.101F2000.  
 G3X0.Y12.101I-12.101J0.F594.  
 G1Y11.34F2000.  
 Z-6.7F50.  
 G3X11.34Y0.I0.J-11.34F594.  
 G1X9.354  
 G2X9.354Y0.I-9.354J0.F1196.  
 G1X11.34F2000.  
 G3X0.Y11.34I-11.34J0.F594.  
 G1Y10.219F2000.  
 Z-6.9F50.  
 G3X10.219Y0.I0.J-10.219F594.  
 G1X9.985  
 G2X9.985Y0.I-9.985J0.F1500.  
 G1X10.219F2000.  
 G3X0.Y10.219I-10.219J0.F594.  
 G1Z5.F2000.  
 M9  
 M5  
 M2

## APPENDIX E

### REGRESSION ANALYSIS OF THE FINISH CUT EXPERIMENTS

In order to predict the geometrical error value for various applications, regression analysis is performed. Coefficients of the linear regression model ( $\beta$  values) are computed as follows:

$$\beta = (X^T X)^{-1} X^T y \quad (\text{E.1})$$

where X is the matrix obtained from the input parameters, step over, feed, cutting speed and y is the vector of the geometrical error. The variable coefficients are computed by applying the least square method to the experimental data.

$$X = \begin{bmatrix} 1 & 0,1 & 0,03 & 130 & 0,003 & 13 & 3,9 & 0,01 & 0,0009 \\ 1 & 0,1 & 0,04 & 130 & 0,004 & 13 & 5,2 & 0,01 & 0,0016 \\ 1 & 0,1 & 0,05 & 130 & 0,005 & 13 & 6,5 & 0,01 & 0,0025 \\ 1 & 0,2 & 0,03 & 130 & 0,006 & 26 & 3,9 & 0,04 & 0,0009 \\ 1 & 0,2 & 0,04 & 130 & 0,008 & 26 & 5,2 & 0,04 & 0,0016 \\ 1 & 0,2 & 0,05 & 130 & 0,01 & 26 & 6,5 & 0,04 & 0,0025 \\ 1 & 0,3 & 0,03 & 130 & 0,009 & 39 & 3,9 & 0,09 & 0,0009 \\ 1 & 0,3 & 0,04 & 130 & 0,012 & 39 & 5,2 & 0,09 & 0,0016 \\ 1 & 0,3 & 0,05 & 130 & 0,015 & 39 & 6,5 & 0,09 & 0,0025 \\ 1 & 0,1 & 0,03 & 170 & 0,003 & 17 & 5,1 & 0,01 & 0,0009 \\ 1 & 0,1 & 0,04 & 170 & 0,004 & 17 & 6,8 & 0,01 & 0,0016 \\ 1 & 0,1 & 0,05 & 170 & 0,005 & 17 & 8,5 & 0,01 & 0,0025 \\ 1 & 0,2 & 0,03 & 170 & 0,006 & 34 & 5,1 & 0,04 & 0,0009 \\ 1 & 0,2 & 0,04 & 170 & 0,008 & 34 & 6,8 & 0,04 & 0,0016 \\ 1 & 0,2 & 0,05 & 170 & 0,01 & 34 & 8,5 & 0,04 & 0,0025 \\ 1 & 0,3 & 0,03 & 170 & 0,009 & 51 & 5,1 & 0,09 & 0,0009 \\ 1 & 0,3 & 0,04 & 170 & 0,012 & 51 & 6,8 & 0,09 & 0,0016 \\ 1 & 0,3 & 0,05 & 170 & 0,015 & 51 & 8,5 & 0,09 & 0,0025 \end{bmatrix} \quad (\text{E.2})$$

$$\text{Geom\_error} = \begin{bmatrix} 20,5 \\ 27 \\ 32,5 \\ 34,5 \\ 39 \\ 42,5 \\ 45 \\ 49,5 \\ 55,5 \\ 21,5 \\ 28,5 \\ 33,5 \\ 36,5 \\ 41,5 \\ 44 \\ 45,5 \\ 51 \\ 57 \end{bmatrix} \quad (\text{E.3})$$

$$x = X^T \cdot X \quad (\text{E.4})$$

$$\beta = x^{-1} \cdot X^T \cdot \text{Geom\_error} \quad (\text{E.5})$$

$$\beta = \begin{bmatrix} -19,083 \\ 156,67 \\ 831,25 \\ 0,0278 \\ -250 \\ 2,016 \cdot 10^{-13} \\ 0,2083 \\ -75 \\ -3750 \end{bmatrix} \quad (\text{E.6})$$

$$\text{Geom\_error} = \beta_0 + \beta_1 a_e + \beta_2 f_t + \beta_3 V_c + \beta_4 a_e f_t + \beta_5 a_e V_c + \beta_6 f_t V_c + \beta_7 a_e^2 + \beta_8 f_t^2 \quad (\text{E.7})$$

$$\text{Geom\_error} = -19.083 + 156.67 a_e + 831.25 f_t + 0.0278 V_c - 250 a_e f_t + 2.016 \cdot 10^{-13} a_e V_c + 0.2083 f_t V_c - 75 a_e^2 - 3750 f_t^2 \quad (\text{E.8})$$